CNIC-00965
CNDC-0016
INDC(CPR)-034/L

COMMUNICATION OF NUCLEAR DATA PROGRESS

No. 13(1995)

China Nuclear Information Centre
Chinese Nuclear Data Center
Atomic Energy Press

CNIC-00965
CNDC-0016
INDC(CPR)-034 / L

COMMUNICATION OF NUCLEAR DATA PROGRESS

No. 13 (1995)

Chinese Nuclear Data Center

China Nuclear Information Centre

Atomic Energy Press

Beijing, June, 1995

EDITORIAL NOTE

This is the thirteen issue of *Communication of Nuclear Data Progress* (CNDP), in which the nuclear data achievement and progress in China during the last year are carried, including the measurements of Fe, Ni(n,xp), ^{58}Ni(n,α), $^{106,\ 110,\ 116}$Cd(n,2n), ^{111}Cd(n,p), $^{196,\ 198,\ 199}$Hg(n,p), ^{196}Hg(n,x)^{195}Au reaction cross sections, Be(n,n), ^{58}Ni(n,α) angular distributions, and Fe, Ni(n,xp) DDCS; the theoretical calculations of P+^{11}C, d+^{11}C and n+$^{63,\ 65}$Cu reaction cross sections; nuclear data evaluation method and evaluation system, the Q–value for natural element, the revision of inelastic scattering cross section of ^{238}U for CENDL–2.1, the evaluations of neutron monitor cross sections for $^{54,\ 56\sim 58,\ Nat}$Fe(n,x)^{51}Cr, $^{52,\ 54,\ 56}$Mn and $^{63,\ 65,\ Nat}$Cu(n,x)$^{56\sim 58,\ 60}$Co reactions; the benchmark testing of CENDL–2 for homogeneous fast reactor and U–fuel thermal reactor; modification and improvement of CENDL–2, progress on Chinese Evaluated Nuclear Parameter Library (CENPL) (IV); radiative loss for carbon plasma impurity; and activities and cooperations on nuclear data in China in 1994.

For limited experience and knowledge, there might be some shortcomings and errors, welcome to make comments on them.

Please write to Drs. Liu Tingjin and Zhuang Youxiang
Mailing Address : Chinese Nuclear Data Center
China Institute of Atomic Energy
P. O. Box 275 (41), Beijing 102413
People's Republic of China
Telephone : 86–10–9357729 or 9357830
Telex : 222373 IAE CN
Facsimile : 86–10–935 7008
E–mail : CIAEDNP@ BEPC 2.IHEP.AC.CN

CONTENTS

I EXPERIMENTAL MEASUREMENT

Progress on Nuclear Data Measurement at Peking University in 1994

Chen Jinxiang Tang Guoyou Shi Zhaomin

(Institute of Heavy Ion Physics, Peking University)

In 1994, the considerable progress was made on development of facilities and nuclear data measurement. The main works are described briefly as follows :

1 Development of Accelerator Facilities

The 4.5 MV Van de Graaff accelerator which was designed and constructed at Peking University has been developed as a monoenergetic neutron source through several years operation and improvement. The monoenergetic neutrons generated by this machine in the range of 0.03～7.20 MeV and 14～20 MeV. Since Nov. 1991, monoenergetic neutron has been supplied to carry out neutron studies on more than ten subjects for more than 2000 hrs effective DC beam time on this machine. The operational stability and reliability has been satisfactory.

During the past year, the progress had been made on establishing a beam pulsing system to meet the needs of the neutron TOF experiment. A RF ion source with high proton ratio has been installed to replace the previous PIG source. High quality ion beam is essential for the bunching facilities. The extracted current of hydrogen ions ranges from 240 μA to 500 μA at the exit of ion source. The ratio of H^+ : H_2^+ is more than 80%. The energy dispersion for the source being used now lies between 50～100 eV and the source emittence lies between 2.3 to 6.6 mm–mrad–$MeV^{1/2}$. The beam pulsing system consists of a pair of deflecting plates, to which 1.5 MHz RF voltage is applied, and a Klystron type buncher inserted between the deflecting plate and the chopping aperture, to which bunching voltage of 9 MHz is applied. The pulsed beam with

width of 1.8 ns (FWHM) has been obtained at the end of the target at a 3 MHz repetition rate. The identification test has been carried out for the performance of the accelerator. A summary of the performance thus achieved is as follows :

(1) status of continuous ion beams :

terminal voltage (no beam loading) : 4.70 MV

terminal voltage (Max achieved, beam loading) : 4.57 MV

stability of terminal voltage : $< \pm 1.5$ kV

efficiency of beam transfer : can be > 95%

duration of once running time : can be > 300 h

Typical beam intensities obtained at various terminal voltages are given on Table 1.

Table 1

ion species	terminal voltage (MV)	non analyzed beam (μA)	analyzed beam (target) (μA)
d	0.429	5.8	4.8
d	1.293	14	11
d	1.879	14	12
d	2.985	14	12.5
d	4.074	14.5	11.5
p	4.452	17.5	14
p	4.569	17.5	12

(2) status of pulsing beam :[1]

beam pulse width (FWHM) : 1.8 ns

repetition rate : 3.0 MHz

mean current of analyzed beam : can be > 1.0 μA

(3) beam line pump : 1×10^{-6} torr

2 Experimental Preparation for Measuring Neutron Spectrum and Double Differential Cross Section

A good precision neutron time–of–flight equipment has been constructed

for the purpose of measuring neutron spectrum and double differential cross section. The equipment includes a monoenergetic neutron source produced a pulsed ion beam, pulsed beam pick–off, deuterium gas target assembly and heavily shielded neutron TOF spectrometer–goniometer. The main neutron detector is a 105 mm in dia. and 50 mm thick ST451 scintillator, optically coupled to a XP2040 photomultiplier tube. After improvement of the PMT voltage divider, the time resolution of the detector is about 512ps (dynamic range 5 : 1). A low mass, fast ionization mini–chamber of ^{252}Cf source is used as the fission fragments detector, and the time resolution of the spectrometer is about 1.4 ns. The detection efficiency[2] and the effective neutron detection threshold to relative electron response[3] for the main detector have been measured by means of a practical method which uses a TOF measurement of the prompt fission neutron spectrum of ^{252}Cf. Relative detection efficiencies have been obtained for threshold settings of 0.420, 0.625, 0.885, 1.168, 1.565 and 1.880 MeV for energies from several hundred keV to 10 MeV. The experimental results were compared to calculated efficiency curves with the Monte Carlo code NEFF7 and the consistencies are rather satisfactory. The effective neutron threshold and relative electron response for the detector in the neutron energy range up to 7.0 MeV were also obtained. Now the measurement of the project is ready to carry out at our 4.5 MV Van de Graaff accelerator.

3 Measurement of $^{7}Li(n,n'\gamma)^{7}Li^{*}$ (478 keV) Inelastic Angular Distribution

This work recently completed is the IAEA contract project. The nuclear data of ^{7}Li has become very important with the development of controlled nuclear fusion reactor, and the double differential cross section is indispensable for neutron transport calculations in the reactor blanket. However, because of the time resolution limit of the TOF technique, it is very difficult to separate the inelastic scattering neutrons of $^{7}Li^{*}$ (478 keV) from the elastic scattering neutrons when the incident energy is higher than 6 MeV. So these measured data are very few. In 1986, Liskien et al. developed the Doppler broaden and shifted gamma–ray method for measuring the neutron angular distribution with the incident energy below 8.5 MeV. But comparing the measured data with the earlier calculation, the consistencies are not so satisfactory. Therefore, at our laboratory the efforts had been made not only in experimental measurement but also in theoretical calculations.

In the experimental measurement : Before the last year, we had completed measurement at neutron energy 14.9 MeV in 5 Lab angles. During the past year

the measurement was done at incident neutron energy of 9, 9.5 and 10 MeV via the method of shape analysis of Doppler shifted γ ray spectra[4]. This work was cooperated with the China Institute of Atomic Energy. The measured γ spectra were fitted to the Monte Carlo simulation results to get the Legendre coefficients of the angular distributions in CM system. The incident neutron energy has been greatly extended on measurement of $^{7}Li(n,n')^{7}Li^{*}$ inelastic angular distribution.

In theoretical calculations: Direct process is dominant for the reaction $^{7}Li(n,n')$ (478 keV) at rather high incident energy. The usual model for calculation of direct inelastic scattering cross section is the DWBA and the Coupled Channel Approximation (CCA). In this work, the calculation was performed with the modified DWUCK4 code based on the zero-range approximation DWBA. In order to do calculation better, we added a subroutine in the DWUCK4, which was used for automatically searching the optical potential parameters, residual interaction potential parameters and the deformation parameter. Some original subroutines were changed slightly to fit the parameter searching. Using the code, the double differential cross sections of the reaction $^{7}Li(n,n')$ (478 keV) in the energy range from 8 to 20 MeV were calculated. The calculated results are compared with the corresponding measured data. The agreements are rather good. As an example, the comparisons between the experimental data and the calculated results are shown in Fig. 1.

4 Measurement of Angular Distribution and Cross Section for $^{58}Ni(n,\alpha)^{55}Fe$ and $^{54}Fe(n,\alpha)^{51}Cr$ Reactions

Nickel, iron and their alloys are widely used as reactor materials and radiation protection shielding materials. It is therefore very important to measure accurately the cross section and angular distribution of emitted charged particles for determining the radiation resistant ability of alloys. Up to now, because of experimental difficulties, the (n,α) cross section data for Fe and Ni are still scarce and large discrepancies exist among the evaluations. Therefore, the α-particle production cross sections of Fe and Ni are required for the region of wide incident neutron energy up to 14 MeV.

We have reported[5] the cross section of $^{58}Ni(n,\alpha)^{55}Fe$ at 5.1 MeV using Gridded Ionization Chamber (GIC). The past year, we extended the measurements of ^{58}Ni to $E_n = 6.0$ MeV, 7.0 MeV and began to measure cross section of ^{54}Fe at 6.9 MeV. The incident monoenergetic neutrons were obtained by the D(d,n) reaction on the 4.5 MV Van de Graaff accelerator. The total neutron fluences were determined by a fission chamber of ^{238}U. The total

weight of ^{238}U sample (purity : 99.997%) was obtained by international calibration and it is 547.2 (1 ± 1.3%) μg. The target sample of ^{58}Ni (purity : 99.95%) was a metal disk with 4.0 cm in diameter and 1.047 mg / cm^2 in thickness. ^{54}Fe powder (enriched to 99.87%) evaporated on a 0.3 mm thick aluminum foil was used as the target sample with 4.0 cm in diameter and 0.96 mg / cm^2 in thickness. During the experiment, solid angles subtended for neutron source by the target sample and sample ^{238}U remained unchanged. The details of the GIC construction and experimental method have been reported in Ref. [6]. But the GIC was filled with gas of 97.5% Kr and 2.5% CO_2 at 1.40 atm, because it can achieve high stopping power and low back ground production. The typical double–parameters spectrum of anode and cathode for reaction of $^{58}Ni(n,\alpha)$ and $^{54}Fe(n,\alpha)$ are shown in Fig. 2. The angular distribution can be obtained by the two–dimensional data processing. The data analysis and calculation are in progress.

5 Activation Cross Section Measurement for the $^{64}Zn(n,p)$, (n,γ) Reactions

In the areas of activation and neutron scattering cross sections, there are still deficiencies in the nuclear data. Activation cross sections were found to be unsatisfactory in 83 of the 183 reactions reviewed by D. L. Smith. The excitation curve for $^{64}Zn(n,p)^{64}Cu$ reaction has been measured by different authors. All of these measured cross sections are not in very good agreement with each other. And experimental data of $^{64}Zn(n,\gamma)^{65}Zn$ are still lack. So it is necessary to measure these cross sections.

The cross sections for $^{64}Zn(n,p)$, (n,γ) reactions were measured with activation technique and the cross sections of $^{58}Ni(n,p)^{58}Co$ and $^{197}Au(n,\gamma)^{198}Au$ were used as reference for neutron fluence rate measurement, respectively. We have reported the cross section measurement of $^{64}Zn(n,p)^{64}Cu$ reaction from 4 to 7 MeV[7]. In the past year, the incident neutron energy was extended to 1.8 MeV for the cross section measurement of $^{64}Zn(n,p)$. We have completed measurement of $^{64}Zn(n,\gamma)$ cross section in incident neutron energy from 165 keV to 1150 keV. The neutrons were generated via the D(d,n) and T(p,n) reactions on the 4.5 MV Van de Graaff accelerator. The results of measurement are shown in Fig. 3. and Fig. 4.

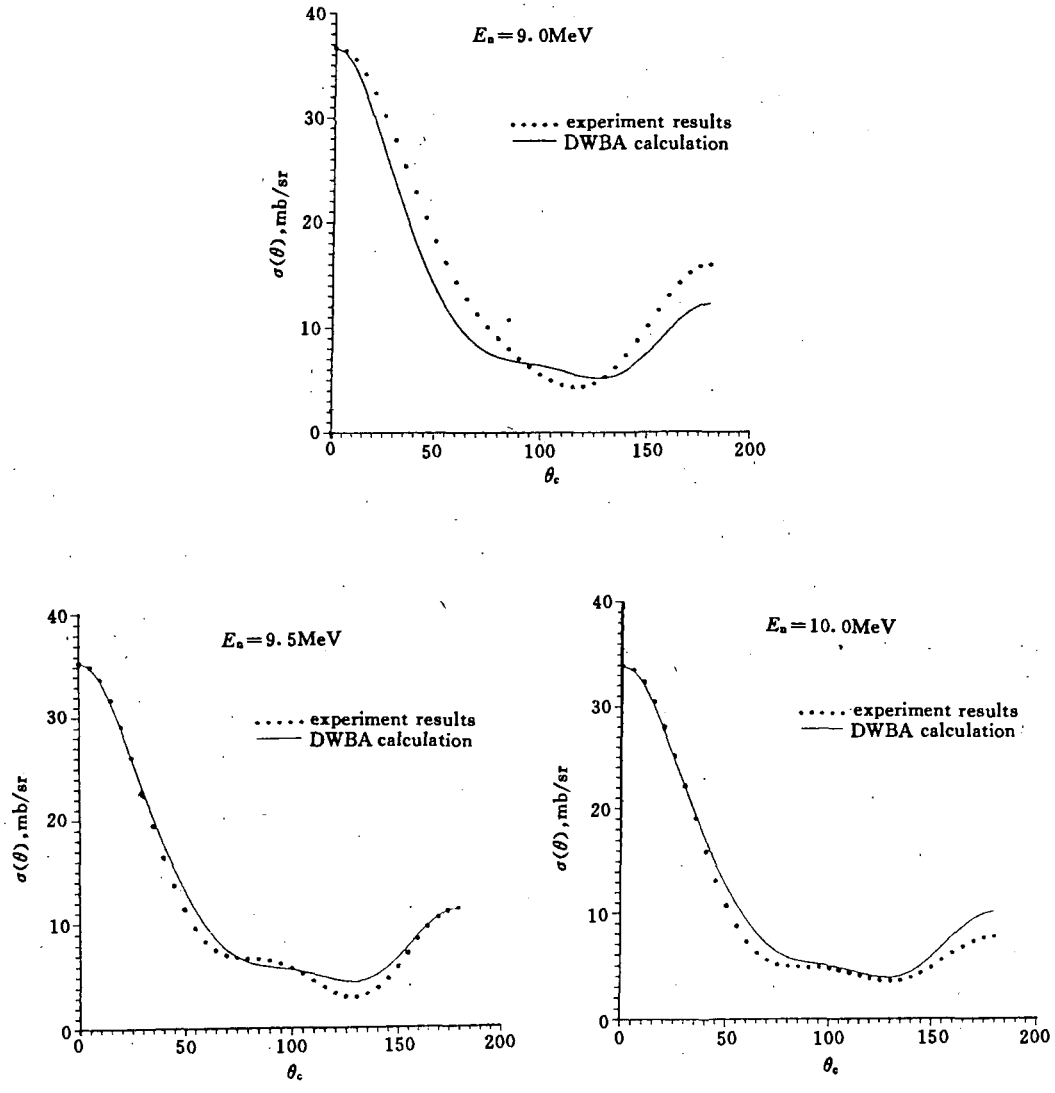

Fig. 1 The comparisons of the experimental and DWBA calculated inelastic scattering angular distribution at 9, 9.5 and 10 MeV

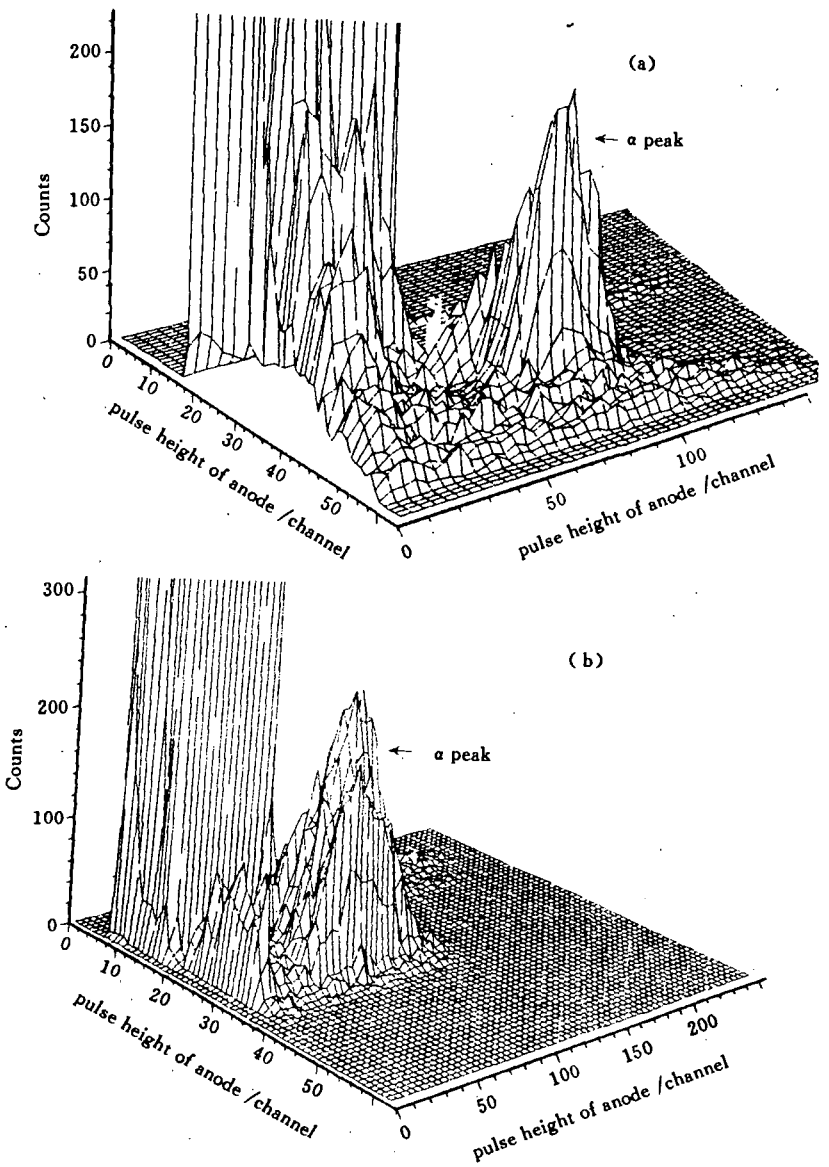

Fig. 2 The two-dimensional picture of pulse heights from gridded ionization chamber

(a) $^{54}Fe(n,\alpha)^{51}Cr$ at $E_n = 6.9$ MeV

(b) $^{58}Ni(n,\alpha)^{55}Fe$ at $E_n = 7.0$ MeV

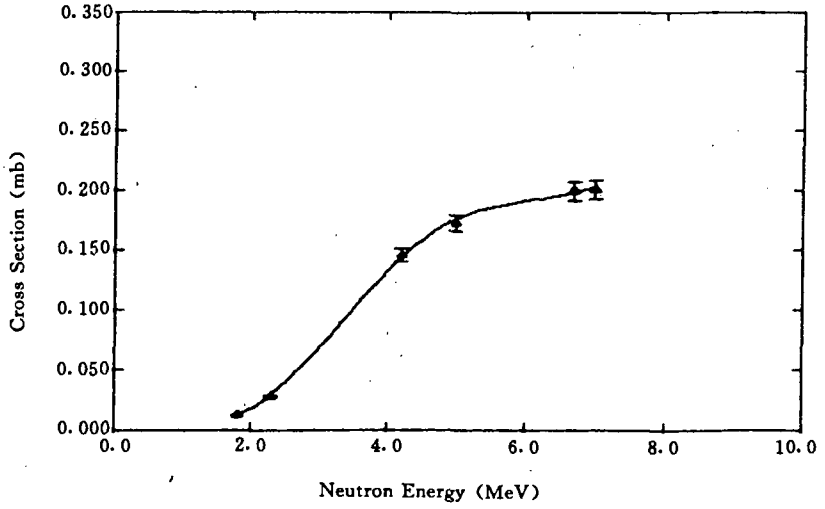

Fig. 3 $^{64}Zn(n,p)^{64}Cu$ cross sections

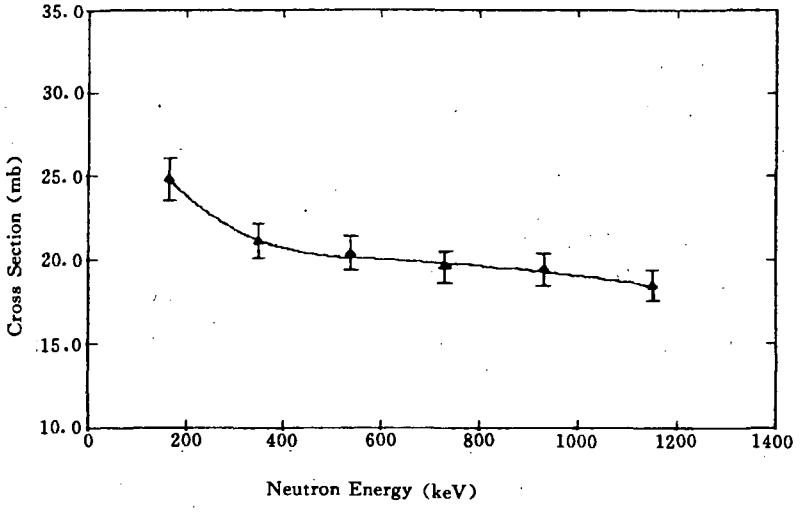

Fig. 4 $^{64}Zn(n,\gamma)^{65}Zn$ cross sections

References

[1] Lu Jianqin et al., Beam pulsing system for the 4.5 MV electrostatic accelerator. Nucl. Instrum. Methods, in Phys. Res. A, A346 : 31, 1994

[2] Chen Jinxiang et al., Experimental determination of the relative fast neutron efficiency of a liquid scintillation detector with a thin ^{252}Cf source. Nucl. Electr. & Detect Tech. 13(6) : 323, 1993

[3] Chen Jinxiang et al., Accurate determination of the effective neutron detection threshold and relative electron response for the neutron scintillation detector. Nucl. Electr & Detect Tech. 14(3) : 140, 1994

[4] Huang Feizeng et al., The inelastic scattering neutron angular distribution of reaction $^{7}Li(n,n')^{7}Li^{*}$ (478 keV) derived from shape analysis of the Doppler broadened spectra at 9, 9.5, and 10 MeV. Nucl Instrum Methods, in Phys. Res. A in press, (1995)

[5] Tang Guoyou et al., Measurement of angular distribution and cross section for $^{58}Ni(n,\alpha)$ reaction at 5.1 MeV. Chin. J. of Nucl. Phys., 16(3) : 1, 1994

[6] Tang Guoyou et al., Angular distribution and cross section measurements for the reaction $^{40}Ca(n,\alpha)^{37}Ar$ using gridded ionization chamber, Nuclear Techniques, 17(3) : 129, 1994

[7] Tang Guoyou et al., Cross section measurement of $^{64}Zn(n,p)^{64}Cu$ reaction from 4 to 7 MeV. Communication of Nuclear Data Progress, No. 11, INDC(CPR)–032 / L, p. 1, 1994

Progress on Measurement of $^{58}Ni(n,\alpha)$ Reaction Cross Sections and Angular Distribution at 6.0 MeV and 7.0 MeV

Fan Jihong Cheng Jinxiang
Tang Guoyou Shi Zhaomin Zhang Guohui

(Institute of Heavy Ion Physics, Peking University, Beijing)

Yu M Gledenov G Khuuhenhuu

(Joint Institute for Nuclear Physics, Dubna 141980, Russia)

1 Measurement

To study energy and angular distribution of α particles produced, a gridded ionization chamber (GIC) with multi-parameters data acquisition and processing system was employed[2]. In the present experiment, structure of the GIC, and the target sample of ^{58}Ni are the same as those in Ref. [1]. To get better particle resolution, 97.5% Kr + 2.5% CO_2 was used as counting gas of the GIC to obtain high stopping power and low background. The pressure of the mixture gas is 1.40 atm. During the experiment, the signals from cathode and both anodes of the GIC were got at the same time. While one anode signal is the signal of event in the angle region 0~90 degree, the other is the background of the 90~180 degree region; if one anode signal is the signal of background of 0~90 degree, the other is the event of 90~180 degree. The neutron flux is determined by the methods described in Ref. [1]. The spectrometer is calibrated by the mixture Pu α source and ^{234}U α source.

2 Primary Results

Comparing with the results of neutron energy at 5.1 MeV, the peak for α_1 is clearer when neutron energy increases to 6.0 MeV and 7.0 MeV, as shown in Figs. 1~3. In comparison of Fig. 1 with Fig. 2, the angular distribution of the α_0 are different from α_1 . When neutron energy is 6.0 MeV, the area of α_0 is

about 40% of total α area at 60 degree, and about 70% of total α area at 120 degree, as shown in Table 1. If the ^{58}Ni sample is thinner, it would be possible to get α_1, α_0 cross sections and angular distributions. We plan to carry out a new measurement with a ^{58}Ni sample of $0.3 \sim 0.5$ mg / cm^2 thick and will get further information about α_1.

Table 1 The area of α_0 and the area of α_1 in total α peak area

angle	area of α_0	area of α_1
60 degree	40 %	60 %
120 degree	70 %	30 %

We wish to thank the operating crew of 4.5 MV Van De Graaff Accelerator for their help during the experiments.

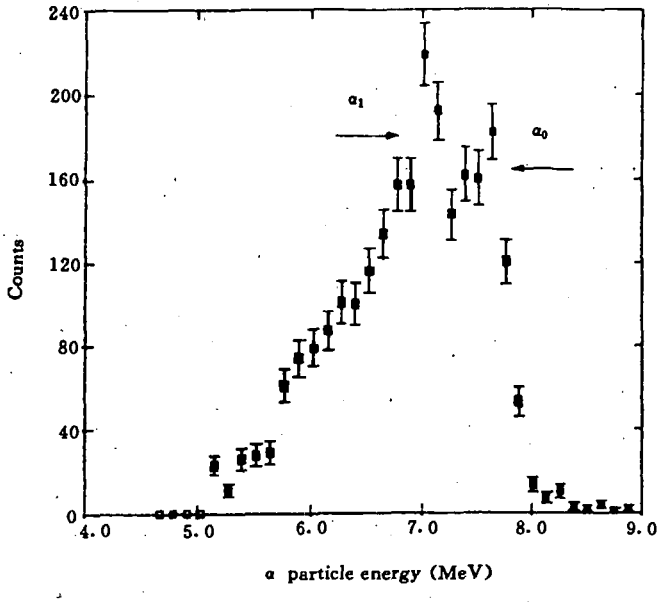

Fig. 1 α particle energy spectrum at $\theta_1 = 60°$, $E_n = 6.0$ MeV

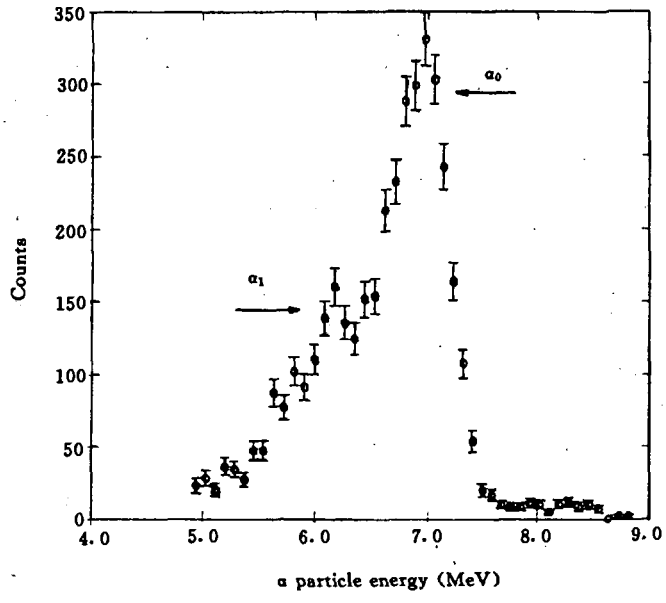

Fig. 2 α particle energy spectrum at $\theta_1 = 120°$, $E_n = 6.0$ MeV

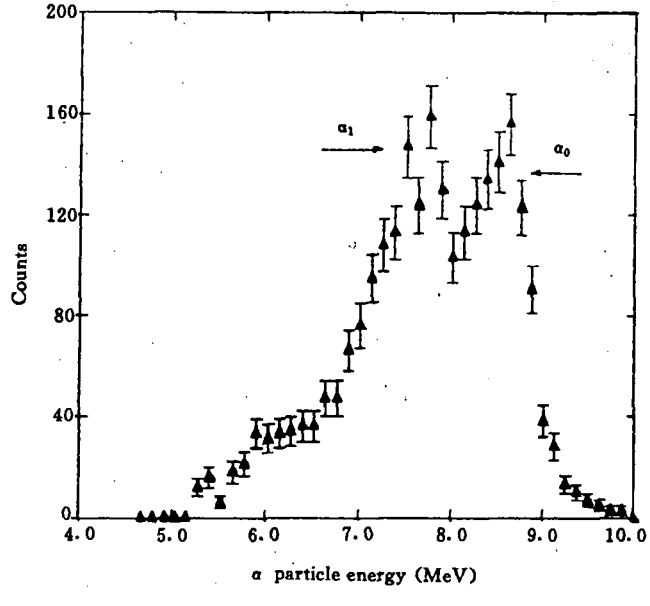

Fig. 3 α particle energy spectrum at $\theta_1 = 60°$, $E_n = 7.0$ MeV

References

[1] Tang Guoyou et al., Communication of Nuclear Data Progress, No. 10, p. 14, (1993)

[2] Tang Guoyou et al., Nuclear Techniques (in Chinese), Vol. 17, No. 3, p. 129, (1994)

Cross Section Measurements for $^{111}Cd(n,p)^{111m}Ag$, $^{106}Cd(n,2n)^{105}Cd$, $^{110}Cd(n,2n)^{109}Cd$, $^{116}Cd(n,2n)^{115m}Cd$ and $^{116}Cd(n,2n)^{115g}Cd$ Reactions

Kong Xiangzhong Wang Yongchang Yuan Jungqian Yang Jingkang

(Department of Modern Physics, Lanzhou University)

Abstract

Activation cross sections for cadmium were measured in the neutron energy range from 13.40 MeV to 14.80 MeV using the $T(d,n)^4He$ reaction as neutron source. The cross sections of $^{27}Al(n,\alpha)^{24}Na$ reaction is used as standard one.

Introduction

Natural cadmium has eight stable isotopes, they are ^{106}Cd (1.25%), ^{108}Cd (0.89%), ^{110}Cd (12.49%), ^{111}Cd (12.80%), ^{112}Cd (24.13%), ^{113}Cd (12.22%), ^{114}Cd (28.73%) and ^{116}Cd (7.49%); therefore, natural cadmium sample has very complex gamma-ray spectrum after irradiations. This fact brings about great difficulties to the analysis of cross sections. So far only a few data have been published and there are gross disagreements among them. In this experiment, the cross sections of $^{111}Cd(n,p)^{111m}Ag$, $^{106}Cd(n,2n)^{105}Cd$, $^{110}Cd(n,2n)^{109}Cd$, $^{116}Cd(n,2n)^{115m}Cd$ and $^{116}Cd(n,2n)^{115g}Cd$ reactions were measured in the neutron energy range of 13.50～14.80 MeV.

1 Experimental Procedure

1.1 Irradiation

The experiment was carried out at the ZF-300-Ⅱ Intense Neutron Generator of Lanzhou University, which has a neutron yield about $(1\sim 3)\times 10^{12}$ n / (4π • s). The neutrons were produced by $T(d,n)^4He$ reaction with an effective average energy of deuteron beam about 125 keV and beam current

about 20 mA. The thickness of T–Ti target was about 0.9 mg / cm^2. The samples were placed at the angles 0～140 ° relative to the beam direction and were irradiated for 6.6 hours. The cross sections of the reactions were determined relatively to the cross sections of $^{27}Al(n,\alpha)^{24}Na$ reaction, which were used as monitors. In this experiment, the samples of Al and Cd 20 mm in diameter and 0.1 mm and 0.8 mm in thickness and 99.999% and 99.6% in purity were made of natural metal foils, respectively. The Cd sample in each group was sandwiched between two Al foils. The groups of samples were placed at 5～28 cm away from the neutron source. The neutron energies for various directions were determined by the cross section ratios of $^{90}Zr(n,2n)^{89m+g}Zr$ and $^{93}Nb(n,2n)^{92m}Nb$[1, 2].

1.2 Activity Measurement

The activities of ^{105}Ag, ^{111m}Ag, ^{109}Cd, ^{115m}Cd, ^{115g}Cd and ^{24}Na were determined by CH8403 coaxial HPGe detector made in China with a relative efficiency of 20% and an energy resolution of 3 keV (1.33 MeV). The efficiency of the detector was calibrated with the standard gamma source SRM4275. The error in the absolute efficiency curve at 2 cm was less than 1.5%, while the error of the activity of the standard source was less than 1%[3].

The abundance and half–lives of residual nuclei, together with the characteristic gamma–ray energies and absolute intensities[4] are listed in Table 1.

In the measurement of gamma activities, some corrections were made for the gamma–ray self–absorption in the samples, the cascade decay, the counting geometry, etc.. At the same time, the corrections were also made for the effect of neutron fluence fluctuation.

Table 1 Parameters of concerned reactions

Reactions	Abundance (%)	Half–life	γ–ray energy (keV)	γ–ray intensity (%)
$^{27}Al(n,a)^{24}Na$	100	14.956 h	1368.598	100
$^{111}Ca(n,p)^{111m}Ag$	12.8	7.47 d	245.384	1.24
$^{106}Ca(n,2n)^{105}Ca\rightarrow^{105}Ag$	1.25	41.29 d	280.52	31.0
$^{110}Cd(n,2n)^{109}Cd$	12.49	1.2665 y	88.0341	3.6
$^{116}Cd(n,2n)^{115m}Cd$	7.49	44.6 d	933.847	2.00
$^{116}Cd(n,2n)^{115g}Cd$	7.49	2.228 d	527.910	27.5

2 Results

The measured cross sections of $^{111}Cd(n,p)^{111m}Ag$, $^{106}Cd(n,2n)^{105}Cd$, $^{110}Cd(n,2n)^{109}Cd$, $^{116}Cd(n,2n)^{115m}Cd$ and $^{116}Cd(n,2n)^{115g}Cd$ reactions are shown in Table 2. The major uncertainties of cross sections were calculated as quadratic sum of the errors such as the error of reference cross sections, efficiency of Ge(Li) detector, correction of sum peak, γ–absorption in sample, variation of neutron flux during irradiation, counting statistics, γ–ray intensities and so on.

Table 2 Measured cross sections (mb)

E_n MeV	$^{111}Cd(n,p)^{111}Ag$	$^{106}Cd(n,2n)^{105}Cd$	$^{110}Cd(n,2n)^{109}Cd$	$^{116}Cd(n,2n)^{115m}Cd$	$^{116}Cd(n,2n)^{116g}Cd$
13.40 ± 0.10	14.5 ± 0.7	1121 ± 61	1232 ± 81	652 ± 27	826 ± 45
13.70 ± 0.10	15.1 ± 0.8	1146 ± 62	1245 ± 85	654 ± 27	828 ± 45
14.25 ± 0.13	16.1 ± 0.8	1144 ± 62	1235 ± 81	658 ± 28	822 ± 45
14.50 ± 0.15	16.9 ± 1.0	1150 ± 63	1226 ± 79	632 ± 26	784 ± 44
14.80 ± 0.16	18.5 ± 1.0	1152 ± 63	1221 ± 79	626 ± 26	784 ± 44

References

[1] Lewis V. E. and Zieba K. J., Nucl. Instrum. Method, 174, 141(1980)

[2] Lewis V.E., Metrologia., 20, 49(1984)

[3] Wang Yongchang et al., High Energy Phys. and Nucl. Phys. 14, 919(1990)

[4] Browne E. and Fireatone R. B., Table of Radioactive Isotopes, 1986

Cross Section Measurements for $^{199}Hg(n,p)^{199}Au$, $^{198}Hg(n,p)^{198}Au$, $^{196}Hg(n,p)^{196}Au$ and $^{196}Hg(n,d+np+pn)^{195}Au$ Reactions

Yuan Junqian Kong Xiangzhong Yang Jingkang

(Department of Modern Physics, Lanzhou University)

Wang Huaiyi

(Northwest Institute of Nuclear Science, Xian)

Introduction

The importance of nuclear data for fusion power reactor design has been acknowledged, in particular for safety, environment reasons and economics. The 14 MeV neutron activation cross sections are the key nuclear data for environmental impact, material recycling, waste handling. Due to the large number of materials and traces of alloy elements and contamination, there are requirements for a complete database covering large number of nuclides. For $^{196}Hg(n,p)^{196}Au$ and $^{196}Hg(n,d+np+pn)^{195}Au$ reaction, the existing cross sections data are unsatisfactory [1], so we have measured cross sections for $^{199}Hg(n,p)^{199}Au$, $^{198}Hg(n,p)^{198}Au$, $^{196}Hg(n,p)^{196}Au$ and $^{196}Hg(n,d+np+pn)^{195}Au$ reactions by using the activation method at the Lanzhou University Intense Neutron Generator.

1 Experimental Procedure

The irradiation of samples was carried out at the ZF-300-II Intense Neutron Generator at Lanzhou University. Neutron were produced by $T(d,n)^4He$ reaction with deuteron beam of 125 keV effective energy and 20 mA current. The thickness of T-Ti target used in the generator was about 0.9 mg/cm^2. The neutron flux was monitored by a uranium fission chamber so that corrections could be made for variance of neutron yields during the irradiation.

The samples were made from natural oxide mercury powder by pressing into disc of 20 mm diameter and being packed in a thin polyethylene foil. Each sample was sandwiched between two iron foils, which used to measure the neutron fluence on the sample. Five groups of samples were placed respectively at five different directions ranging from 0° to 120° angles relative to the beam direction and distances of samples from the target were about 5～25 cm. The neutron energies at various locations, where five samples were simultaneously irradiated, were determined by the method of cross section ratios for zirconium and niobium. The five neutron energies were determined to be 14.8, 14.7, 14.5, 14.1, 13.8 MeV, respectively. The irradiation lasted up to 61 hours with neutron intensity of about $1\sim3\times10^{12}$ n / s in the 4π space.

After irradiation, the activities of the samples and monitors were measured by gamma ray spectroscopy using a CH8403 coaxial HPGe detector made in China in conjunction with a EG & ORTEC 7450 Multichannel Analyzer. The energy resolution of the detector is 2.7 keV for 1.33 MeV gamma ray. The efficiency of the detector was calibrated by using the standard gamma ray source, SRM4275, made in U. S. A.. The error of the relative photopeak detection efficiency of the detector was ± 2%. The decay data used in present work are taken from Ref. [2] and listed in Table 1.

Table 1 The decay data used in present work

Reaction	Abundance (%)	Half-live (day)	Energy of γ-ray (keV)	Intensity of γ-ray (%)
$^{199}Hg(n,p)^{199}Au$	16.84	3.139	208.0	8.76
$^{198}Hg(n,p)^{198}Au$	10.02	2.7	411.8	95.5
$^{196}Hg(n,p)^{195}Au$	0.146	6.18	355.7	88
$^{196}Hg(n,d+np+pn)$	0.146	186.0	98.86	10.9
$^{54}Fe(n,p)^{54}Mn$	0.58	312.2	834.8	99.97

In the measurement of gamma ray activities, some corrections were made for the effects of neutron intensity fluctuation, gamma ray self-absorption in the sample, the sum peak effects in the investigated nuclide and the counting geometry.

2 Result and Discussion

The measured results of the cross sections are listed in Table 2.

Table 2 The measured cross sections (mb)

E_n (MeV)	13.8	14.1	14.5	14.7	14.8
$^{199}Hg(n,p)^{199}Au$			2.4± 0.5	2.6± 0.3	2.7± 0.1
$^{198}Hg(n,p)^{198}Au$		3.1± 0.2	5.7± 0.3	5.9± 0.3	5.6± 0.3
$^{196}Hg(n,p)^{195}Au$		6.2± 0.7	5.2± 0.5	13.3± 1.1	18.0± 1.0
$^{196}Hg(n,d)^{195}Au$	633± 92	664 ± 67	726 ± 82	577 ± 37	604 ± 32

The errors reported in our work are from counting statistics, standard cross sections, detector efficiency, weighting of samples, self–absorption of gamma–ray, coincidence sum effect of cascade gamma–rays.

Strictly speaking, the cross section of the $^{199}Hg(n,p)^{199}Au$ is mixed with the cross section of the $^{200}Hg(n,d)$, (n,pn), (n,np), $^{199}Au(n,pn)$, (n,np) and the cross section of the $^{199}Hg(n,p)^{199}Au$ mixed with the cross section of the $^{199}Hg(n,d)$, (n,np), $(n,pn)^{198}Au$, because our samples were made of natural oxide mercury. A. K. Hankla and R. W. Fink[3] have made the measurement with the enriched Hg sample (83.4% ^{199}Hg) and obtained 2.3± 0.3 mb for $^{199}Hg(n,p)^{199}Au$, 4.5 ± 0.5 mb for $^{198}Hg(n,p)^{199}Au$, 0.4± 0.06 mb for $^{199}Hg(n,d)^{198}Au$ at 14.4 MeV[3]. Our results agree with them within experimental errors.

Up to now, no data have been found for the $^{196}Hg(n,d)$, (n,np), $(n,pn)^{195}Au$ reactions.

References

[1] D. L. Smith et al., ANL / NDM 123, 11(1991)

[2] E. Browne et al., Table of Radioactive Isotopes, 1986

[3] A. K. Hankla et al., Nuclear Physics A 180, 157(1972)

The Differential Elastic Scattering of 14.7 MeV Neutron from Beryllium

Zhang Kun Cao Jianhua Wan Dairong Dai Yunsheng

(Institute of Nuclear Science and Technology, Sichuan University)

A fast neutron associated particle time–of–flight (TOF) spectrometer was used for measuring neutron differential cross sections on beryllium nuclei in this experiment. Source neutrons are detected at 10 angles step between 15 and 135 deg. (laboratory system) in massive shielded ST45 liquid scintillator located at 254 cm from the scattering sample. The relative efficiency curve of neutron detector was determined by measuring the n–P and n–C scattering in polyethylene and graphite respectively.The total error of the differential cross section is from 7.5% to 11.5% including the statistical error 0.5～3.5 and the efficiency calibration error 6～7%.

Introduction

Beryllium can be used as major constituent of controlled fusion reactors because of its unique characteristic of emitting two neutrons for each inelastic neutron interaction. To calculate the tritium breeding rate in proposed reactor vessel walls requires detailed knowledge of the angular distributions of the neutrons emitted from beryllium under the bombarding of the energetic neutrons. For accurate neutron scattering data, it is the important basic work that the elastic scattering cross sections are measured precisely.

1 Experimental Facilities

The neutron source in present experiment was obtained via the $T(d,n)^4He$ reaction with solid tritium–loaded targets cooled by water. A deuteron beam with average energy 250 keV is provided by 400 kV Cockcroft–Walton generator. The emitted neutrons are at angle of 39.82 degrees direction against the incident deuteron beam and the energy is 14.7 MeV, measured by means of an associated particle time–of–flight spectrometer with ST451 liquid scintillator detector of 100 mm in diameter and 50 mm in thickness directly coupled to a

XP–2401 photomultiplier.

The neutron detector was placed in a massive shield which is made from Li_2CO_3, paraffin, Fe and Pb, and set on a turning table. The associated alpha particles are recorded by a plastic scintillator with a thickness of 50 μm coupled to a 56 AVP photomultiplier, and the detector was placed at 135 degrees with the direction of deuteron beam. To check the drift of the primary neutron beam, a small neutron detector is used.

The measurement was completed by using the standard TOF technique. Pulse shape discrimination was used to eliminate the gamma–rays induced events in the scintillators.

The scattering sample, which was machined into the shape of right circular cylinders of 40 mm in diameter and 20 mm in thickness, was set at the place of 254 cm from the neutron detector and 10 cm from target. The TOF information of the scattering neutrons was digitized into about 0.28 ns per channel by time analyzer, which was started by a pulse of neutron from the constant fraction discriminator and stopped by a pulse originated from alpha detector. The data of time spectra were stored in Computer Multi–Channel Analyzer, whose gate signals were got by coincided the fast signals of alpha detector, the slow signals of neutron detector and the pulse–shape discrimination signals.

The efficiency curve of neutron detector was determined by measuring the elastic scattering neutrons from the H(n,n)H reaction with polyethylene sample and C(n,n)C reaction with graphite in the neutron energy range from 0.98 MeV to 14.7 MeV. The measured error of the efficiency is smaller than 7.5% and the statistical error is smaller than 3.5%.

2 Data Processing

The neutron beam was monitored by counting the number of associated alpha particles produced by the $T(d,n)^4He$ reaction and determined by using the n–P scattering cross section at 0 degree as a standard. The scattering samples located at the well–distributed part of the primary neutron beam.

For the time spectra acquired with an associated particle TOF spectrometer, the channel counts on the right of elastic peak are only from accidental coincidence. The average count of these channels is named as average accidental background for the entire time spectra and the effective time spectra are obtained by subtracting the average background from the every channel counts. For the background time–spectrum, there is no difference between the high energy side and the low energy side and their average values are equal.

In the present work, to eliminate the inelastic count of carbon in the

polyethylene time spectra for the efficiency calibration, the graphite and polyethylene samples were measured simultaneously at each angle and the channel counts were normalized in the standard of the elastic scattering peak for the time spectra of graphite.

The measured angular distributions were calculated from the equation

$$\frac{d\sigma}{d\Omega}(\theta,E)=\frac{N(\theta)}{\varepsilon(\theta,E)\,N_{\alpha}\,\Omega\,\gamma\,n} \tag{1}$$

where

$\frac{d\sigma}{d\Omega}(\theta,E)$ = differential cross section for the scattering of neutrons of energy E at laboratory angle θ;

$N(\theta)$ = the count of scattering neutrons at laboratory angle θ;

N_{α} = the monitor count of alpha particles corresponding to the related neutrons;

Ω = solid angle subtended by the detector at sample;

$\varepsilon(\theta,E)$ = efficiency for the neutron detector at energy E;

γ = the thickness of scattering sample;

n = the density of scattering sample.

For getting the final results, the electronics dead time was corrected, and also the anisotropy of the incident neutron flux in scattering sample, the attenuation of the flux, the effects of multiple scattering, and the angular resolution of the detector were taken into account.

3 Experimental Results

The angular distributions of cross section for 14.7 MeV incident neutron scattered to the ground state and first excited state (2.4 MeV) in ^{9}Be were measured at 10 angles step from 15 deg. to 135 deg. in laboratory system. The data were got for each one in 3 or 5 runs, and their consistency was checked. The total error of the differential cross sections is from 7.5% to 11.5%, including the statistical error 0.5～3.5% and the efficiency calibration error 6～7%.

Table 1 Elastic and inelastic (to 12.43 MeV state) differential cross sections of Be(n,n)Be reaction in laboratory system (mb / sr)

θ L (deg)	$\sigma_{n,n}$ (0) (mb / sr)	$\sigma_{n,n'}$ (θ) (mb / sr) (2.43 MeV state)
15	769.388 ± 53.466	31.845 ± 2.427
25	513.971 ± 38.188	29.387 ± 2.333
35	292.426 ± 24.714	21.178 ± 2.059
45	108.840 ± 8.544	16.061 ± 1.285
60	19.884 ± 1.879	18.589 ± 1.739
75	12.458 ± 1.237	15.618 ± 1.518
90	13.567 ± 1.416	12.183 ± 1.302
105	14.074 ± 1.583	7.001 ± 0.678
120	13.137 ± 1.314	7.121 ± 0.658
135	7.440 ± 0.786	4.798 ± 0.446

Table 2 The Legendre coefficient fitting to Be(n,n)Be differential cross sections in CM system

State	σ_0 (mb)	Legendre Coefficients						
		f_0	f_1	f_2	f_3	f_4	f_5	f_6
Elastic	942.38	1.0	0.72271	0.52384	0.32753	0.15587	4.1502×10^{-2}	1.1057×10^{-2}
2.43 MeV state	155.64	1.0	0.24289	2.4115×10^{-2}	2.7800×10^{-2}			

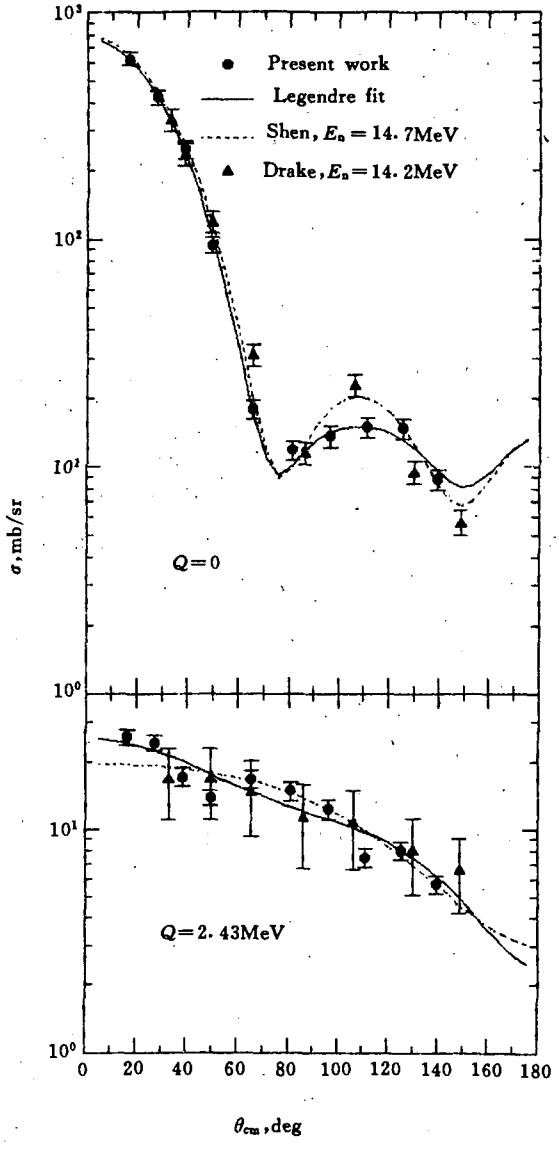

Fig. 1 The beryllium differential elastic and inelastic (2.43 MeV state) neutron cross sections

The scattering differential cross sections and their associated uncertainties are given in Table 1 (laboratory system) and plotted in Fig. 1 (center–of–mass system). The solid line through the experimental points are the results of least–squares fitting of the data with Legendre polynomial expansion in the following form

$$\frac{d\sigma}{dE}\ (\ \theta_{cm}\ ) = \frac{\sigma_o}{4\ \pi} \sum_{l=0}^{L} (\ 2l+1\ )\ f_l\ P_l(\mu)$$

$$\sigma_0 = 2\ \pi \int \frac{d\sigma}{dE}\ (\ \theta_{cm}\ )\ d\mu \qquad (2)$$

$$\mu = \cos\ (\ \theta_{cm}\ ), \qquad -1 \leqslant \mu \leqslant 1$$

Where, σ_0 is the total elastic / inelastic scattering cross section. The polynomial coefficients, expressed in the center–of–mass (CM) system, are illustrated in Table 2. To determine the order L, the two factors were taken into account : the minimization of the reduced χ^2 and no significant change in the zero–order coefficient by inclusion of a high order coefficient. Same previous measurements are compared with present work.

References

[1] D. M. Drake et al., Nucl. Sci. Eng., 63, 401(1977)

[2] Shen Guanren et al., Chinese J. Nucl. Phys., 3, 320(1981)

Progress on Nuclear Data Measurement at STC in 1994

Ye Bangjiao Fan Yangmei Wang Zhongmin

(Department of Modern Physics, University of Science and Technology of China)

1 Developments of System

Some progress has been got for the STC multitelescope system :

1) The energy of detector system was calibrated again by using ^{241}Am α–source. Because energy loss of α–particle in the proportional counters is changed with gas pressure, thus the energy of α–particles received by CsI(T) crystal is different. According to the response curve of CsI(T1) for P and α–particles[1], the energy of system for detecting protons was calibrated and the results was different slightly from that of Ref. [1] at the energy zero–point.

2) The reaction angle function of telescope system was calculated again by using Monte Carlo method[2]. The events of 10^6 was selected in this calculation. A new result which was rather different with that of Ref. [1] was obtained as shown in Fig. 1.

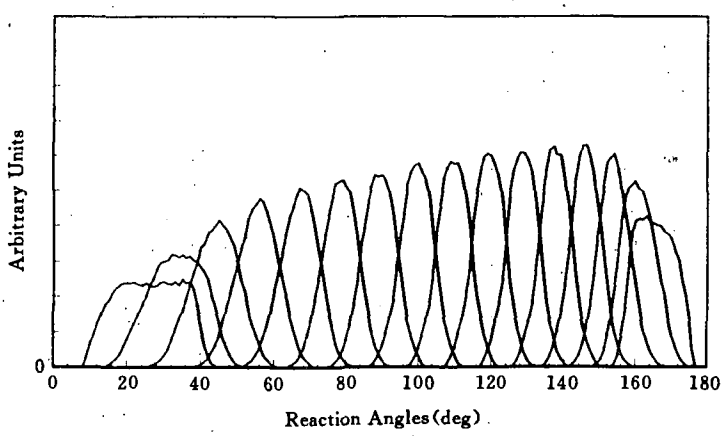

Fig. 1 Reaction angle functions of the multitelescope system

3) The programs for data off-line analysis were further improved. Some programs were revised or rewritten. All programs had been linked.

2 Measurements of ^{Nat}Fe and ^{Nat}Ni(n,xp) Reaction

2.1 ^{Nat}Fe(n,xp) Reaction at E_n = 14.6 MeV

A natural iron target of 0.5 mm thick was used. The whole system was irradiated for about 30 h with a neutron source intensity ~ 1.5×10^9 n / s. The total number of true events turned out to be ~ 170000.

The DDCS of proton emission have been obtained in 16 angle[3]. The angle-integrated proton emission cross sections for ^{Nat}Fe(n,xp) reaction are listed in Table 1. The total proton emission cross section for proton energy > 3 MeV is 170.7 ± 13.7 mb.

Table 1 The angle-integrated proton emission cross sections for ^{Nat}Fe(n,xp) reaction

E_p (MeV)	dσ / dε (mb / MeV)
3~4	33.8 ±3.3
4~5	34.3 ±4.9
5~6	33.9 ±4.2
6~7	24.3 ±3.9
7~8	20.8 ±2.1
8~9	10.9 ±1.6
9~10	7.2 ±1.0
10~11	3.6 ±0.6
11~12	1.2 ±0.5
12~13	0.46±0.2
13~14	0.16±0.07

2.2 ^{Nat}Ni(n,xp) Reaction at E_n = 14.6 MeV

A natural nickel target of 0.5 mm thick was used. The whole system was irradiated for about 40 h at same neutron source intensity as above. The total number of true events turned out to be ~ 450000.

The DDCS of proton emission have also been obtained in 16 angles. The angle-integrated cross sections for ^{Nat}Ni(n,xp) reaction are listed in Table 2.

The total proton emission cross section for proton energy >3 MeV is 612.7 ± 44.8 mb.

Table 2 The angle-integrated proton emission cross sections for ^{Nat}Ni(n,xp) reaction

E_p (MeV)	dσ/dε (mb/MeV)
3~4	142.7± 9.0
4~5	133.9± 11.5
5~6	117.9± 13.8
6~7	84.1± 8.7
7~8	60.1± 8.5
8~9	33.7± 2.8
9~10	20.2± 1.7
10~11	10.3± 1.6
11~12	6.4± 0.8
12~13	2.9± 0.3
13~14	1.1± 0.3

References

[1] Ye Bangjiao et al., CNDP No. 10, 19(1993)

[2] Lin Guan et al., J. of STC, to be published

[3] Ye Bangjiao et al., Nucl. Sci. & Eng., to be published

II THEORETICAL CALCULATION

Progress on Nuclear Reaction Mechanism and Its Application by Theory Group of CNDC

Yan Shiwei

(Chinese Nuclear Data Center, IAE)

1 Nuclear Reaction Mechanism

1.1 The Channel Theory of Fission with Diffusive Dynamics

The neutron Data obtained, by using the 800 MeV pulsed proton beam from LAMPF to produce neutron over a broad energy range (from 100 keV to nearly 800 MeV), show that the results of fission cross section calculated by traditional channel theory of fission calculation are significantly above the experimental data, and provide completely new information about the fission process and a challenge for theorists to develop a model that can describe the behaviors of the fission cross section at the energy above 20 MeV.

In order to understand the fission cross section behaviors at the energy range mentioned above, the pre–equilibrium exciton model, evaporation model and the channel theory of fission with diffusive dynamics have been used to calculate the cross section and spectrum for 3~ 20 MeV and above 20 MeV neutron induced reaction on actinides. The code and the calculations is just on the way. Based on the works above, it is expected that the calculated fission cross sections will be more closed to the experimental data, i. e., the behaviors of the fission cross section at the energy above 15 or 20 MeV could be understood and the systematics research of level density on saddle point with collective enhancement effect for actinide nuclides could be also done by the channel theory of fission with diffusive dynamics.

With the approach mentioned above, the comparison of consistent dynamical and statistical descriptions of fission of hot nuclei is presented and

analyzed.

1.2 The Quantum–Mechanical Preequilibrium Theory

(1) Unified theory of nuclear compound reaction and multistep compound theory

A unified theory formula describing the multistep compound emission of preequilibrium and compound nucleus emission of full equilibrium is presented by using the optical model in the FKK theory.

(2) The FKK theory of Spin 1 / 2 particle

A multistep compound formula with the spin–half particle, a non–zero spin target and the angular momentum coupling treated in j–j representation has been deduced.

(3) Two–component multistep compound theory

The neutrons and protons are distinguished rigorously by isospin in wave function. The formulas of double differential cross–sections, damping and escape width are deduced in this two component theory.

(4) Quasi–quantum model for calculating multistep direct reactions of continuum and discrete levels

In terms of the comparison between the FKK quantum theory and the semiclassical theory, we find that the final equations of the FKK quantum model are very similar to the semiclassical theory. Then, a method for calculating multistep direct reactions both for continuum and discrete levels is proposed. For improving the semiclassical method, the energy–angle correlation scattering kernel is adopted for continuum and discrete levels in the semiclassical approach, in which the angular momentum and parity conservations are considered. Following the FKK quantum MSD theory, the Legendre coefficients of the angular distributions are calculated based on one–step distorted wave Born approximation instead of nucleon–nucleon scattering expressions in nuclear matter. Since the quantum effects are properly considered, we call it as quasiquantum multistep direct (QMSD) theory.

We calculated the reaction p+^{11}B in the energy region of 1~25 MeV with QMSD theory and HF theory. The calculated discrete level neutron angular distributions of $^{11}B(p,n_0)^{11}C$ reaction and the cross sections of $^{11}B(p,n_0)^{11}C$ and $^{11}B(p,n)^{11}C$ reactions reproduce the experimental data reasonably. This approach can also be used to composite particle emissions.

1.3 Intermediate and High Energy Reactions

(1) Averaged analytical forces in intermediate and high energy reactions

By use of the effective Skryme–type potentials, we derived the averaged analytical forces which include the two–body Skryme force, three–body Skryme force, Yukawa force and the Coulomb force. Comparing with the difference method,the application of the analytical forces can raise the calculation speed to 6 times and raise the accuracy significantly.

(2) Light particle emissions in fission diffusion process and the nuclear friction coefficient

In order to include the emissions of other light particles (such as proton, α, ···) into the fission diffusion process, we give out the extensive Smoluchowski equation with the inclusion of these light particle emissions. We also showed the formulas for the multiplicities of these particles, with them the comparisons to experimental data can be made and the nuclear friction coefficient can be extracted.

1.4 The Maximum Entropy Method of Analysis

The maximum entropy method of analysis is successful in fitting experimental data. In order to reveal the underlying physics, we apply both the method and the conventional approach, i. e the exciton model plus the master equation, to three cases. We have found that both approaches produce almost equally good fits to spectra, and yield almost the same average exciton numbers. This implies that there must be similar physics ideas behind the two approaches, and it should be safe to use the maximum entropy method of analysis to fit data or to estimate reaction cross sections.

2 Chinese Evaluated Nuclear Parameter Library (CENPL)

A great progress was made on setting up the CENPL and studying of the relative model parameters in 1994. Three sub–libraries (the first edition), the atomic masses and characteristic constants of nuclear ground states, giant dipole resonance parameters for gamma–ray strength function and fission barrier parameters, have all been finished. The management–retrieval code systems have retrieved a large amount of required data for many users from different research fields.

The data file of the sub–library of the discrete level schemes and gamma radiation branching ratios has been set up, which is translated from the Evaluated Nuclear Structure Data File.

The sub–library of nuclear level density includes two data files : the data

file relative to level density and the data file of the level density parameters (LDP). D_0 and S_0 values come from the data recommended by CNDC in 1993. The LDP file contains eight sets of density parameters for three popular level density formulas which are the four–parameter formula, the back–shifted Fermi gas formula, the generalized superfluid model.

The data file of optical model parameter sub–library includes two parts : the global and regional optical model parameters and nucleus–specific ones. The first part has had specific scope, and another has appeared in an embryonic form.

By fitting the D_0 and N_0 values recommended by CNDC, we got a set of the level density parameters for the generalized superfluid model for 249 nuclides ranging from ^{41}Ca to ^{250}Cf. And comparison of the different level density formulas in low–lying region has been made.

The giant dipole resonance parameters (GDRP) have been extracted for more nuclides with $A < 50$ by fitting the photo–nuclear cross sections and the systematics of the GDRP will be developed.

3 The Nuclear Data Calculation

3.1 Calculation of Angular Distribution with Two–component Exciton Model

Two–component exciton model is presently used to describe the pre–equilibrium emission of compound system instead of normal exciton model. The calculated double differential cross sections are much lower than the experimental data at backward angles. In order to improve the agreement between the calculated results and experimental data, the Fermi motion and Pauli principle are taken into account in two–component exciton model. We take n+^{93}Nb with $E_n = 14.1$ MeV as an example to calculate double differential cross section. A fairly good results are obtained.

3.2 ^{235}U, ^{239,240}Pu Neutron Induced Reaction in $E_n = 0.001 \sim 20$ MeV

For the ^{235}U, ^{239,240}Pu neutron induced reaction in the energy region of $0.001 \sim 20$ MeV, the total cross section ,the cross section of each opened channels, the elastic / inelastic scattering angular distribution and the secondary neutron energy spectra are calculated by using the optical model, Hauser–Feshbach statistical theory with width fluctuation correction and the evaporation model including the preequilibrium statistical theory based on the exciton model. The calculated results show that the calculated results reproduce

the experimental data very well.

3.3 Neutron Monitor Reaction of $^{63, 65, Nat}Cu(n,x)^{56, 57, 58, 60}Co$ in Energy Region up to 70 MeV

The activation isotopes ^{56}Co, ^{57}Co, ^{58}Co, and ^{60}Co can be produced in $n+^{63, 65, Nat}Cu$ reactions. For $n+^{63}Cu$ reaction, ^{60}Co can be produced through (n,α), (n,2n2p), (n,npd), (n,2d), (n,n^3He), and (n,pt) reactions, ^{58}Co, ^{57}Co, and ^{56}Co through more reaction channels especially in higher energy region. $^{56, 57, 58, 60}Co$ can also be produced through $n+^{65}Cu$ reaction, but more complicated reaction channels are needed.

Based on various experimental data of $n+^{63, 65}Cu$ reactions from EXFOR library a set of optimum neutron optical potential parameters in energy region 2 ~ 80 MeV was obtained. The Gilbert–Cameron level density formula is applied in the calculations, and the exciton model constant K is taken as 1800 MeV^3. Because the calculated results for many channels are in pretty agreement with the existed experimental data, the predicted production cross sections of the activation isotopes mentioned above are reasonable.

3.4 Intensity and Spectra of Neutron Source Produced by 70 MeV Proton Accelerator

The intensive beam proton cyclotron is adopted in Beijing Radioactive Nuclear Beam Facility designed by China Institute of Atomic Energy. The design target of this facility is that the proton maximum energy is 70 MeV and the intensity is 200 μA. The white light neutron source can be obtained if the thick target is bombarded by this kind of proton beam.

The calculated results show that the reactions occur for 5.7% incident 70 MeV protons before stopping in W thick target. The total neutron intensity produced by 70 MeV and 200 μA proton beam is 1.26×10^{14} n / s. The average neutron energy is 4.2 MeV. The neutron intensity above 10 MeV is 1.43×10^{13} n / s, for which most of them are emitted in small angle region. This kind of white light neutron source is very useful in practice.

3.5 Proton Produced Medical Radioisotope ^{186}Re on Accelerator Cyclone–30

The radioisotope ^{186}Re (half life is $T_{1/2}$ = 3.777 d) is a kind of useful medical radioisotope. It can be produced by proton accelerator through $^{186}W(p,n)^{186}Re$ reaction. So far no experimental data can be found for

this reaction. The yield and radioactivity of proton produced medical radioisotope ^{186}Re on accelerator Cyclone–30 are calculated and predicted. The calculated results show that it is better to chose the proton energies at 15~18 MeV and the irradiating time less than $T_{1/2}$ = 3.777 d. If the proton energy is 18 MeV and the beam intensity is 350 μA, the radioactivities of the producing ^{186}Re are 2.65 and 4.86 Ci for irradiating time 24 and 48 hours, respectively. Therefore one can say that it is an effective method for producing medical radioisotope ^{186}Re.

3.6 Analyses of p+^{11}B, p+^{11}C, and d+^{11}C Reactions

Aiming at the production of ^{11}C radioactive beam, the various nuclear data of p+^{11}B reaction at incident proton energies spanning 1~25 MeV were calculated with quasiquantum multistep direct (QMSD) theory and Hauser–Feshbach (HF) theory. The calculations basically agree with the experimental data. The angular distributions in lab. frame of ^{11}C produced in the reversed geometry reaction ^{1}H(^{11}B,^{11}C)n were deduced. The cross sections of p+^{11}C and d+^{11}C reactions induced by ^{11}C beam were also predicted. The calculated results show that the experimental measurement to ^{11}C+d reaction is more feasible than ^{11}C+p reaction at HI–13 tandem accelerator.

Progress on Calculations of Nuclear Data at Tsinghua University

Chen Zhenpeng

(Dept. of Phys., Tsinghua University, Beijing)

1 Calculating Cross Sections of Direct Inelastic Scattering Neutron from Ni

The code UNF[1] of Chinese Nuclear Data Center is able to calculate the complete neutron data. In the calculation, the direct inelastic scattering (D. I. S.) cross sections of neutron is input as input data with the format of Legendre Coefficient (L. C.). Nowadays, an effective way for calculating direct inelastic

data is the coupled–channel optical model (CCOM).

The code ECIS88[2] is used, in which some necessary modifications have been done to run it in our VAX – computer, and a new subroutine is programmed to obtain and output L. C. simulataneously. So it's more convenient in the evaluation of the nuclear data. The maximum term of the Legendre polynomials is determined by the code. The output format is :

$$\sigma_{nn'}(E) \qquad A_0 \text{ to } A_{10}$$

The relative formula[3] for calculating differential scattering cross section is :

$$d\sigma(\theta,E) / d\Omega = \sigma_{nn'}(E) / 2\pi \sum_{l=0}^{10} (2l+1) / 2 \; A_l(E) \; P_l(\theta) \qquad (1)$$

Here, $\sigma_{nn'}(E)$ is the integrated cross section of D. I. S., $A_0 \equiv 1$.

We have finished the calculations of D. L. S. for 5 isotopes of Ni. The even–even nuclei of Ni show fairly clear vibrational spectra, so for ^{58}Ni, ^{60}Ni, ^{62}Ni and ^{64}Ni, the harmonic vibrational model is used, but for ^{61}Ni a better way is to use symmetric rotational model approximation. The selected coupled–levels are taken form Ref. [4], they are listed in Table 1.

Table 1 The coupled–levels of $^{58, 60, 61, 62, 64}$Ni

Element	Spin, parity and energy (MeV) of levels				
	Ground	1st level	2nd level	3rd level	4th level
^{58}Ni	0^+ (0.6)	2^+ (1.4545)	4^+ (2.4591)		
^{60}Ni	0^+ (0.0)	2^+ (1.3325)	2^+ (2.1586)	0^+ (2.2849)	4^+ (2.5058)
^{61}Ni	$\frac{3^-}{2}$ (0.0)	$\frac{5^-}{2}$ (0.0624)	$\frac{1^-}{2}$ (0.2830)	$\frac{3^-}{2}$ (0.6672)	$\frac{1^-}{2}$ (0.6672)
^{62}Ni	0^+ (0.0)	2^+ (1.1729)	0^+ (2.0486)	2^+ (2.3018)	4^+ (2.3364)
^{64}Ni	0^+ (0.0)	2^+ (1.3458)	0^+ (2.3163)	2^+ (2.3163)	4^+ (2.6528)

In the calculations, the spherical optical model parameters are used with some modifications on them. These parameters were obtained by fitting the experimental data ranging from 10 keV to 20 MeV. The geometrical parameters are constant. The depths of optical potentials change with energy of incident neutron E_n(lab), mass number A, charge number Z. They are given as follows[5] :

Geometries (fm) : $R_r = R_{so} = 1.1764$, $R_s = R_v = 1.3191$

$a_r = a_{so} = 0.7284$, $A_s = A_v = 0.4110$

Well Depths (MeV) :

$V_r(E_n)=54.103-0.1183E_n-0.0141E_n^2+17.5894\ (\ A-2\ Z\ )/A$

$W_v(E_n)=-1.7484E_n+0.253E_n$

$W_s(E_n)=12.0-0.1545E_n-1.2687E_n^2$

$V_{s0}(E_n)=3.1$

In the coupled-channel calculations the depth of imaginary potential W_s is decreased by a factor of 0.70 to 0.74 (see next section). There are a lot of research work about the deformed parameter of Ni[6] we take photon amplitude $\beta=0.22\pm0.01$ in these calculations.

2 Research on Using Parameters of SOM in Calculation of CCOM

There are a lot of optical model parameters for deformed nuclei, which in fact were got from spherical nuclei approximation (SOM), therefore it is very difficult to search a optimum optical model parameters for a deformed nucleus by using the coupled channel optical model (CCOM).

When we make exact calculation of CCOM for a deformed nucleus for which there are no deformed optical model parameters, an effective way is to use the optical model parameters of SOM of it as primary values, most of them keep originally values, but the few have to be changed to a certain.

A systematics research for some medium heavy nuclei, for example Lu, Hg, Tl and ^{238}U has been done with CCOM code ECIS88[2]. It shows that the depths of imaginary potential and the radii of real potential are the most sensitive. The range of change is different for the different deformed parameter β_2. For β_2 from 0.1 to 0.25, the depths of imaginary potential must be decreased by 25 to 35 percent, the radius of real potential must be increased by 1 to 3 percent.

The criterion for changed range is that the calculated total cross section and elastic differential scattering cross section of CCOM are agreement with the values of SOM.

In calculation of harmonic vibrational model with CCOM, the depths of imaginary potential must be decreased too. Because the imaginary parts of SOM include the contribution of direct inelastic scattering, but in CCOM this contribution is excluded from W_s and W_v, so the W_s and / or W_v used in CCOM must be decreased.

3 The Reduced R-matrix Analysis of n+^{16}O Between 6.2 and 10.5 MeV

The R–matrix analysis on n+^{16}O for $E_n < 6.2$ MeV has been finished in Ref. [7]. Two channels (n,^{16}O) and (α_0,^{13}C) only were considered in that work. When $E_n > 6.2$ MeV, some other channels give out rather large contribution. As a further development of Ref. [7] to higher energies, the reduced R–matrix code RAC92[8] is employed to analyze the data of n+^{16}O for $E_n = 6.2$ to 10.5 MeV. The Lane and Thomas[9] formula were adopted in RAC92, in which

$$R_{c'c} = \sum_{\lambda\lambda'} \gamma_{\lambda c'} \gamma_{\lambda' c} A_{\lambda\lambda'} \tag{2}$$

$$[A^{-1}]_{\lambda\lambda'} = (E_\lambda - S (E_\lambda) - E) \delta_{\lambda\lambda'} - \frac{1}{2} \Gamma_{\lambda\lambda'} \tag{3}$$

Where c and c′ are the channels, $R_{c'c}$ is the reduced R–matrix element, γ is the reduced amplitude of residual channel, $A_{\lambda\lambda}$ is the level–matrix element, E_λ is the position of level, $\Gamma_{\lambda\lambda'}$ is the total reduced width of all eliminated channels. In this work n+^{16}O and α_0+^{13}C are taken as residual channels, other channels is represented by one channel–eliminated channel, the relative parameter is $\Gamma_{\lambda\lambda'}$.

The used experimental data are σ_{tot} of Cierjack et al.[10], the elastic scattering differential cross sections of Schrack[11] Kiney[12], Glendnning[13] and Borker[14]; $\sigma_{n\alpha_0}$ of Bair et al.[15], which is renormalized with factor 1.7 to match Ref. [7]. The details of relative data and channel configuration are listed in Table 2.

Table 2 The channel configuration and relative data

order	channel	radius (fm)	l_{max}
1	n+^{16}O	4.4326	4
2	α_0+^{13}C	6.1639	4
3	reduced	no	no
Reaction	E_n (MeV)	Type	Points
^{16}O(n,n)^{16}O	6.2 to 9.8	$d\sigma_{nn}/d\Omega$	320
n+^{16}O	6.2 to 10.5	σ_{tot}	280
^{16}O(n,α_0)^{13}C	6.2 to 8.8	$\sigma_{n\alpha_0}$	156
Total		3	756

In this analysis 84 levels are involved. For $0 < E_\lambda < 5.8$ MeV, there are 31 levels, which were taken from Ref. [7] and the parameters of them were fixed. There are 11 distant background levels with fixed positions E_λ. So about 90

parameters were adjusted to fit the experimental data. Fig. 1 shows that the agreement between the calculated values and the experimental data for σ_{tot} and $\sigma_{n\alpha_0}$ is very good. The results for fitting $d\sigma_{nn}/d\Omega$ are good too.

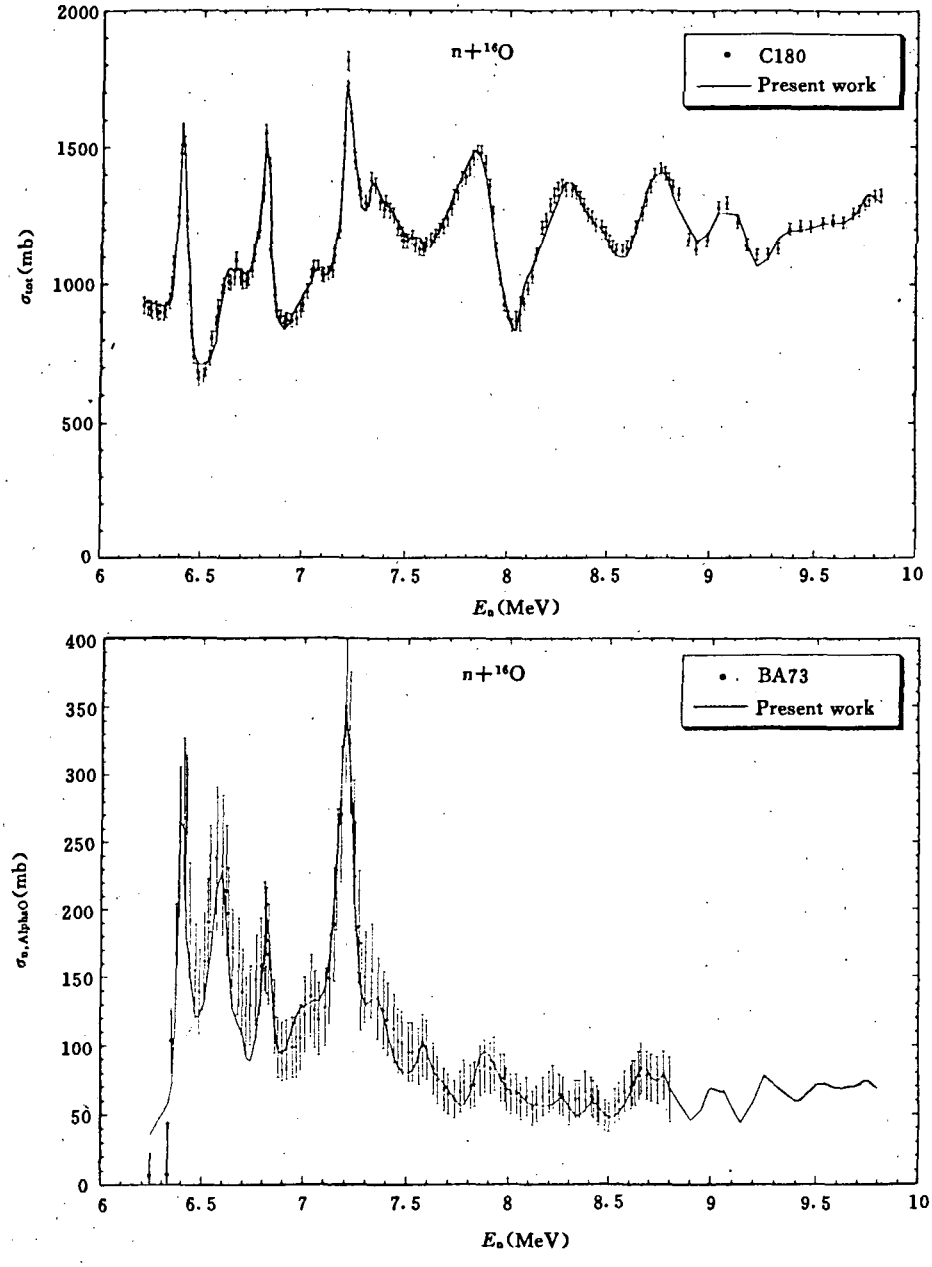

Fig. 1 Total cross section (upper) and (n,α) cross section (down)

References

[1] Zhang Jingshang, CNDP, No. 7, 14(1992)
[2] J. Raynal, ECIS88, ENA 0850
[3] P. F. Rose et al., ENDF / B–6 format manual 4.3 (1986)
[4] L. K. Peker, NDS Vol. 61, 189(1990)
[5] Ma Gonggui, Private Communication, Sichuan University, (1993)
[6] P. O. Guss et al., Nucl. Phys. A 438, 187(1985)
[7] G. M. Hale et al., summary report on at ^{16}O in ENDF / B–6, (1990)
[8] Z. P. Chen, comment of R–matrix code RAC92, (1992)
[9] A. M. Lane et al., Thomas, Rev. Mod. Phys., 30 257(1958)
[10] S. Cierjack et al., Nucl. Meth. 169, 185(1980)
[11] R. Schrack, BAPS 17, (1972)
[12] W. E. Kiney, Perey, F. G., ORNL–4780 (1972)
[13] S. Glendinning et al., Nucl. Sci. Eng., 82, 393(1982)
[14] B. Borker et al., PTB–N–1 (1989)
[15] J. K. Bair, Haas, F. X., Phys. Rev. C7, 1356(1973)

Progress in FKK Multistep Compound Reaction Theory

Li Baoxian Su Zongdi

(Chinese Nuclear Data Center, IAE)

The three refinements to the FKK multistep compound reaction (MSC) theory are given as described below.

1 Angular Momentum in MSC Theory

The original FKK theory[1] treaded the incident nucleons as being spinless and assumed that the target nucleus spin is zero, so the double–differential cross section formula and the transition matrix elements are given in the l–s coupling. In present work, the angular momentum coupling factors are deduced in both the transition matrix element and the geometrical coefficient in the differential cross section formula, when the incident nucleon is treated as a

spin–half particle, the target nucleus has its real spin and the angular momentum coupling is treated rigorously. Thus a multistep compound formalism with the spin–half incident particle and the angular momentum coupling treated in j–j representation has been deduced.

2 Entrance Strength Function and r–Stage

Firstly, the entrance strength function can be obtained in a consistent way with the optical model (OM) by equating it to the OM transmission coefficients. Secondly the escape widths of the equilibrium emission in the r–stage can be evaluated by the OM transmission coefficients. A unified theory formula described the multistep compound emission of preequilibrium and compound nucleus emission of full equilibrium is presented.

The entrance strength function of primitive formula[1, 2] can be replaced by OM transmission coefficients as the formation factor of a compound system. Thus, the results of MSC theory are consistent with OM and are restricted by OM if the direct reaction can be neglected.

When full equilibrium in the r–stage has been established, the detailed balance principle is justifiable, the escape width and total width can be evaluated by the transmission coefficient of OM in the r–stage too.

In view of the refinements mentioned above, a unified formula for the MSC of pre–equilibrium emission and compound nucleus emission of full equilibrium is presented in the representation j–j coupling. The emission description of the equilibrium system is fully consistent with the Hauser–Feshbach theory if pre–equilibrium emission is neglected.

3 Two–Component MSC Theory

In the present work, the neutrons and protons are distinguished rigorously by isospin in wave function. Because the two–body residual interacting is of zero–range and the wave–function of compound system must be antisymmetry, if the nucleon spin is 1 / 2 and the neutrons and protons are not distinguishable, the total spin of the system of interacting two nucleons must be zero. If the neutrons and protons are distinguishable, then the total spin of the system can be zero or one, so the interaction matrix elements[3] become more complicated. The formulas of double differential cross–section, damping and escape width are deduced in the two component theory.

The two–component theory leading to (n,n) emission cross section is enhanced and (n,p) reaction cross section becoming smaller. The explanation is

presented for $Vt = 1.6$ Vs in phenomenological potential[4] from the interaction matrix elements. In order to satisfy the experimental results of (n,n) and (n,p) reaction, R parameter[5] (2.89) which is the rate of n–p and n–n residual interaction strength was phenomenologically introduced in the exciton model of the two–component theory. The average R parameter is 2.75 from calculation without any phenomenological parameter in present work.

References

[1] H. Feshbach et al., Ann. Phys. 125, 492(1980)

[2] R. Bonetti et al., Phys. Rep. 202 No. 4, 171～231(1991)

[3] Li BaoXian, Master's thesis CIAE. (1994)

[4] Hu Jimin " Nuclear Theory " 56, No. 1

[5] G. Reffo et al., Beijing International Symposium on " Fast Neutron Physics ", 9～13 Sep., 155(1991)

Sensitivities of Optical–Model Parameters

Liu Tong Zhao Zhixiang Shen Qingbiao

(Chinese Nuclear Data Center, IAE)

Abstract

Sensitivities of the neutron total, nonelastic cross section, and the angular distribution for elastic scattering to nine Optical–Model Parameters (OMP) — the depths, radii and diffuseness for real, imaginary surface and imaginary volume absorption potential have been studied. The results for targets ^{51}V, ^{54}Fe, ^{63}Cu and ^{85}Rb are given. The code APOM94 — a new version of code APOM[1] has been involved in this work.

Introduction

The sensitivities of nuclear model parameters is useful to generate the uncertainty of quantities calculated through nuclear model, for example, the sensitivities of OMP can be used to estimate the uncertainties of elastic angular distribution. Recently, the sensitivities of calculated cross section of ^{56}Fe to model parameters have been studied by K. Shibata[2]. In this paper, the relationship of the sensitivities dependence on the mass of target are shown and the sensitivities to elastic angular distribution are presented.

1 Optical–Model Parameters

A processing code system for searching the optimal optical model parameters has been developed in CNDC[3]. The optimal optical model parameters for three nuclei ^{63}Cu, ^{51}V and ^{85}Rb have been adjusted by using this system. The parameters of ^{54}Fe are taken as same as those for ^{56}Fe which has been obtained in Ref. [4]. The Woods–Saxon optical potential shape is used[4]. The optical potential parameters for neutron (the optical model parameters for charged particle are same with those for ^{56}Fe[4]) are presented in Table 1.

Table 1 The optimal optical-model parameters for neutron

Parameter	^{54}Fe	^{63}Cu	^{51}V	^{85}Rb
A_R, fm	0.6071	0.6570	0.7528	0.7037
A_S, fm	0.4818	0.3613	0.5531	0.5638
A_V, fm	0.7587	0.6216	0.3718	0.3954
A_{SO}, fm	0.6072	0.6840	0.6840	0.6840
R_R, fm	1.1895	1.1799	1.1411	1.1810
R_S, fm	1.2564	1.3904	1.2855	1.2932
R_V, fm	1.2823	1.1423	1.4009	1.4848
R_{SO}, fm	1.1895	1.2057	1.20569	1.20569
R_C, fm	1.2500	1.2500	1.2500	1.2500
U_0, MeV	−1.0236	−1.1416	−1.5080	−2.3521
U_1, MeV	0.172	0.2107	0.1902	0.2226
U_2, MeV	0.0016	−0.0006	0.0006	0.0051
V_0, MeV	56.8317	52.4389	54.3022	53.729
V_1, MeV	−0.5072	−0.1790	−0.2982	−0.2952
V_2, MeV	0.0024	−0.0006	−0.0001	0.0074
V_3, MeV	−24.000	−24.000	−24.000	−24.000
V_4, MeV	0.0000	0.0000	0.0000	0.0000
V_{SO}, MeV	6.2000	6.2000	6.2000	6.2000
W_0, MeV	12.0235	14.3009	9.7678	11.9804
W_1, MeV	−0.2940	−0.1639	−0.3067	−0.4408
W_2, MeV	−12.000	−12.000	−12.000	−12.000

2 The Sensitivities of Optical-Model Parameters

The sensitivities of model parameters are defined as follows :

$$S(p) = \frac{\partial f(p)}{f(p)\ \partial p}$$

where p is the OMP and $f(p)$ is the physical quantities to be calculated.

Nine model parameters are studied and the pictures are plotted. Figs. 1～4 show the sensitivities of total cross section and nonelastic cross section to optical–model parameters. The sensitivities for angular distribution of elastic scattering are shown in Figs. 5～6.

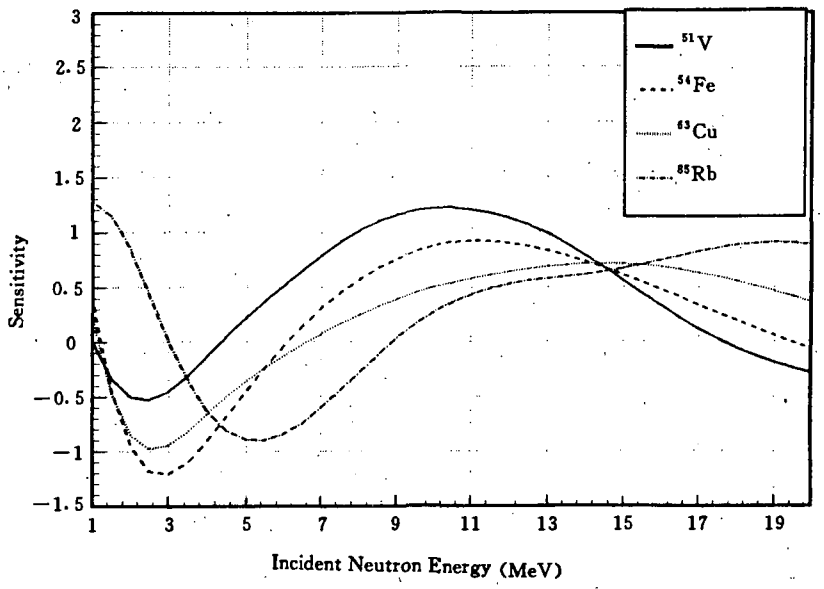

Fig. 1 Sensitivity of total cross section to real depth

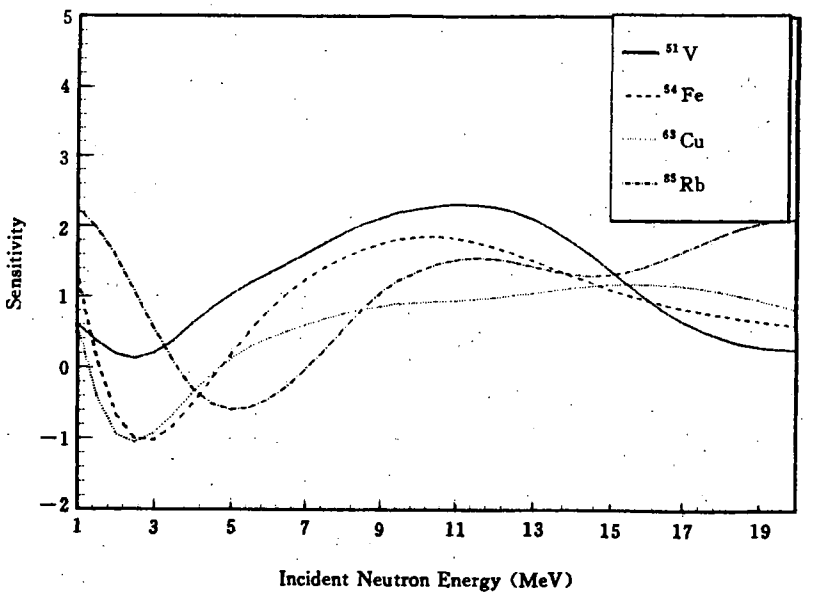

Fig. 2 Sensitivity of total cross section to real radius

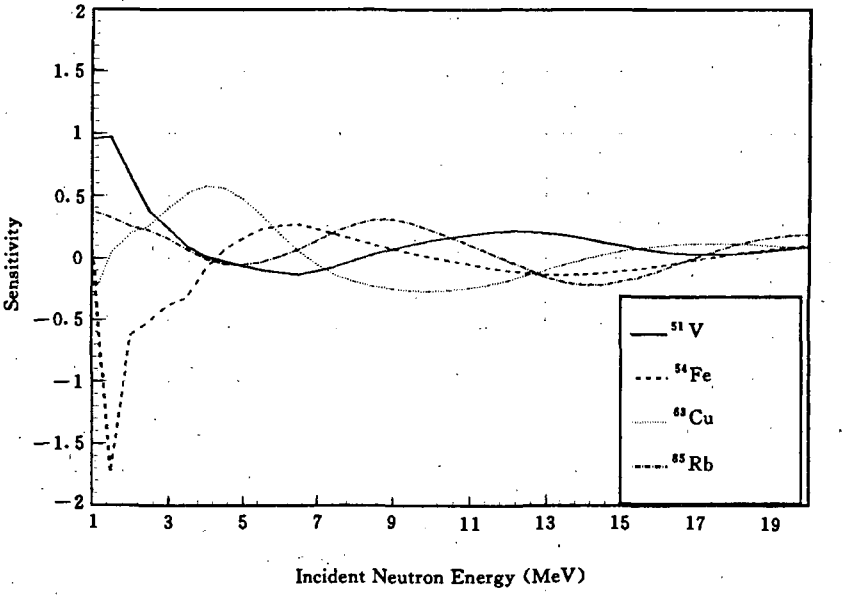

Fig. 3 Sensitivity of nonelastic cross section to real depth

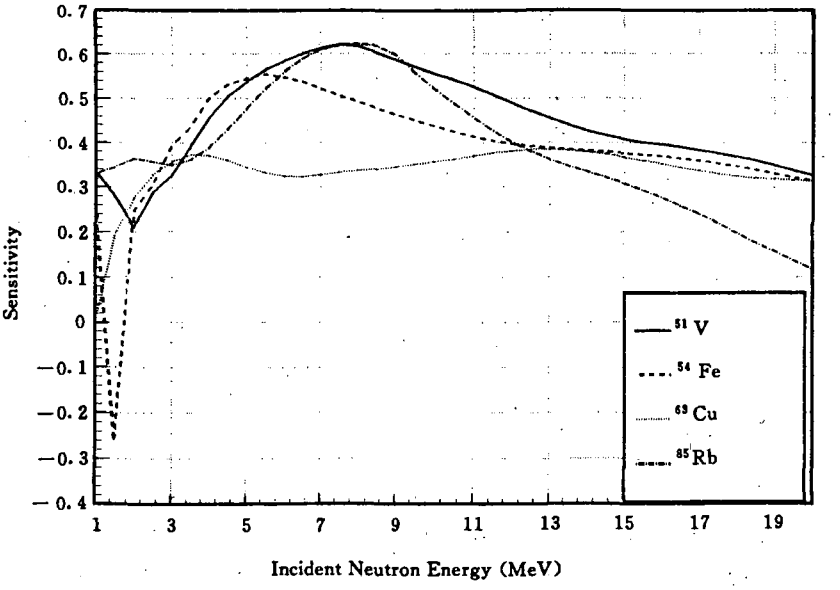

Fig. 4 Sensitivity of nonelastic cross section to imaginary surface absorption diffuseness

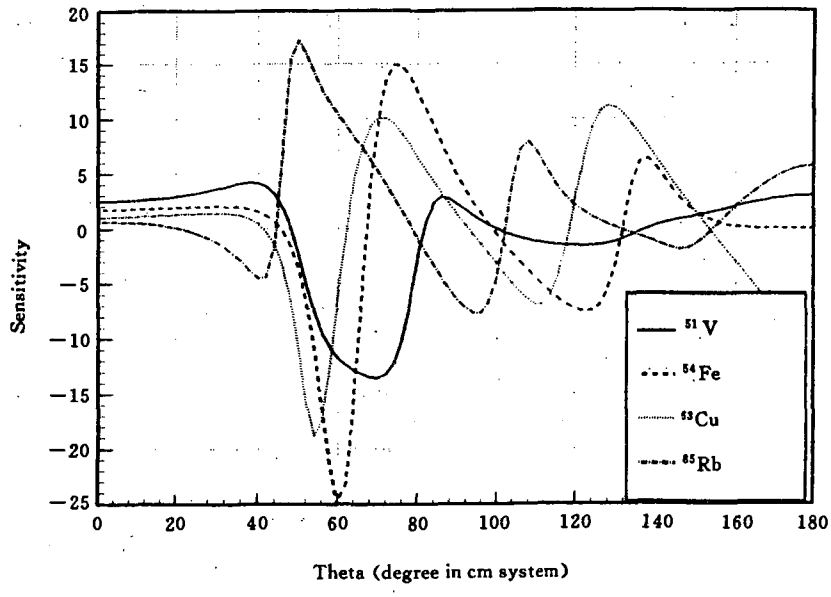

Fig. 5 Sensitivity of the angular distribution of elastic scattering to real depth at the incident energy 10 MeV

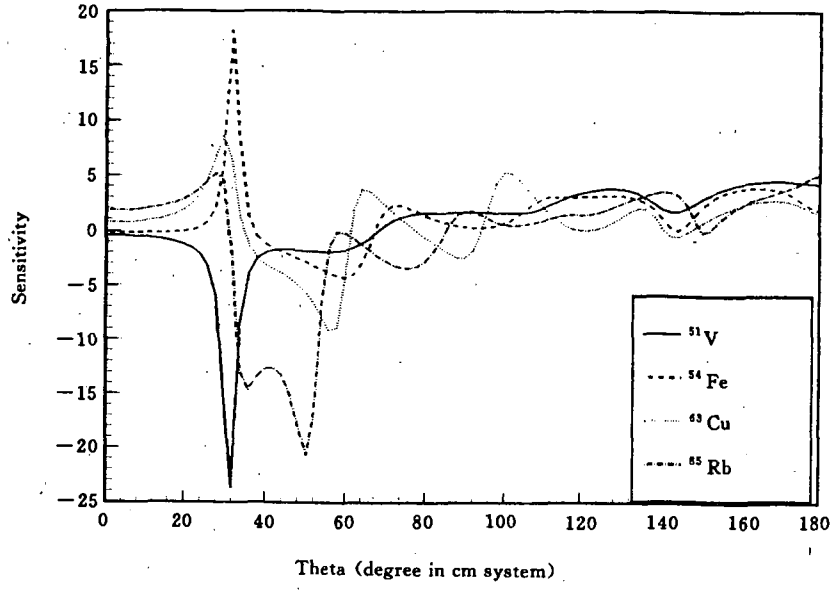

Fig. 6 Sensitivity of the angular distribution of elastic scattering to real depth at the incident energy 20 MeV

3 Conclusion

It is found from the figures that the sensitivities to the diffuseness parameters are smaller than those to other parameters.

The sensitivities of total cross section, nonelastic cross section and the angular distribution have the similar behaviors among different masses of targets.

Acknowledgement

The authors would like to give their thanks to " The Science Foundation for Young Scientist of CIAE " for its support to this work.

References

[1] Shen Qingbiao, " APOM — A Code for Searching Optimal Neutron Optical Potential Parameters ", CNDP, No. 7, p. 43, 1992

[2] K. Shibata, " Sensitivities of Calculated Cross Section of ^{56}Fe to Model Parameters ", OCED / GD(94)21

[3] Liu Tong et al., " A Processing Code System AUTOOPT Searching for Optimal Neutron Optical Potential Parameters ", CNDP, No. 12, p. 35. 1994

[4] Zhao Zhixiang et al., " Evaluation of Neutron Induced Data on ^{56}Fe ", CNDP, No. 11, p. 72, 1994

Prediction of the Cross Sections of p+^{11}C and d+^{11}C Reactions for Energy up to 25 MeV

Shen Qingbiao Zhang Jingshang Han Yinlu

(Chinese Nuclear Data Center, IAE)

Abstract

^{11}C (half time is 20.3 min) is a proton–rich radioactive nucleus. The cross sections of p+^{11}C and d+^{11}C reactions were predicted in energy region up to 25 MeV. From the calculated results one can see some features of nuclear reactions of proton–rich radioactive nuclei. The calculated results also show that the experimental measurement to ^{11}C+d reaction is more feasible than to ^{11}C+p reaction at HI–13 tandem accelerator.

Introduction

The production and use of unstable, radioactive nuclear ion beams is of considerable interest. The radioactive nuclear ion beams provide a new opportunity for studying nuclear phenomena in a wider field. The nuclear data of the secondary radioactive beam induced reactions are of fundamental importance for astrophysical studies and some nuclear engineering designs. Many laboratories have made a lot of efforts in producing the secondary radioactive beams for nuclear physics research[1]. Recently, some reactions in reversed geometries were proposed for producing the kinematically compressed beams of ions[2] and ^{11}C, ^{17}F secondary beams have been successfully tuned with China's first radioactive nuclear beam line at HI–13 tandem accelerator in CIAE[3]. A ^{11}C beam was produced with intensity 1.2×10^{5} particles per second and energy 41 ± 1.0 MeV through the reaction ^{1}H(^{11}B,^{11}C)n at the incident ^{11}B energy 66.12 MeV. One of the most important purposes for producing radioactive beam is to measure the nuclear data of the unstable, radioactive nuclei. The theoretical predictions of the nuclear data for secondary reactions have important reference value to experiment scientists.

1 Theory Codes and Parameters

The calculations were made with quasiquantum multistep direct (QMSD) theory and Hauser–Feshbach (HF) theory[4]. The charged particle induced reaction code CUNF[5], the searching optimal charged particle optical potential parameter code APCOM[6], the direct (n,p) and (p,n) knock–out reaction code KORP[7], and the distorted wave Born approximation code DWUCK4[8] were used in the calculations.

Based on the experimental reaction cross sections of p+^{11}B and p+^{9}Be[9], a set of optimum proton optical potential parameters up to 40 MeV was obtained with the code APCOM[6] and is given as follows :

$$V = 53.9591 - 0.3194E - 0.0004943E^2 + 24.0\ (N-Z)/A + 0.4Z/A^{1/3} \quad (1)$$

$$W_S = \max\ \{\ 0.0,\ 16.99 - 0.05824E + 12.0\ (N-Z)/A\ \} \quad (2)$$

$$W_V = \max\ \{\ 0.0,\ -2.7085 + 0.3085E - 0.006505E^2\ \} \quad (3)$$

$$U_{SO} = 6.2 \quad (4)$$

$$r_r = 1.2191,\ r_S = 1.1153,\ r_V = 1.0281,\ r_{SO} = 1.25,\ r_C = 1.5 \quad (5)$$

$$a_r = 0.6368,\ a_S = 0.3102 + 0.7(N-Z)/A,$$
$$a_V = 0.7871 + 0.7\ (N-Z)/A,\ a_{SO} = 0.55 \quad (6)$$

The calculated reaction cross sections of p+^{11}B and p+^{9}Be reactions up to 40 MeV with this set of optical potential parameters are shown in Fig. 1, which fit the experimental data very well.

The deuteron optical potential parameters were taken from Ref. [10]. The universal parameters of the other particle optical potential and level density were taken, or less changes were made for them. The exciton model constant was adopted to be $K = 300$ MeV^3 in the calculations.

2 Calculated Results and Discussion

The measurement of the secondary reaction induced by the radioactive ^{11}C is especially payed attention to. Fig. 2 shows the various calculated cross sections of the reaction p+^{11}C in the incident proton energy region 5~ 25 MeV. When incident proton energy < 9.5 MeV (corresponding incident ^{11}C energy < 103.8 MeV, this energy is too high for HI–13 tandem accelerator) only (p,p′) channel is open. When incident proton energy > 9.5 MeV, the main reac-

tion channels are (p,p′) and (p,2p). Above calculated results are easier to be understood because the target ^{11}C is proton–rich nucleus and it is also bombed by a proton. The threshold of the (p,n) channel is 16.4 MeV. Since the proton binding energy in ^{11}N formed through (p,n) channel is negative, the proton would be emitted immediately and the real (p,n) channel does not exist.

Fig. 3 shows the various calculated cross sections of the reaction d+^{11}C in the incident proton energy region 1～ 25 MeV. Since the target ^{11}C is a proton–rich nucleus, the cross sections of the (d,p) and (d,2p) channels are larger than others in the most part of the energy region. When the incident deuteron energy < 12.5 MeV (corresponding to the incident ^{11}C energy < 68.3 MeV), the reaction channels (d,p), (d,2p), (d,α), (d,np), (d,n), (d,d′), and (d,^{3}He) are all open. The ions ^{12}C, ^{11}B, ^9B, ^{11}C, ^{12}N, and ^{10}B may be detected in order to measure some nuclear data of the reaction d+^{11}C. Fig. 4 shows the calculated (d,n), (d,n_0), and (d,n_c) cross sections of the reaction $^{11}C(d,n)^{12}N$. It can be seen clearly that basically the (d,n) cross sections are all contributed by the channel (d,n_0). It is because if the residual nucleus ^{12}N stays at the first and higher excitation states the proton may be emitted from ^{12}N continuously.

From above calculated results one can see some features of nuclear reactions of proton–rich radioactive nuclei. The calculated results also show that the experimental measurement to ^{11}C+d reaction is more feasible than to ^{11}C+p reaction at HI–13 tandem accelerator as the limitation of the accelerator energy. These theoretical results have important reference value to experiment scientists.

The authors would like to thank Prof. Bai Xixiang for helpful discussions and suggestions.

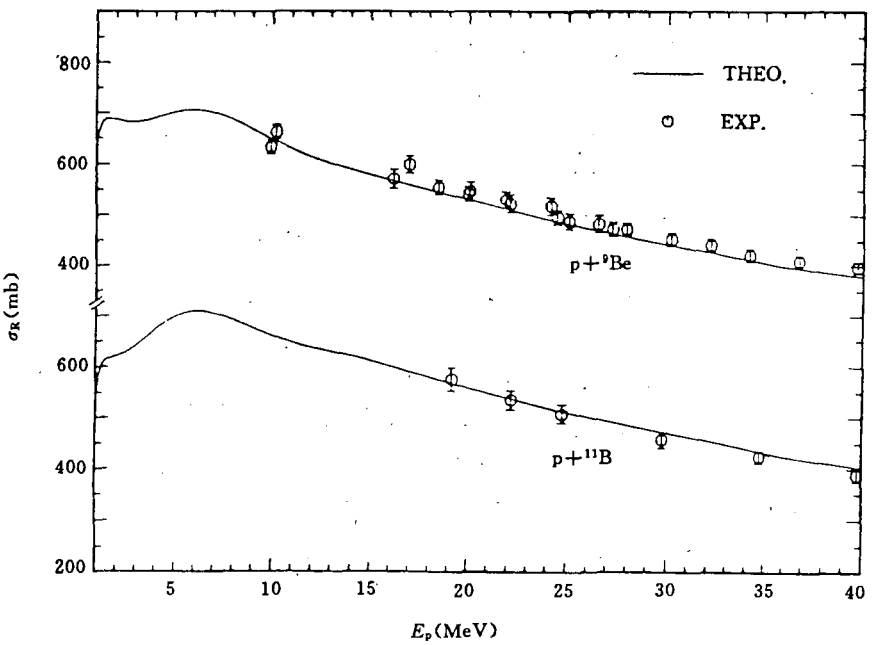

Fig. 1 The comparison of the p+^{11}B and p+^{9}Be reaction cross sections

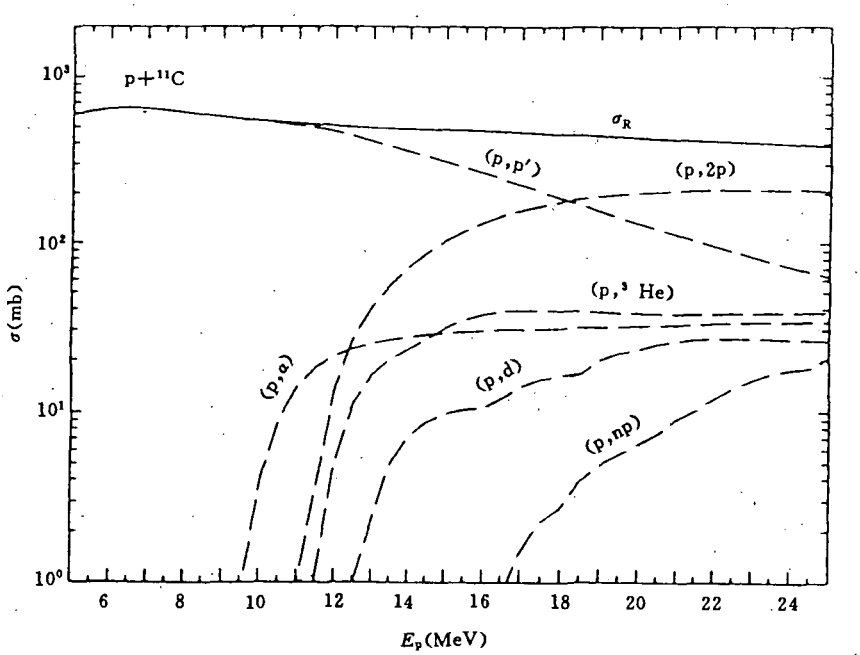

Fig. 2 The calculated p+^{11}C reaction cross sections

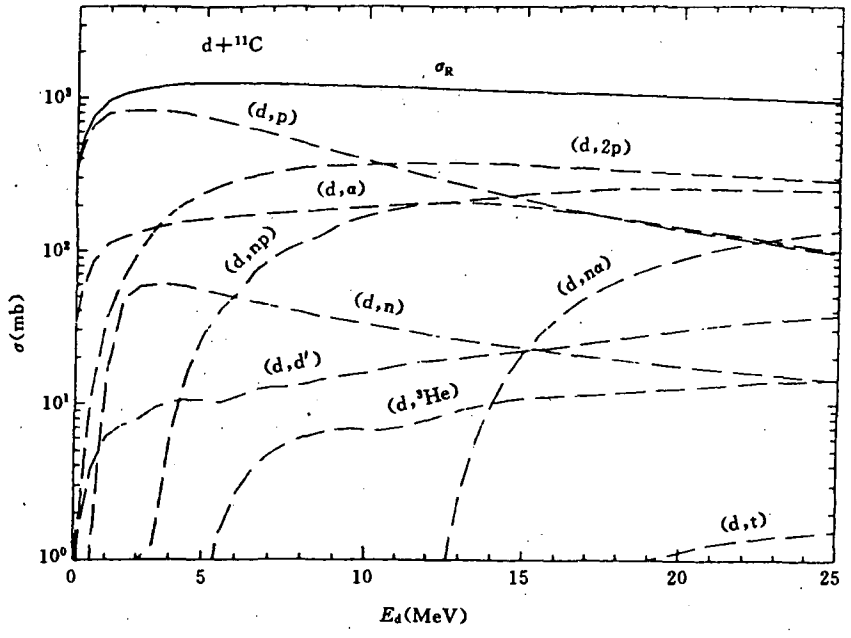

Fig. 3 The calculated d+^{11}C reaction cross sections

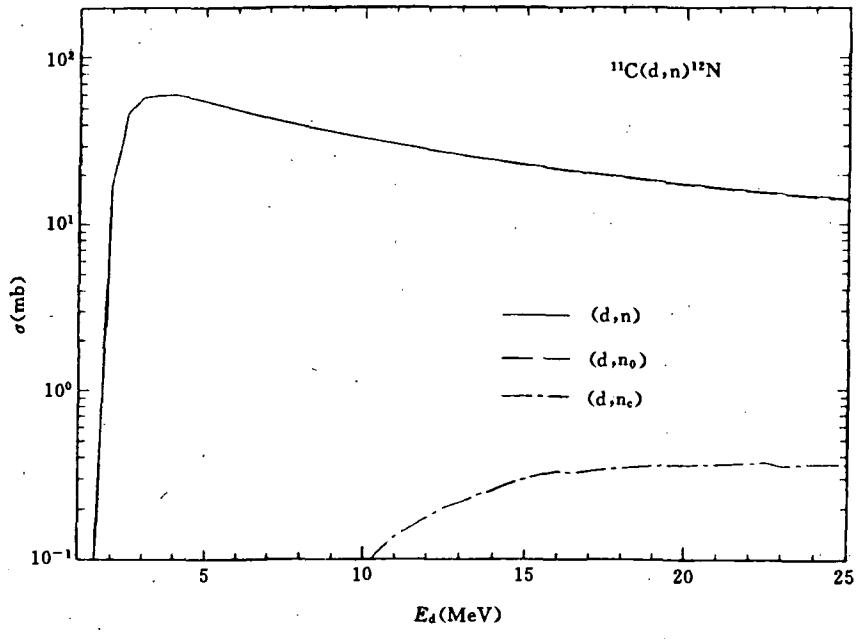

Fig. 4 The calculated ^{11}C(d,n)^{12}N reaction cross sections

References

[1] W. D. Myers, Nitschke J. M., Norman E. B., Proc. First Int. Conf. on Radioactive Nuclear Beams, Singapore : World Scientific, 1990

[2] Bai Xixiang et al., "On the Feasibility of Producing Secondary Radioactive Nuclear Beams Using Reactions in Reversed Geometries at HI–13 Tandem Accelerator", Atomic Energy Sci. Technol., 27, 385(1993)

[3] Bai Xixiang et al., "The Production of ^{11}C and ^{17}F Secondary Radioactive Beams", Chin. J. Nucl. Phys., 16, 100(1994)

[4] Shen Qingbiao et al., "Approach for Calculating Multistep Direct Reactions of Continuum and Discrete Levels", Phys. Rev., C 50, 2473(1994)

[5] Zhang Jingshang, "The Charged Particle Induced Reaction Code CUNF", China Institute of Atomic Energy (unpublished)

[6] Shen Qingbiao et al., "APCOM – A Code for Searching Optimal Charged Particle Optical Potential Parameters in $E<50$ MeV Energy Region", Commun. of Nucl. Data Prog., 7, 41(1992), INDC(CPR) – 027 / L

[7] Yu Ziqiang et al., "KORP1 — A Program for Calculating the Direct (n,p) and (p,n) Reaction by Using DWBA Method", China Nuclear Science and Technology Report, CNIC–00736, 1993, Atomic Energy Press of China

[8] P. D. Kunz, "Distorted Wave Code DWUCK4", University of Colorado, USA (unpublished)

[9] W. Bauhoff, "Tables of Reaction and Total Cross Sections for Proton– Nucleus Scattering below 1 GeV", Atom. Data and Nucl. Data Tables, 35, 429(1986)

[10] W. Fitz et al., "Scattering and Pick–up Reactions with Deuterons on Be, B, C, N and O at 11.8 MeV", Nucl. Phys., A101, 449(1967)

Calculations of Various Cross Sections for $n+^{63,65}Cu$ Reactions in Energy Region up to 70 MeV

Shen Qingbiao Yu Baosheng Cai Dunjiu

(Chinese Nuclear Data Center, IAE)

Abstract

A set of neutron optical potential parameters for $^{63,65}Cu$ in energy region of 2~ 80 MeV was obtained with available experimental data. Various cross sections of $n+^{63,65}Cu$ reactions are calculated and predicted in the energy range up to 70 MeV.

Introduction

The activation isotopes ^{56}Co (half life is 77.3 d), ^{57}Co (half life is 271.8 d), ^{58}Co (half life is 70.88 d), and ^{60}Co (half life is 5.271 a) can be produced from $n+^{63,65,Nat}Cu$ reactions. For $n+^{63}Cu$ reaction, ^{60}Co can be produced through (n,α), (n,2n2p), (n,npd), (n,2d), (n,n^{3}He), and (n,pt) reactions, ^{58}Co, ^{57}Co, and ^{56}Co through more reaction channels especially in higher energy region. $^{56,57,58,60}Co$ can also be produced through $n+^{65}Cu$ reaction, but more complicated reaction channels should be considered. There are more experimental data to be used to obtain the model parameters for $n+^{63,65}Cu$ reactions. If the calculated results are in pretty agreement with the existed experimental data, the production cross sections of the activation isotopes mentioned above can be predicted.

In Sec. 1, the theories and parameters used in our calculations are described. The calculated results and analyses are given in Sec. 2. Finally, a summary is given in Sec. 3.

1 Theories and Parameters

The calculation was made with the program SPEC[1] including the first to the sixth particle emission processes. In this program, the optical model, evaporation model, and the master equation of exciton model[2] are included. The

preequilibrium and direct reaction mechanisms of γ emission[3] are also included in this program. The direct inelastic scattering cross sections were obtained by the collective excitation distorted-wave Born approximation[4]. The compound-nucleus elastic scattering contributions were calculated by Hauser-Feshbach model.

For composite particle emissions, the pick-up mechanism of cluster formation[5~7] was included in the first and second particle emission processes.

Firstly, based on various experimental data of n+$^{63,\ 65}$Cu reactions from EXFOR library and recent information, a set of optimum neutron optical potential parameters in the energy region 2~80 MeV was obtained as follows :

$$V = 52.4390 - 0.17904E - 0.0005869E^2 - 24.0(N-Z)/A \quad (1)$$

$$W_S = \max\{0,\ 14.3009 - 0.16389E - 12.0(N-Z)/A\} \quad (2)$$

$$W_V = \max\{0,\ -1.14157 + 0.21069E - 0.0006034E^2\} \quad (3)$$

$$U_{SO} = 6.2 \quad (4)$$

$$r_r = 1.19185,\ r_S = 1.39041,\ r_V = 1.14228,\ r_{SO} = 1.19185 \quad (5)$$

$$a_r = 0.65701,\ a_S = 0.36129,\ a_V = 0.62164,\ a_{SO} = 0.65701 \quad (6)$$

The Gilbert-Cameron level density formula[8] was applied in our calculations, and the exciton model constant K was taken as 1800 MeV[3].

2 Calculated Results and Analyses

Fig. 1 shows the comparison of neutron total cross sections between the calculated values and the experimental data in the energy region 2~ 100 MeV for n+^{Nat}Cu reaction. The theoretical values are in good agreement with the experimental data.Fig. 2 shows that the calculated neutron nonelastic cross sections are in good agreement with the experimental data for n+^{Nat}Cu reaction. Fig. 3 and Fig. 4 show the comparison of the calculated elastic scattering cross sections and angular distributions with the experimental data for n+^{65}Cu reaction. They and those for n+^{63}Cu reaction are all in good agreement with the experimental data. Based on above fitting situation, a set of neutron optical potential parameters in the energy region 2~80 MeV for n+$^{63,\ 65}$Cu reactions are determined.

The calculated neutron inelastic scattering cross sections of ^{63}Cu are shown in Fig. 5. Fig. 6 gives the comparison of calculated and experimental (n,2n) cross sections of ^{63}Cu. Fig. 7 shows the calculated (n,α) cross sections

of ^{63}Cu.They and those for (n,d), (n,α–em) reactions are all basically in agreement with the experimental data.

Figs. 8, 9 give the comparisons of calculated and experimental (n,2n) and (n,nα) cross sections of ^{65}Cu. The calculated results for (n,inl), (n,2n), (n,n α), (n,d), (n,α), (n,α–em) and (n,p–em) cross sections of ^{65}Cu are all basically in agreement with the experimental data.

Fig. 10 shows the calculated $^{55\sim62}$Co production cross sections for n+^{63}Cu reaction in the energy range up to 70 MeV. The corresponding calculated results for n+^{65}Cu reaction can also be obtained and the calculated results for n+^{Nat}Cu reaction can be obtained through summation according to abundance in natural copper. Because the calculated results for many channels are in pretty agreement with the existed experimental data, the predicted production cross sections of the activation isotopes are reasonable.

3 Summary

Based on the available experimental data, a set of neutron optical potential parameters for ^{63,65}Cu in the energies of 2～80 MeV was obtained. Then many nuclear data for n+^{63,65}Cu reactions were calculated based on optical model, evaporation model, and the master equation of exciton model. Because the calculated results for many channels are in pretty agreement with the existed experimental data, the predicted production cross sections of the activation isotopes are reasonable. For n+^{63}Cu reaction, there are many (n,α) experimental data in low energy region, through which the activation isotope ^{60}Co can be produced. The evaluation for these experimental data and the final evaluated production cross sections of activation isotopes $^{56\sim58,60}$Co produced through n+^{63,65,Nat}Cu reactions will be given in another evaluation paper[9].

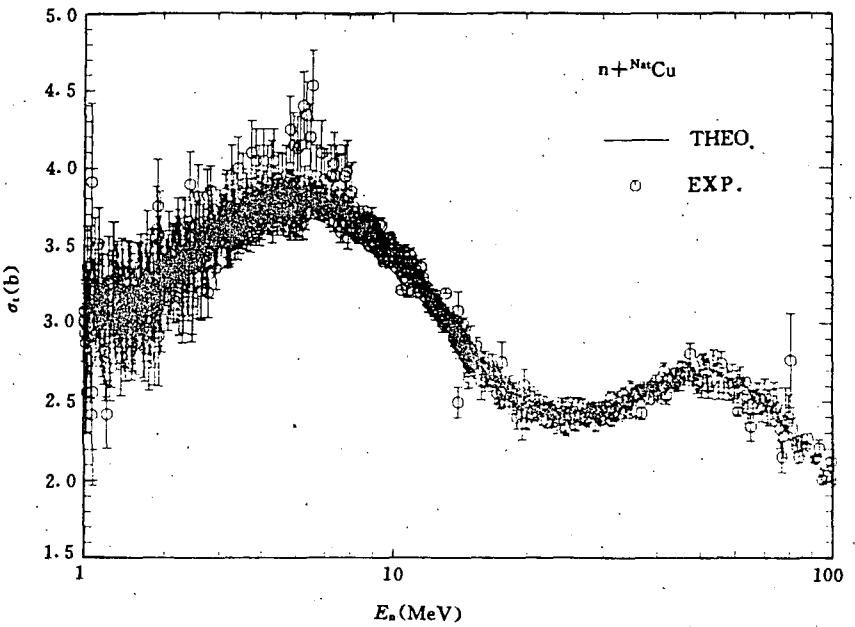

Fig. 1 , Comparison of neutron total cross sections of ^{Nat}Cu between the calculated values and the experimental data

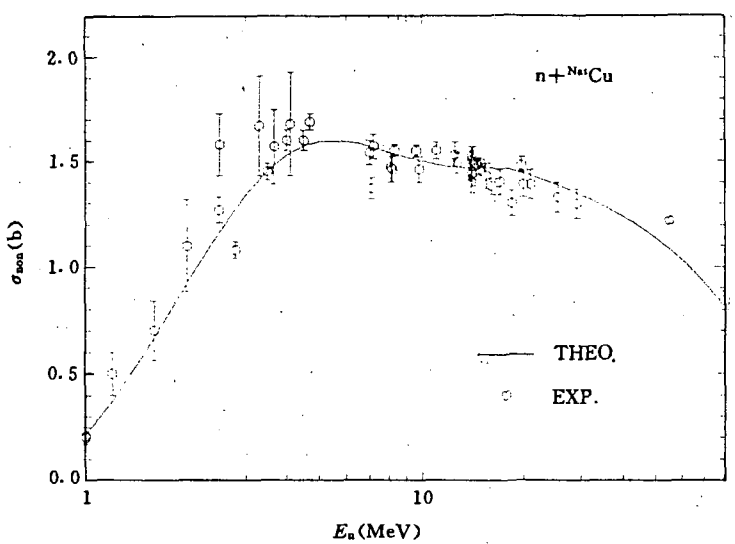

Fig. 2 Comparison of neutron nonelastic scattering cross sections of ^{Nat}Cu between the calculated values and the experimental data

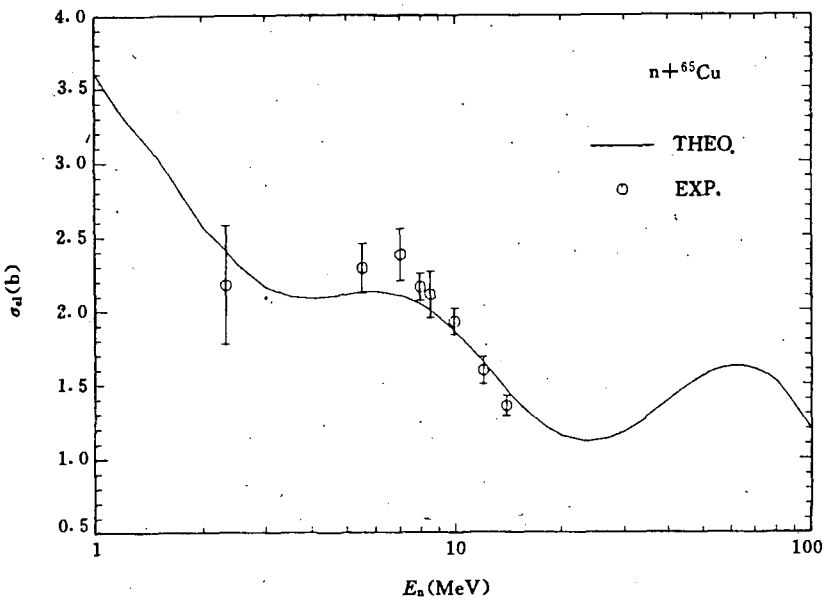

Fig. 3 Comparison of neutron elastic scattering cross sections between the calculated values and the experimental data of ^{65}Cu

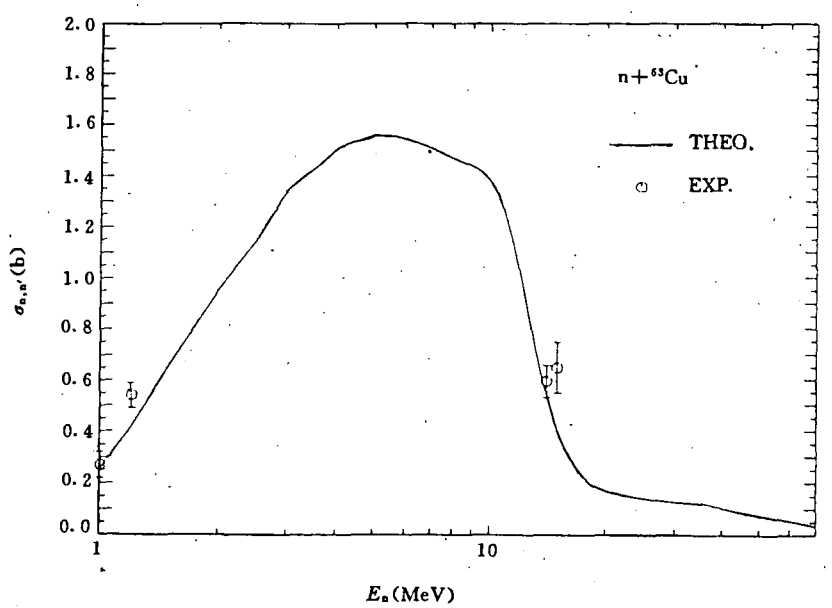

Fig. 5 Comparison of neutron inelastic scattering cross sections of ^{63}Cu between the calculated values and the experimental data

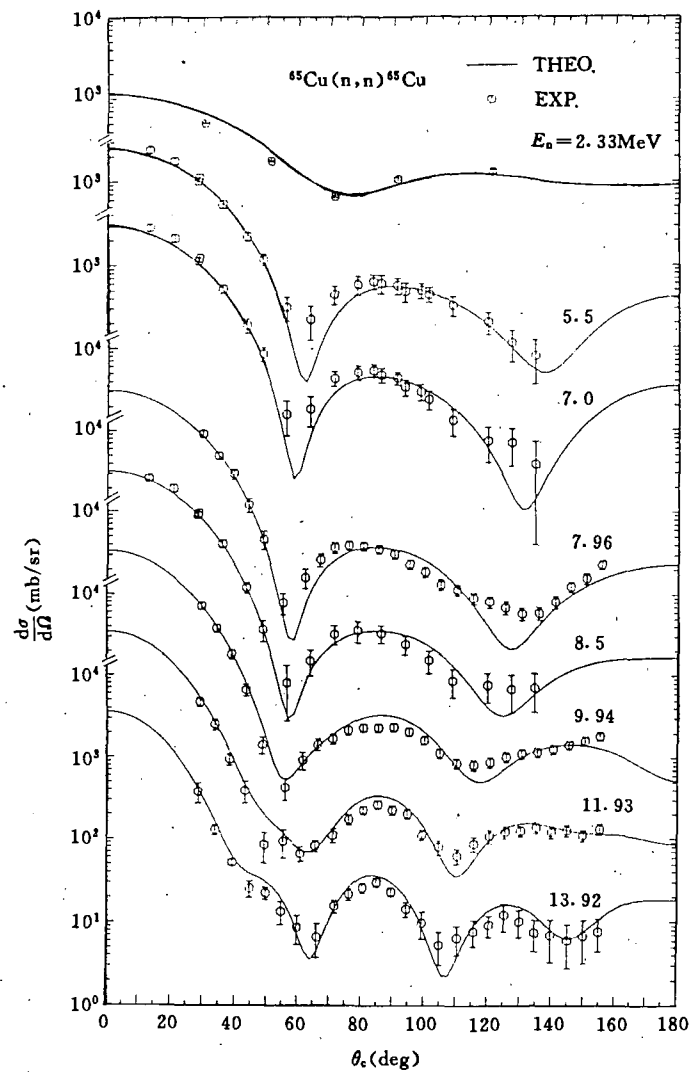

Fig. 4 Comparison of neutron elastic scattering angular distributions between the calculated values and the experimental data of ^{65}Cu

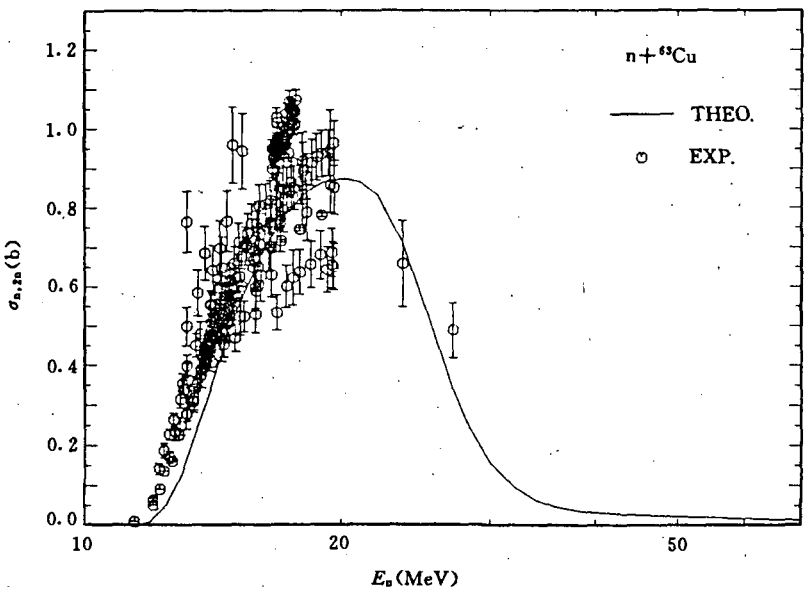

Fig. 6 The same as Fig. 5 but for (n,2n) cross sections

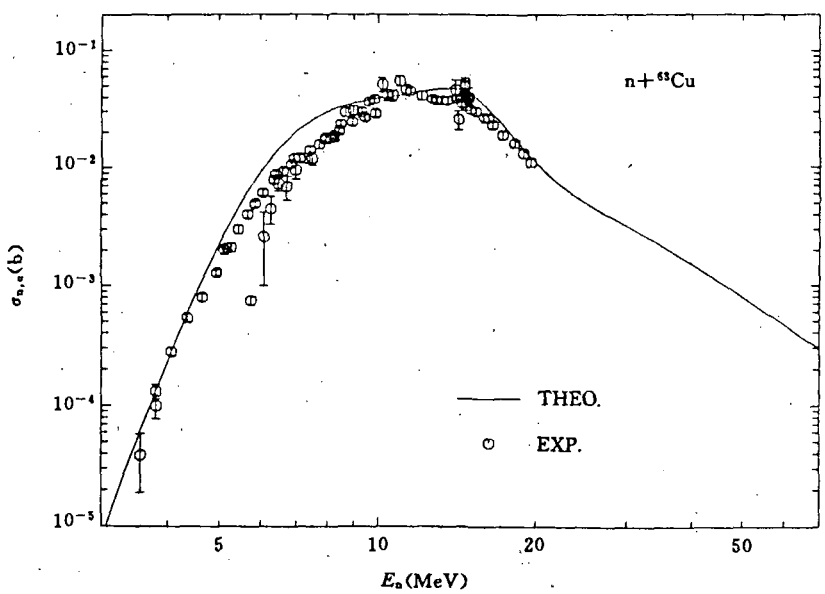

Fig. 7 The same as Fig. 5 but for (n,α) cross sections

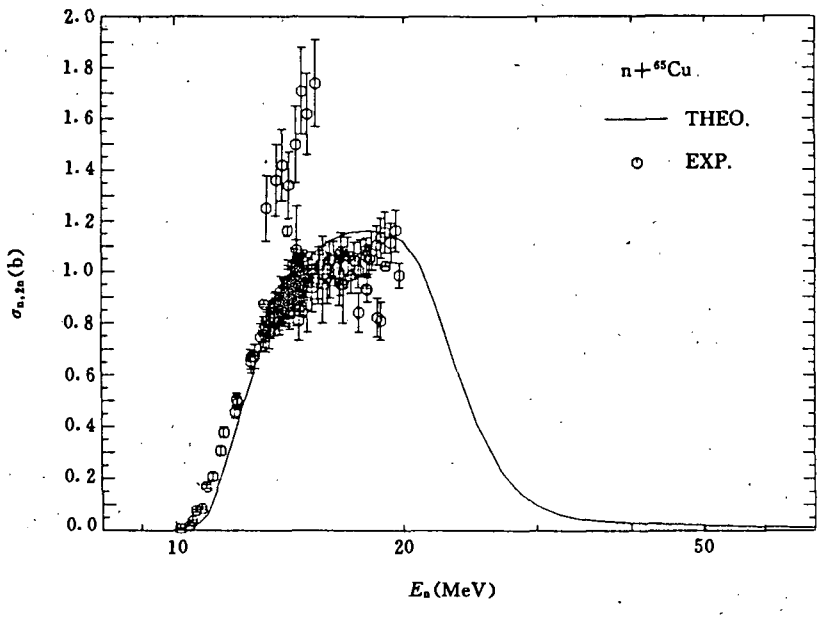

Fig. 8 Comparison of (n,2n) cross sections of ^{65}Cu between the calculated values and the experimental data

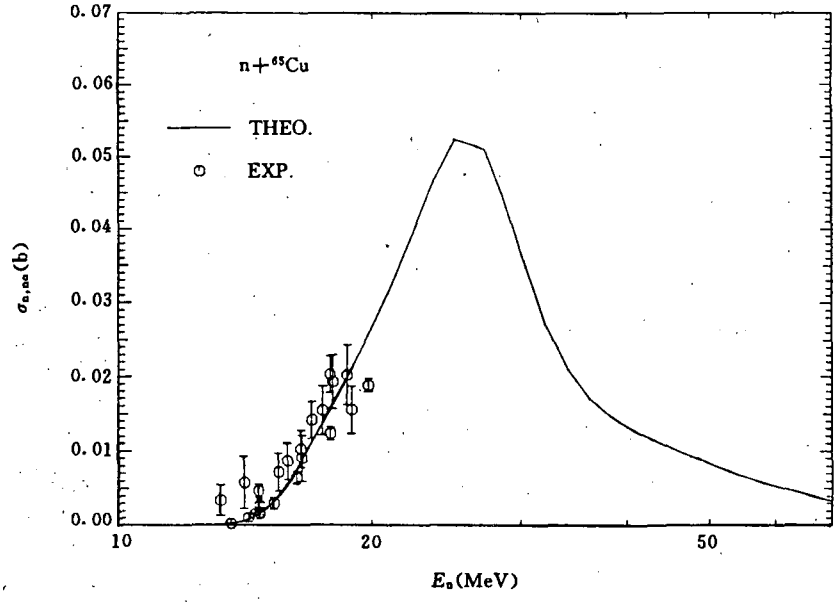

Fig. 9 The same as Fig. 8 but for (n,nα) cross sections

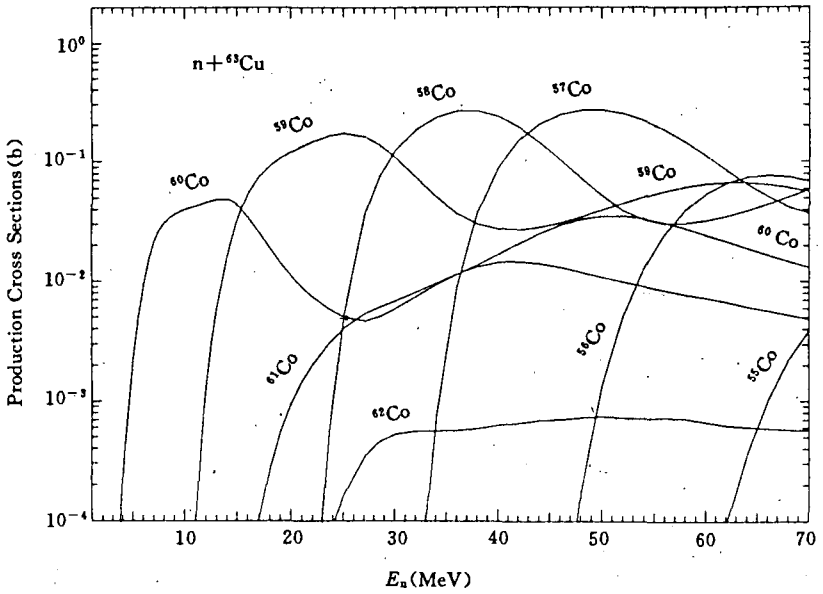

Fig. 10 The calculated cobalt isotopes production cross sections for n+^{63}Cu reaction

References

[1] Shen Qingbiao et al., Commun. of Nucl. Data Prog., 11, 28(1994)

[2] M. Blann, Ann. Rev. Nucl. Sci., 25, 123(1975)

[3] J. M. Akkermans et al., Phys. Let., 157B, 95(1985)

[4] P. D. Kunz, "Distorted Wave Code DWUCK4", University of Colorado

[5] A. Iwamoto et al., Phys. Rev., C26, 1821(1982)

[6] K. Sato et al., Phys. Rev. C28, 1527(1983)

[7] Zhang Jingshang et al., Commun. in Theor. Phys., (Beijing, China), 10, 33(1988)

[8] A. Gilbert et al., Can. J. Phys., 43, 1446(1965)

[9] Yu Baosheng et al., to be published

III DATA EVALUATION

Nuclear Data Evaluation Method and Evaluation System

Liu Tingjin

(Chinese Nuclear Data Center, IAE)

To complete the nuclear data evaluation in China, the evaluation methods and Nuclear Data Evaluation System have been developed. The system was on computers Acos–500 and PDP–11 / 70 in the late seventies and early eighties[1]. Since then, a new version of the System has been established on Micro–VAX 2 computer,which is supported by IAEA under the technology assistance program. The new version is not only suitable for new computer, not only developed in program and software technology, but also much more new physical ideas, methods and programs for data and covariance matrix evaluation and processing are included.

The flow chart of the system is shown in Fig. 1.

1 The Retrieval Analysis and Pre–processing of Experimental Data in EXFOR Format

Using the EXFOR software system[2], which was developed in USA and transplanted on CNDC Micro VAX 2 computer from NDS / IAEA, the measured data are retrieved directly from master experimental neutron data library in EXFOR format. The retrieval can be done according to the nuclides, reaction quantities and / or measured years, or access number.

As well known that the EXFOR format is very flexible and complicated, so the format, especially the data table, need to be changed and standardized for using and processing the data conveniently later, this includes unit conversion, column exchange, data normalization, error correction etc. and is completed with codes FORM[3] and SIG[4]. It is worth to mention that in some cases (e. g. some total cross section measured with white light source) too many data points are given, the energy points need to be selected or merged in the

evaluation. With the code, the number N (for each N, one energy point is selected or merged into) can be chosen according to the requirement and the points at peaks or volleys always kept. After the pre–processing, the EXFOR data table is standardized.

Code SIG is a powerful and convenient tool for physical analysis and evaluation of EXFOR experimental data. With it, the description information of EXFOR data can be displayed on screen. The data measured by different libraries can be plotted and compared; the data can be renormalized and the error can be corrected.

It is very important in the physical analysis and evaluation of experimental data to pay attention to the following things : 1) experimental methods,for example, white light source or certain energy point for total cross section, activation or large liquid scintillator for (n,2n) cross section, time of flight method or others for energy spectrum, etc.; 2) identify the measured quantity, for example, total (n,2n) cross section or to isomeric state, (n,x), (n,n′x) cross section or the sum of both, etc.; 3) whether the background was already reasonably subtracted, the necessary correction were already done; 4) whether the standard cross section used is newest, internationally recommended one, otherwise, renormalization need to be done with new standard.

2 Data Processing

Data processing is a very important step in the evaluation. In the system,it includes the data processing at certain energy point, curve fitting and simultaneous evaluation.

2.1 The data at certain energy point are very significant for determining the absolute position of the recommended curve in the evaluation, but traditional method to the matter is applicable only for the independent data and make senses at extreme cases[5]. We developed a method [6] to deal with not only independent data, but also correlative data, not only statistical error, but also possibly existing negligence error. A statistical model was presented for isolating the possibly existing negligence error, adjusting the original data and estimating the combination–mean of the correlative data. A practical code was developed, and the features of correlative data mean were studied. It was found that in some cases, the combination mean could be out of all input data, an example for three dimension case is shown in Fig. 2.

2.2 The curve fitting is essential treatment in the experimental data evaluation.

Through it, the smooth optimum values in mathematics can be got as the recommended data. For this purpose, the spline methods and programs SPF, SPD, SPC[7~9] have been developed. Comparing with previous works[10, 11], in summary, the following developments have been made in our works :

1) Knot optimization. The knot for spline fitting can be automatically optimized with the total knot number plus one to make the χ^2 minimum for each iteration. The only thing should do for users is to give the initial knots. An example is given in Fig. 3, from which it can be seen that the χ^2 value decreases to a reasonable level only through 3~5 times of iteration for all 4 sets of different initial knots. The knot optimization is convenient to users, also it minimizes the arbitrariness of the fit result due to the arbitrary knot selection (traditionally, spline knots are given by users).

2) Any spline order. Traditionally, in general, only three order spline is used [10, 11]. Now, the order of spline function can be chosen for different curve shape, for example, one order for linear line, two order for parabola, three order for peak structure etc..

3) Strict error calculation. The formulas for calculating the fit values and their errors for multi-sets of data were deduced[7]. It was found that the error calculation formulas in previous works[11, 12] are approximate ones, only suitable to the case where is only one set of data. Comparing the calculated results, it was found that the differences between the strict and approximate formulas are quite large when the width for each set of data becomes larger (Fig. 4).

4) Correlative data and covariance. Traditionally, the curve fit is only for independent data and only the error of the fit values is calculated. Now, the code SPC can be used for correlative data (there is correlation among the data at different energy points). The covariance of the fit values can be calculated (traditional error only is diagonal elements). An example is given in Fig. 5. For correlative data fitting, it is very different from the traditional independent data fitting that the fit values are changed not only with knot, width of each set of data, but also with the correlation coefficients of the data. In some cases (e. g. both the correlation coefficient and the discrepancy of the data are larger), so called PPP problem[12] could happen, an example is given in Fig. 6. The code has a function to deal with the matter by using iteration (for input absolute covariance matrix) method or appropriately selecting the order and knots of the spline function. An example is given in Fig. 7.

2.3 Simultaneous evaluation is a advanced evaluation method, developed in last ten years. With the method, more information is included, and consist (between cross sections and ratios or the cross sections and standards etc.) can be

got.

We have developed a simultaneous evaluation method and a code SESP relative to ratio[13, 14]. The logarithms of the cross sections and their ratios are fitted with spline function, the consistent fit values and their covariance are calculated. Comparing with previous work[15], the fitting is with B–spline and the method can be used for the correlative data, the covariance matrix can be calculated not only for the different energy points of the same kind of cross sections, but also for the same and different energy points of different kinds of cross sections. It means that the correlations among the fit results are given not only for the same kind of cross sections, but also for the different kind of cross sections. The method and program have been used to evaluate the fission cross sections of $^{235, 238}$U and the capture cross section of ^{238}U. An example of the results is shown in Fig. 8, comparing with individual evaluation and simultaneous evaluation without correlation. All of the curves are based on the same experimental data in the figure.

3 Covariance Data Evaluation

With the development of the reactor physics and computer technology, the covariance matrix of nuclear data becomes more and more important for nuclear engineering. For evaluators and experimenters, the data information is given out completely only in the case that the data themselves and their covariance matrix are given, because the error, as traditionally given, is only the diagonal elements of the covariance matrix and describes the accuracy of the data, nothing about the correlation of the data is given.

Some methods and codes for covariance data evaluation of experimental data have been developed and included in the system[16, 17].

3.1 Parameter Analysis[17]

If the conditions of an experiment, especially the information about the error are well known, the covariance matrix can be constructed according to the formula

$$\mathrm{Cov}\ (f_i, f_j) = \sum_k \frac{\partial f}{\partial \chi_k}\Big|_i \frac{\partial f}{\partial \chi_k}\Big|_j \rho_{ij}^k \Delta\chi_{ki} \Delta\chi_{kj}$$

Where quantity f to be measured is a function of some parameters χ, which

could be measured directly, ρ_{ij}^{k} is the correlation coefficient of parameters χ at energy points i and j. If the function or the errors $\Delta\chi_k$ of the directly measured parameters are not known, the covariance matrix can be calculated like this

$$\mathrm{Cov}\ (\ f_i,\ f_j\ ) = \sum_k \rho_{ij}^{k}\ \Delta f_{ki}\ \Delta f_{kj}$$

Where Δf_{ki} is the error of the indirectly measured data contributed from k–th parameter at energy point i.

A practical program CMP was developed, some explicit form of function f, commonly used for various experimental methods, are included. To insure the covariance is reasonable in mathematics and physics, the positive definite feature of the constructed covariance matrix is checked by using the method of calculating the eigenvalues of the correlation coefficient matrix. An example with the method and code is given in Table 1 for Na(n,2n) reaction cross section in the energy region 13.0~ 18.0 MeV,measured by Prof. Lu[18] with activation method at six energy points.

3.2 Mathematics Calculation

For cross section or other quantities, if there are multi–sets of measured correlative data and their covariance matrices are all known, the data can be fitted with spline function and the covariance matrix of the fit values can be calculated strictly in mathematics :

$$V_{\hat{y}} = EV_y\ E^T$$

Where $E = B^T\ (\ W - U^T D U\ )$ and V_y is the covariance matrix of the input measured vector Y, B is base spline function matrix and W, U, D are the matrices corresponding different weights respectively[8]. In practice,the program SPC as introduced in section 2.2, can be used. Using the program, the features of the fit value covariance matrix were studied, it was shown that the correlation among fit values at different energy point results mainly from the propagation of the input covariance matrices, and also somewhat producing in the fitting.

3.3 Physical Analysis

The data that their covariance is not given and the error information is not well known, which is usual case faced by the data evaluators, must be analyzed carefully in physics, and the total error, especially the systematical error should be found out as much as possible based on the realistic situations and available information. The key point here is to distinguish the statistical and systematical error, or the short, middle and long range error, the latter contributes to correlation. Usually, the errors of the sample quantification, standard cross section etc. are long range error, and the errors of detector efficiency calibration, some correction etc. are the middle range error. It should be pointed out that original statistical error could acts as systematical one in some case of the covariance analysis and evaluation, for example, the statistical part of the standard cross section error, the counting error of the monitor. Another thing should be emphasized is that the systematic error, in general case, could not be found by the experimenter themselves, but it could be found by the evaluators when they put the same kind of data together, measured by different libraries. In this case, the systematic difference among the different measurements can be taken as systematic error. An example is given in Fig. 10, which is a part of the covariance data evaluations by author for oxygen data[19].

For convenient, a processing code CMC was developed. With the code, explicit covariance matrix can be calculated and output in ENDF / B–6 format, using the systematic error information given through above analysis in physics and the evaluated total or statistical error (e. g. through curve fitting), taking into account of whether the systematic error needs to be added to the diagonal elements.

4 Comprehensive Adjusting and Library File Making

4.1 In general,the experimental data are not enough to recommend complete set of data, especially for angular distributions and energy spectra. So it is necessary to supplement with theoretical calculation. Lotsof model calculation programs have been developed and used for developing CENDL. For statistical calculation, most commonly used program for CENDL–2 is MUP–2[20], and now the one commonly used is UNF[21], which was finished recently and can be used to calculate double differential cross section (including recoil nucleus) and γ–production data. For direct reaction, some codes transplanted from abroad are used when they are necessary. The parameters for model calculation can be retrieved directly from Chinese Nuclear Parameter Library[22], which is being developed now. Programs RETRIVE and ESS is used for retrieving the

necessary data from the theoretically calculated data.

4.2 It is commonly defined that in "general purpose file" the neutron energy is from 10^{-5} eV to 20 MeV. In so large energy range, the data are divided into two regions : "resonance" and "smooth" at the boundary energy about several keV to hundreds keV depending on the nuclides. The methods and programs described above are only suitable to the smooth region, and the resonance parameters are given for the resonance region. Some method and programs for resonance parameter evaluation have been developed [23]. But for the resonance parameters in complete neutron data, due to the limit of the practical condition, at present in China, only thing can do is to evaluate the parameter themselves or to recommend some existing parameters (such as BNL–325). However, when take these parameters and put them into the file, it must be checked if the data at the resonance boundary are smoothly linked with "smooth" region, if not, find the reason as much as possible and adjust them. For example, in the complete neutron data evaluation of natural iron completed by author[24], the resonance parameters were taken from the recommendation of CNDC[25], but the average value at the boundary region (380～400 keV) of the total cross section and elastic scattering cross section calculated from the parameters are twice larger than the measured data and the data given in the smooth region (Fig. 11). Comparing with the parameters given in BNL–325, the both are basically same. Adjusting the width of the main s–wave resonances, there is no much effect on it. Taking into account of the interference effect, four large s–wave resonances ($\Gamma_n = 400 \sim 7700$ keV) above 400 keV were added, and then the calculated cross sections decrease much more and consistent with the experimental data.

4.3 To extend the data as low as 10^{-5} eV, either some negative resonances are given, or the point–wise cross section is presented in the region below resonance low boundary. In both cases, the cross section should be consistent with the experimental data in the thermal neutron energy region, especially at thermal energy point 0.0253 eV, where the total, elastic scattering and capture cross sections are usually measured and recommended. If the negative resonance parameters are given, the cross section should be calculated with them to compare. In the case of giving point–wise data, the cross section is usually extrapolated from thermal energy point with $1/v$ law for capture cross section and with constant for potential scattering, if there are no data in this energy region. For γ–production cross section of (n,γ) reaction, usually its multiplicity is extrapolated as a constant from the smooth region down to 10^{-5} eV.

To calculate the point–wise cross section from resonance parameters, either check program[26] of ENDF / B system or MSBW2 code[23] can be used.

4.4 The comprehensive adjusting is to make the evaluated data file satisfy the requirements in physics and format. The former includes making cross section consistent, angular distribution non–negative value etc., and the latter includes making energy spectrum normalization, the energy points of some cross section include all the energy points of its partial cross sections, energy region covers the same range for all files etc.. To make the cross section consistent, usually elastic cross section is got by subtracting nonelastic cross section from total cross section, nonelastic cross section by summing the cross sections of all nonelastic reaction channels or inelastic cross section by subtracting the cross sections of all other nonelastic reaction channels from nonelastic cross section,continuous inelastic cross section by subtracting all the discrete inelastic cross section from total inelastic cross section.

The library file making and comprehensive adjusting, including supplementing with theoretical calculated data, adding resonance parameter file, extending the energy region to 10^{-5} eV, making the cross section consistent etc., are mostly completed with code CRECTJ5[27], which was transplanted from Japan Nuclear Data Center and very convenient to be used, for many operations can be completed simultaneously in batch and input and output are in standard ENDF / B–4, 5 format. For making cross section consistent, the code CCSC3[1] was mostly used before and in some cases it is still used now.

5 Check and Intercomparison

5.1 The library file, or the new evaluated data need to be checked in format and physics before it is entered into CENDL. These can be done with programs CHECKR,FIZCON and PSYCHE[26], which were transplanted from NNDC, USA.

It has been found that in many cases the cross sections are not consistent in some energy points, although they had been adjusted. This could be caused by the interpolation when the energy mesh is not dense enough. In this case, the data can be corrected with codes CRECTJ5 or CCSC3 by adding or subtracting the given differences. Another problem is the data are not smoothly linked at the resonance boundary. In this case, the resonance parameters must be adjusted, as pointed above, or adding the necessary background cross section in file 3. The mostly found problem is that the energy is not in balance,namely the energy taking by the outgoing particles (including neutron, γ, charged particles

and recoil nucleus) is larger or much smaller than the available energy offered by the incident neutron and reaction Q value. The problem is quite complicated and is a comprehensive one, because it concerns the secondary particle spectra, γ production multiplicities, reaction Q values etc. To solve the problem, physical analysis should be done concretely and the reason should be found as much as possible,and then make some adjusting or correction to the spectra, multiplicities or Q values concerned.

5.2 The new evaluated data need to be compared with available experimental data and exsisting evaluated data. This can be completed with intercomparison plot system ICPL, consisting of ICPLN[28] and ICPLG[29] for neutron data (files (2)3～5(6)) and γ-production data (files 12～15(6)) respectively.

The functions of the system, in summary, are as follows. 1) Directly retrieve the experimental data from EXFOR master library and exsisting evaluated data from evaluated nuclear data libraries, with which the new evaluated data need to be compared. 2) Interpolate according to given interpolation models for cross section, angular distribution (for incident neutron energy) and energy spectrum (for incident neutron energy and secondary neutron, γ energy). 3) Transform coordinate system between laboratory and mass-center systems for angular distribution and spectrum. 4) Calculate neutron and γ-production emission cross section and spectrum by summing the corresponding data of all reaction channels, including making the Gassian extension for discrete neutron or γ-rays. 5) Calculate γ-production multiplicity, γ-production spectrum from the γ transition probability arrays given in file 12. 6) Get secondary neutron and γ spectrum in 4π space from the angular-energy distributions given in file 6. 7) Calculate the natural element's cross section, differential cross section and spectrum of neutron and γ-production by summing its corresponding isotopes' data taking the abundance as weight. 8) Plot, automatically choose the minimum and maximum values of the data and coordinate scale, output with various devices, such as printer, laser jeter and graphic terminal screen.

The system ICPL not only has very strong data processing and plot function, but also is very convenient to use, for it can run in batch, many operations, such as retrieving, data processing and plotting, can be completed in one run, the input parameters by users are decreased to minimum. Some examples are shown in Figs. 12～ 15 for cross section, angular distribution and neutron, γ emission spectra intercomparison respectively.

Conclusion Remarks

Nuclear data evaluation is being developed now, so is the evaluation method and system. For last ten years, the main efforts have been put on the double differential cross section, covariance data and evaluated data library validation. Correspondingly, the evaluation methods concerned, such as calculation programs for double differential cross section, evaluation methods for covariance matrix and intercomparison system have also been developed in China and included in the Chinese Nuclear Data Evaluation System. It should be pointed out that so far some problems, e. g. energy balance, Q value for natural element, interpolation for energy spectrum etc., are still being studied and need to be resolved further.

The developed evaluation method and Chinese Nuclear Data Evaluation System have been widely used at CNDC and in Chinese Nuclear Data Network for CENDL, for special purpose file evaluation, for the intercomparison of structural material Fe, Cr, Ni complete neutron data from CENDL–2, BROND–2, ENDF / B–6 and JENDL–3. Some of the methods and programs have also been offered to experimenters and abroad.

The Chinese Nuclear Data Evaluation System is already an embryonic form of intelligence specialist nuclear data evaluation system. Taking it as a base, the Chinese Intelligence Specialist Nuclear Data Evaluation System will be developed in future.

Table 1 The correlation coeffcient matrix and error for ^{23}Na(n,2n) reaction

E_n / ρ / E_n	13.5 MeV	14.10 MeV	14.64 MeV	14.87 MeV	16.95 MeV	17.98 MeV
13.50 MeV	1.0000					
14.10 MeV	0.5543	1.0000				
14.64 MeV	0.6398	0.6281	1.0000			
14.87 MeV	0.6423	0.6201	0.7140	1.0000		
16.95 MeV	0.5094	0.4390	0.5122	0.5325	1.0000	
17.98 MeV	0.4720	0.3897	0.4571	0.4834	0.5435	1.0000
σ	0.14	0.45	0.78	0.87	2.69	4.05
σ^*	0.16	0.50	0.80	0.90	3.0	4.3

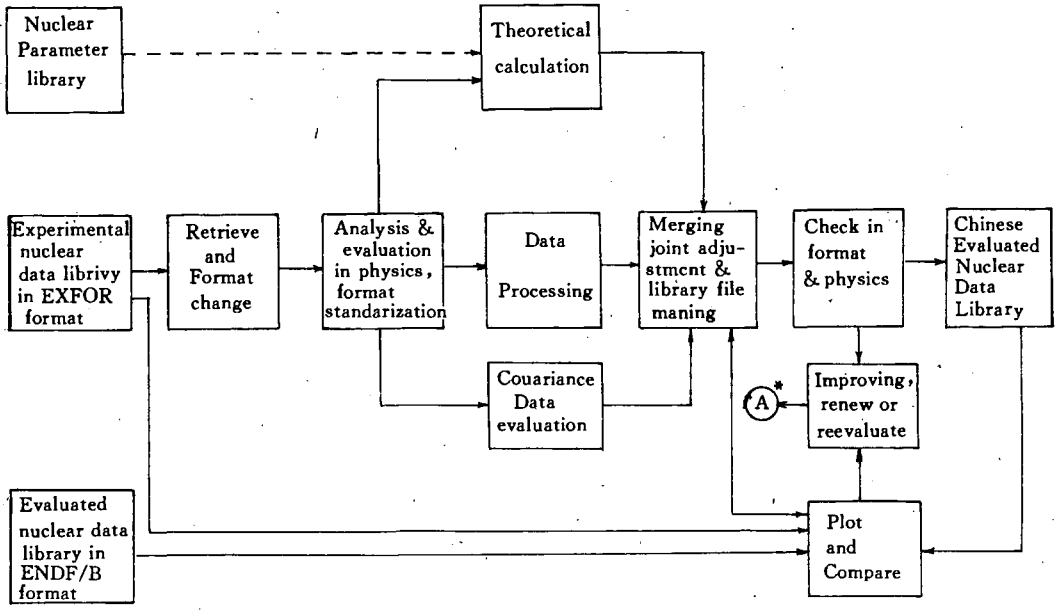

Fig. 1 The flow chart of Chinese Nuclear Data Evaluation System

Ⓐ* Any place, from which the improving, renew or reevaluation need to be done

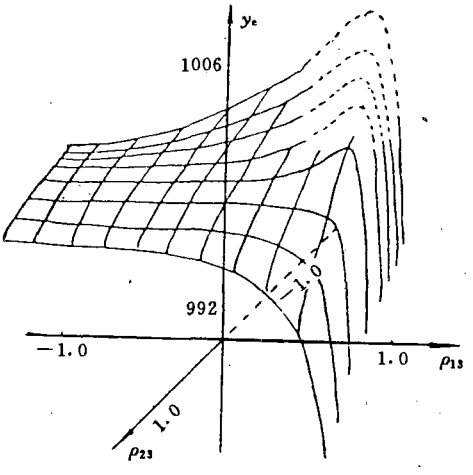

Fig. 2 The effect of correlation in three dimension case

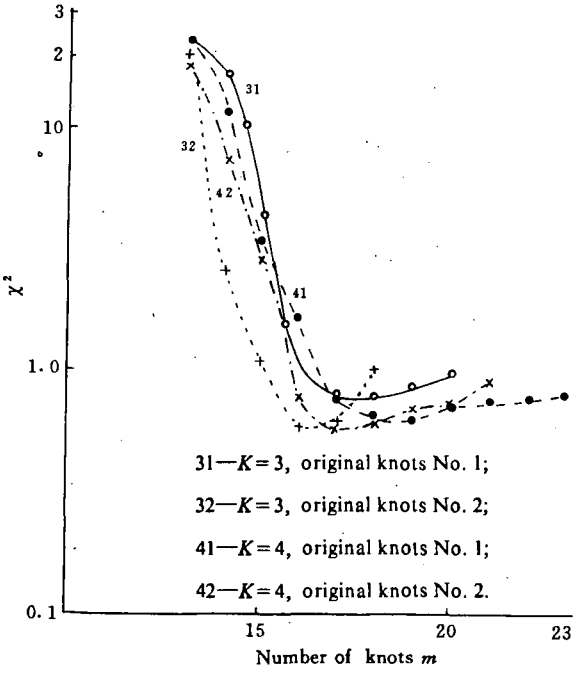

Fig. 3 Knot optimization of spline fitting

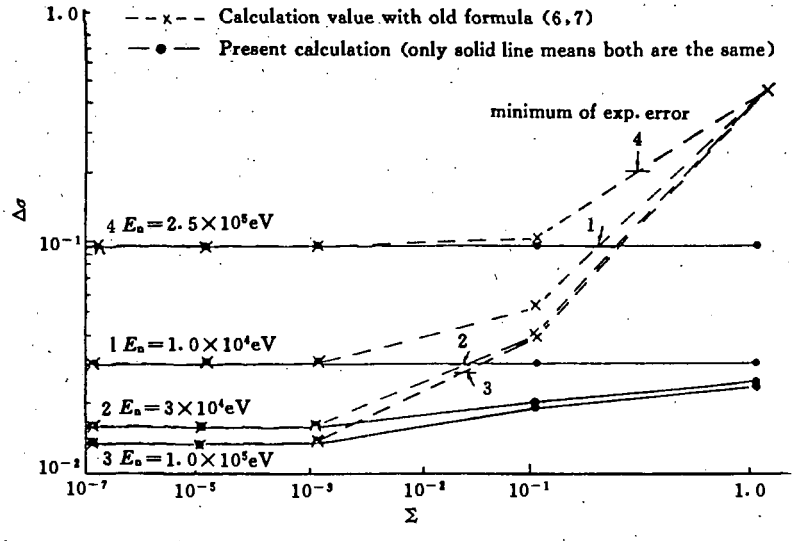

Fig. 4 The variation of fit value error with the width of each set of data

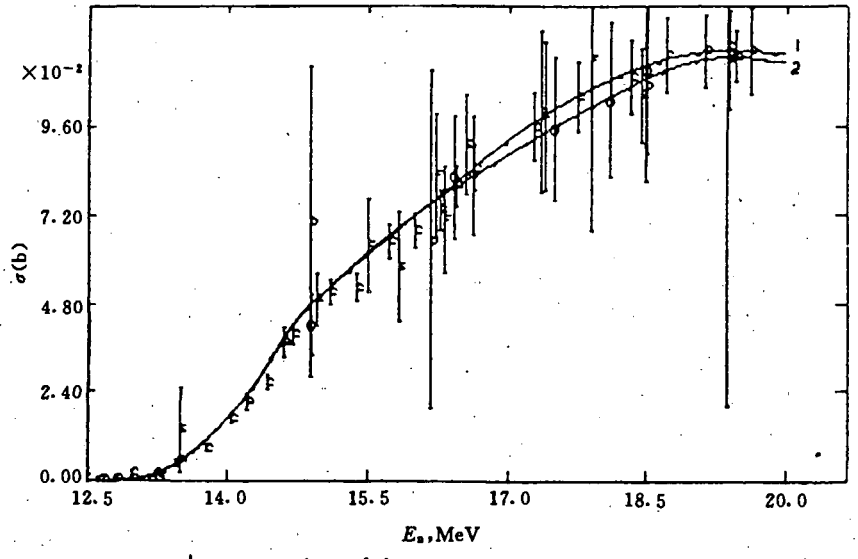

etc. experimental data;

curve 1. Input data are correlative; curve 2. Input data are not correlative.

Fig. 5 A practical example of spline function fitting for correlative data ^{23}Na(n,2n) cross section

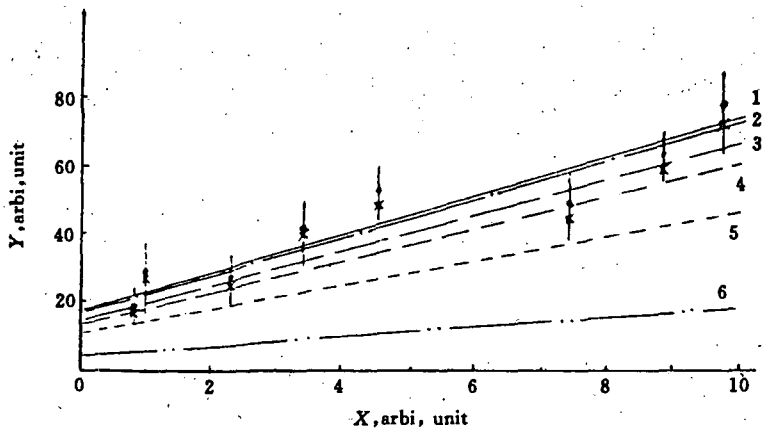

Fig. 6 The variation of fit value with correlation coefficient r

curve 1, r = 0.0; 2, r = 0.2; 3, r = 0.4; 4, r = 0.6; 5, r = 0.8; 6, r = 0.95.

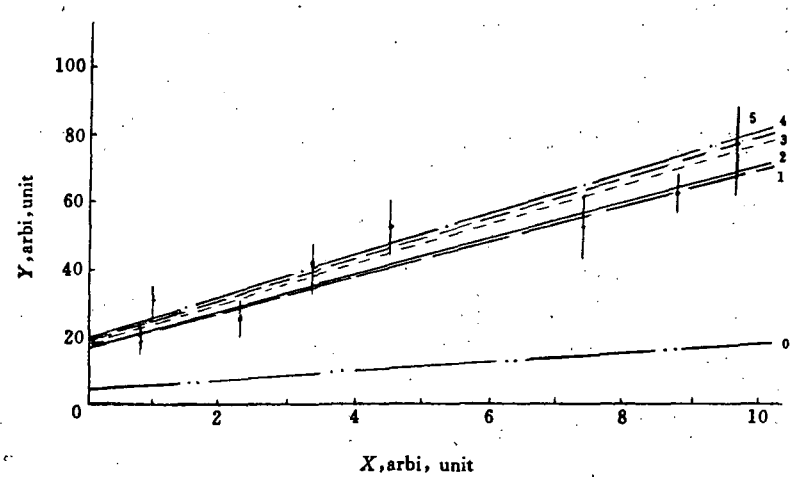

Fig. 7 The variation of fit value with iteration

(for input covariance matrix) times (r = 0.95)

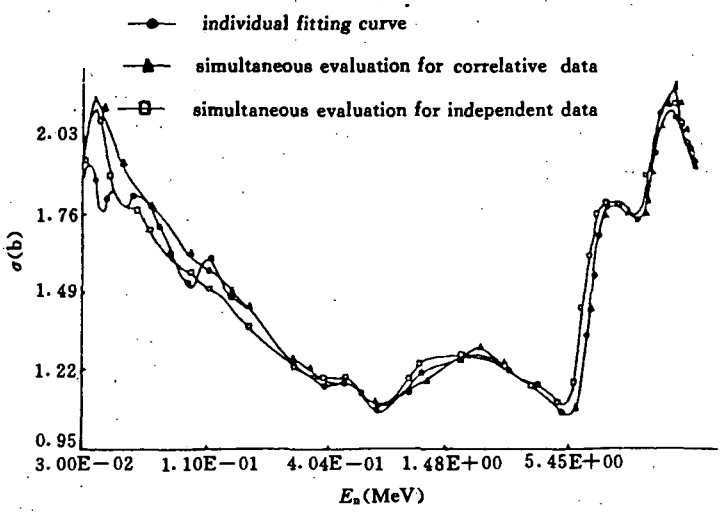

Fig. 8 An example of simultaneous evaluation results : ^{235}U fission cross section

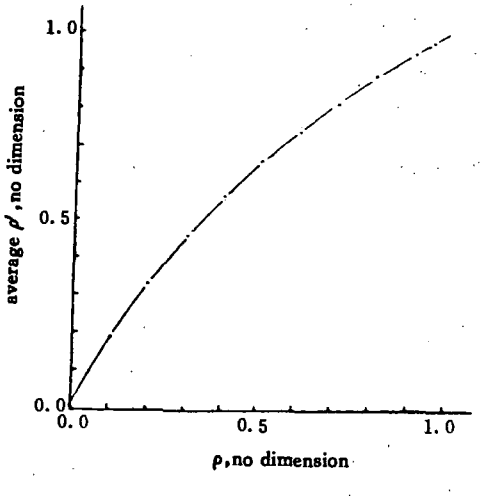

Fig. 9 The changing of average correlation coefficient ρ' of fit values with input correlation coefficient ρ

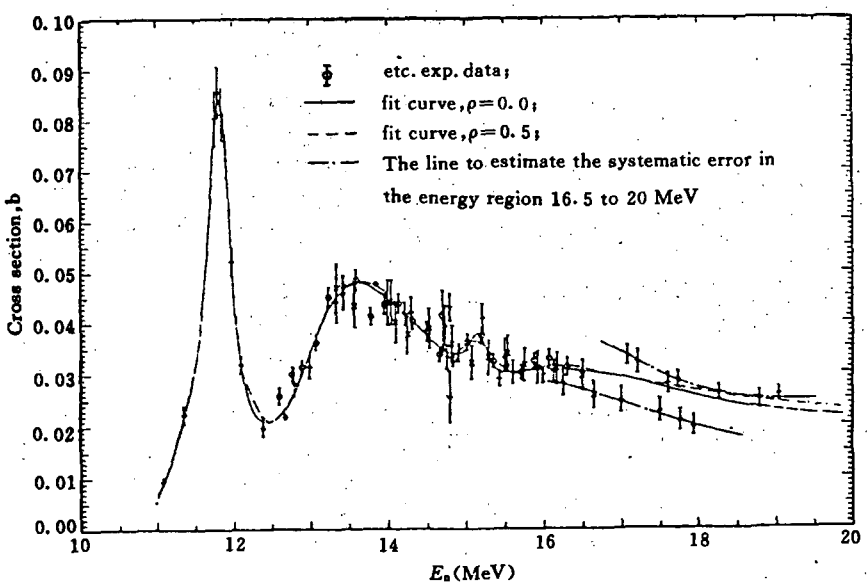

Fig. 10 An example taking the difference as systematic error : O(n,p) cross section

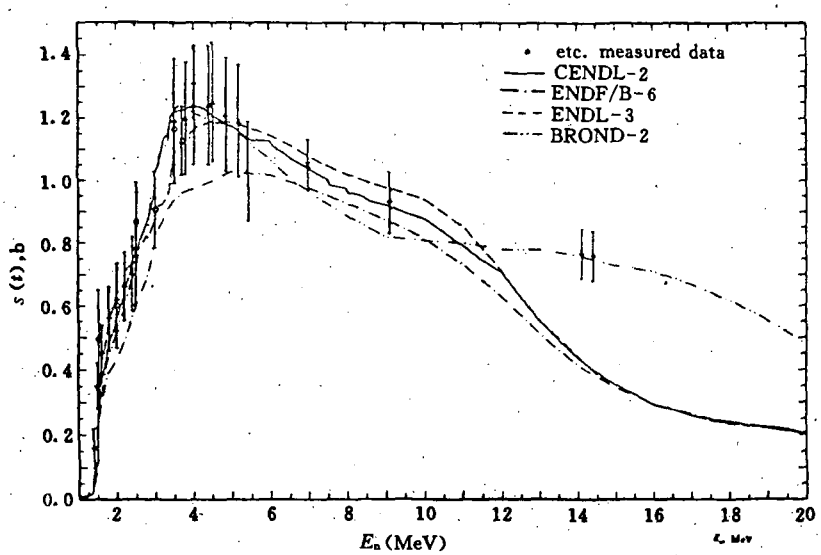

Fig. 12 An example of cross section intercomparison :
Ni inelastic scattering cross section

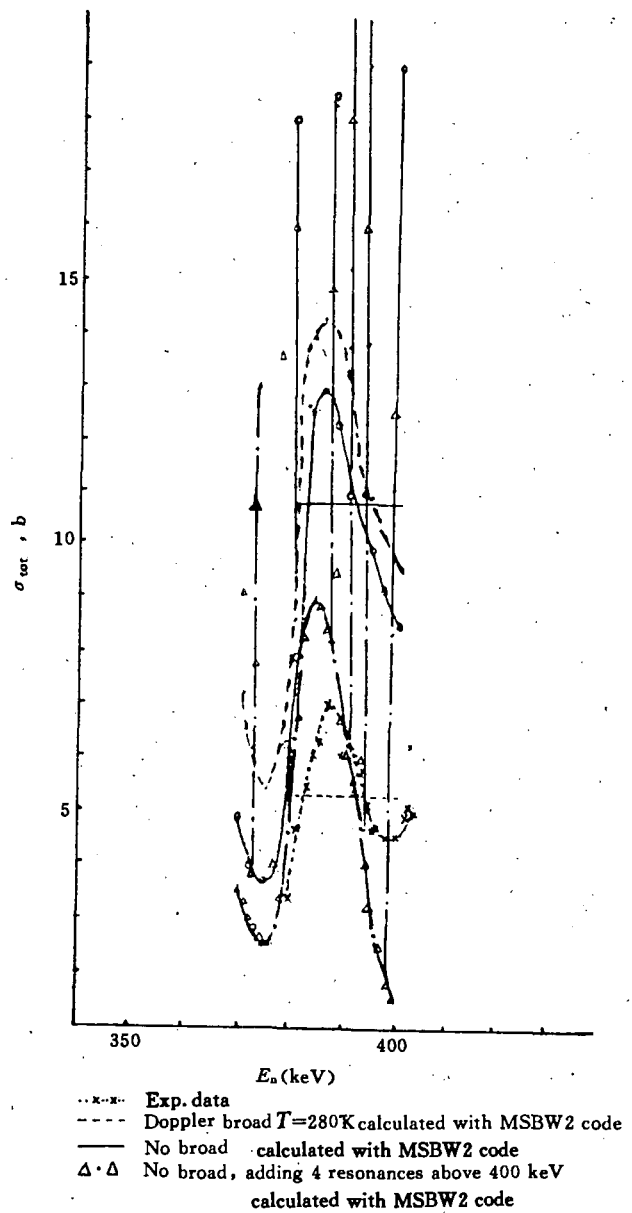

Fig. 11 The adjusting of Fe resonance parameters (Fe total cross section)

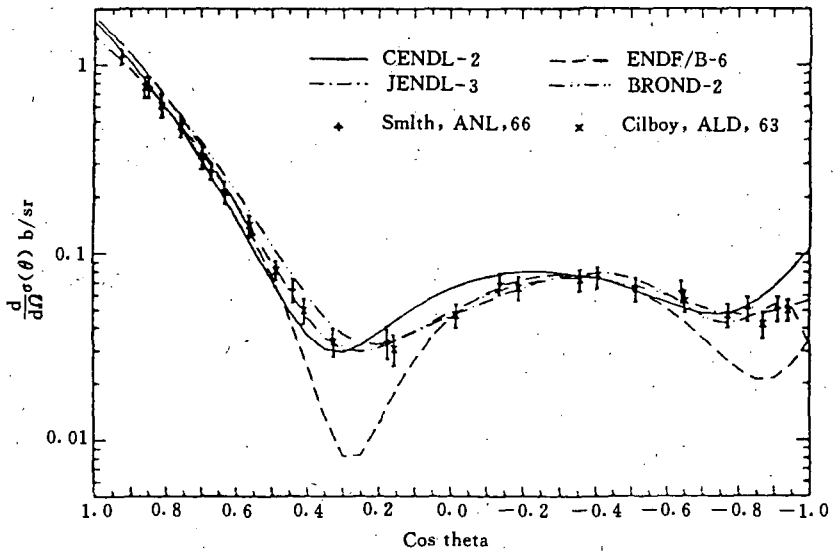

Fig. 13 An example of angular distribution intercomparison : Cr elastic differential cross section at 4.0 MeV

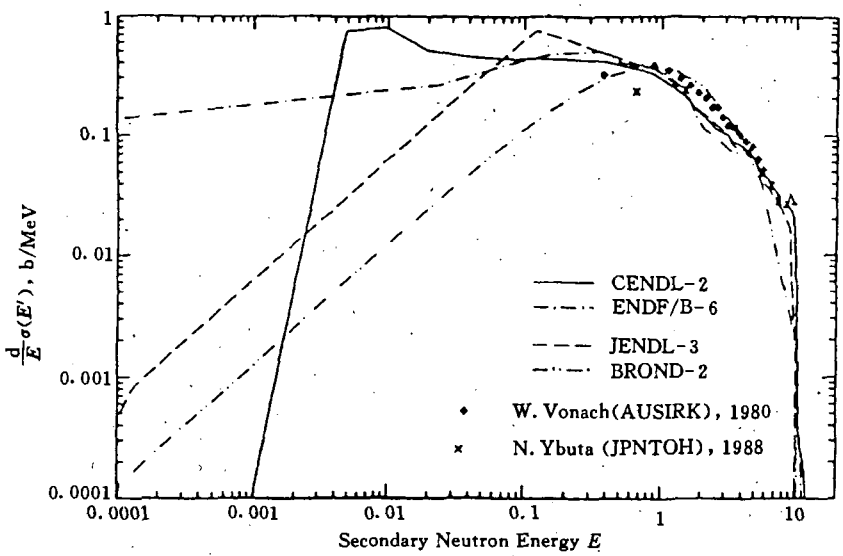

Fig. 14 An example of energy spectrum intercomparison : Ni secondary neutron emission spectrum at 14.1 MeV

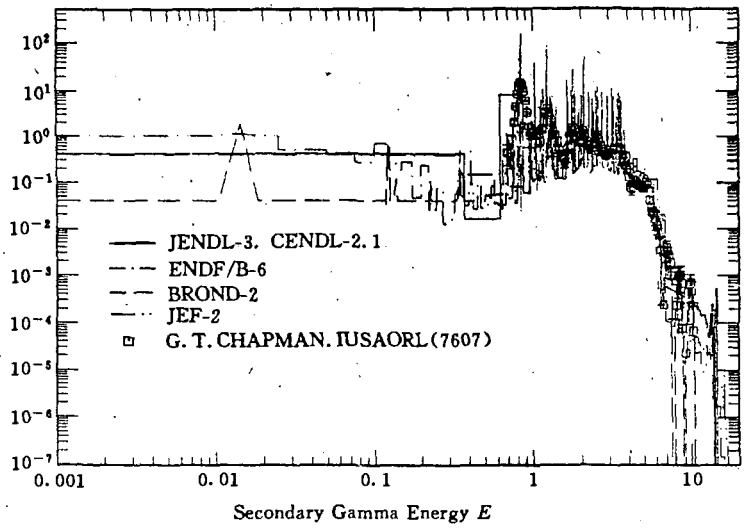

Fig. 15 An example of γ-production spectrum intercomparison : Fe γ emission spectrum at 6.76 MeV

Acknowledgement

The author would like to give the thanks to Drs. Liang Qichang, Shen Linxing, Zhou Hongmo, Chen Baoqian, Liu Renqiu, Zhang Jianhua, Sun Zhengjun, Ma Lizhen for their participating some works on developing the methods and system, to Drs. Zhang Jingshang, Cai Chonghai, Su Zongdi, Zhao Zhixiang, Lu Guoxiong, Zhuang Youxiang for their works relative to this subject. The thanks are also given to C. L. Dunford and Dr. T. Nakagawa for their developing and transplanting ENDF / B system and program CRECTJ5 on Micro-VAX-2 at CNDC respectively.

References

[1] Liu Tingjin et. al., Chinese J. of Nucl. Scie. & Tech., 1, 79(1988)
[2] V. Mclane, Private Communication (1988)
[3] Shen Linxing, Internal Report (1986)
[4] Shen Linxing et. al., Internal Report (1986)
[5] Liu Tingjin et. al., Nuclear Tech., 10, 7(1986)

[6] Zhang Jianhua et. al., CNDP, 10, 132(1993)
[7] Liu Tingjin et al., CNDP, 2, 58(89)
[8] Liu Tingjin et al., CNDP, 11, 116(1994)
[9] Zhou Hongmo et al., Chinese J. of Atomic Ener. Scie. & Tech., 28(5), 403(1994)
[10] A. Horsley et al., Nucl. Instr. & Meth., 62, 29(1968)
[11] Liu Ruizhe, Chinese J. of Atomic Ener. Scie. Tech., 30, 316(1980)
[12] P. Peelle, Private Communication (1987)
[13] Liu Tingjin et al., CNDP, 4, 49, (1990)
[14] Liu Tingjin et al, Chinese J. of Atomic Ener. Scie. Tech., 28(5), 413(1994)
[15] Y. Uenohara et. al., Nucl. Data for Sci. & Tech., 639(1982)
[16] Liu Tingjin, Proc. of Specialists' "Meeting on Covariance Data Evaluation and Processing", Oak Ridge, USA (1992); CNDP, 9, 76(1992)
[17] Liu Tingjin et al., Chinese J. of Nucl. Physics, 14(2), 173(1992)
[18] Lu Hanlin et al., Private Communication (1990)
[19] Liu Tingjin, CNDP, 6 Supplement, 3(1992)
[20] Cai Chonghai et al., Chinese J. of Atomic Ener. Scie. Tech., 23(2), 7 (1989)
[21] Zhang Jingshang, CNDP, 7, 14(1992)
[22] Su Zongdi et al., CNDP, 11, 92(1994)
[23] Lu Guoxiong et al., Private Communication (1988)
[24] Liu Tingjin et al., CNDP, 6, 128(1991)
[25] CNDC, "Neutron Resonance Theory and Parameters", 342(1981)
[26] C. L. Dunford, IAEA–NDS–29 (1993)
[27] T. Nakagawa, Private Communication (1990)
[28] Liu Tingjin et al., Proc. of Symp. on Nucl. Data Eval. Methodology, BNL, USA, 37(1992)
[29] Liu Tingjin et al., (to be published)

The Q—Value for Natural Element

Liu Tingjin

(Chinese Nuclear Data Center, IAE)

Introduction

It is well known that nuclear reaction Q–value is defined[1] as the total kinetic energy of all objects and γ–ray energy produced in the reaction minus the one inducing the reaction. In ENDF / B–6 format, the international adopted format for evaluated neutron nuclear data, two Q–values QM and QI are defined[2]. QM is the mass–difference Q–value, defined as the mass of the target and projectile minus the mass of the residual nucleus in the ground state and masses of all other reaction products. QI is the reaction Q–value for the (lowest energy) state defined by the given MT value in a simple two–body reaction or a breakup reaction. It is defined as QM for the ground state of the residual nucleus (or intermediate system before breakup) minus the energy of the excited level in this system. For the reaction, where the residual nucleus stays at ground state, the two Q–values are the same.

Anyway, the Q–value is definite for given reaction on one nuclide or isotope. But on natural element, consisting of its isotopes, there are different Q–values for the different isotopes. How the Q–value for natural element can be defined, and how make it reasonable in physics and adopted in format of evaluated nuclear data, this is mostly faced and more concerned by the nuclear data evaluators and users, and so far it is ambiguous and vague and need to be studied further.

In ENDF / B–6 format, there is a stipulation for natural element Q–value. It said that if the value of QM is not well defined (as in elements or for summation reactions like MT = 5), use the value of QM which gives the threshold. If there is no threshold, use the most positives Q–value of the component reaction. But it is also pointed out that these ill–defined values of QM can not be relied on for energy–release calculations. It is worth to investigate to what extent the definition is reasonable and why it is ill–defined.

1 Reaction Cross Section

From the standpoint of reaction cross section, only thing is that the reaction threshold is determined by Q–value. It is clear that the reaction for natural element is open, when the reaction is open for any one of all isotopes, no matter how much whose abundance is. An example is given in Fig. 1. So when the reaction Q–values are negative for all isotopes, the reaction threshold is determined by the smallest (absolute value) one of the Q–values, therefore, the smallest Q–value should be taken as the Q–value of the natural element. When the Q–values of all or some isotopes are positive, the reaction for element is non–threshold one, nothing from Q–value could effect the cross section, so in this case, only from the viewpoint of the cross section, any value, e. g. 0 or most positive one, is all right.

2 Energy Spectrum

As well known, in a nuclear reaction, various particles, e. g. neutron, γ–ray and charged particles, could be emitted, and they have own energy distributions. From the standpoint of energy spectrum, the maximum energy of the spectrum of outgoing particle is determined by its reaction Q–value. For natural element, the maximum of the outgoing particle spectrum is determined by the largest one of all reaction Q–values (for negative Q–value, the absolute value smallest one). An example is given in Fig. 2. So the largest one of all isotopes' Q–values should be taken as the Q–value of natural element.

3 Energy Balance

The energy taken by outgoing particles is very important in nuclear engineering calculation. So more and more attention has been payed to energy balance in complete nuclear data evaluation[3], and there is a special code in ENDF / B utility program system[4] for checking it.

As well known, in a nuclear reaction, the total available energy is determined by the incident particle energy and reaction Q–value, and the energy taken by outgoing neutron and / or charged particle, recoil nucleus and γ–rays emitted following the deexcitation of residual nucleus can be calculated from their spectra and γ–production multiplicity. Both the "available" and "taken" energy should be equal with each other, that is called as energy balance. It can be seen that the energy balance is a quite complicated matter. Firstly, the "taken" energy concerns the spectra of all outgoing particles and γ–production multiplicity. All of these must be correct to insure the "taken" energy is a correct one. Secondly, the "available" energy concerns the reaction Q–value. This

is simple for a nuclide, but is more complicated and somewhat ambiguous for natural element, need to be discussed here.

The secondary neutron (others are the same) spectrum produced from natural element is the sum of all isotopes' spectra, taking $R_i(E)$ as the weight, the cross section ratio

$$R_i(E) = \frac{A_i \sigma_i(E)}{\sum_i \sigma_i(E) A_i} \tag{1}$$

where A_i is the abundance of i–th isotope in the element and $\sigma_i(E)$ is the reaction cross section of i–th isotope at the same energy point E for the same kind of reaction. Correspondingly, the contribution to the "available" reaction energy of i–th isotope

$$Q_{ai}(E) = Q_i \; R_i(E) \tag{2}$$

where Q_i is the Q–value of i–th isotope. So the available Q–value for natural element should be

$$Q_a(E) = \sum_i Q_{ai}(E) \tag{3}$$

Here, the available Q_a–value is relative to the cross section, so it is relative to the incident particle energy.

4 Conclusion Remarks

It can be seen from the discussed above that from different view of point, the reasonable Q–value in physics for natural element is different : for cross section Q = minimum $\{ |Q_i| \}$; for energy spectrum Q = maximum $\{ Q_i \}$; for energy balance, $Q = Q_a(E) = \sum Q_i \; R_i(E)$. So for different purpose, different Q–value should be taken for natural element to make it reasonable in physics.

So far as the Q–value definitions and some stipulations for natural element in ENDF / B–6 format, it is reasonable for cross section and spectrum, but is ill–defined for energy balance. According to the format, the minimum absolute Q and most positive Q are taken as natural element Q–value for negative and positive Q–value respectively. All of these, the "available" energy is overestimated, especially in the case that the abundance of the isotope corre-

sponding Q–value taken is very small and the difference of the Q–value with others is large.

So, in this case, if the spectra of outgoing particles and the γ–production multiplicity are correct,the "taken" energy must be much smaller than "available" energy, and if there are some problems for the spectra and / or multiplicity, the "taken" energy could be much larger than the correct "available" energy, but may be not than this one. It should be specially emphasized here that for natural element, even there is no warning pointed out by the check program, that does not mean no problem for energy balance if the Q–value is given according to the ENDF / B–6 stipulation.

It is better to define a Q–value for natural element according to formulas (2), (3). This is energy relative, and could be put into the table head of files 5 or 6 in ENDF / B–6 format for each incident neutron energy and specially used for energy balance checking. It is suggested that this could be considered when the ENDF / B–6 format is updated in future.

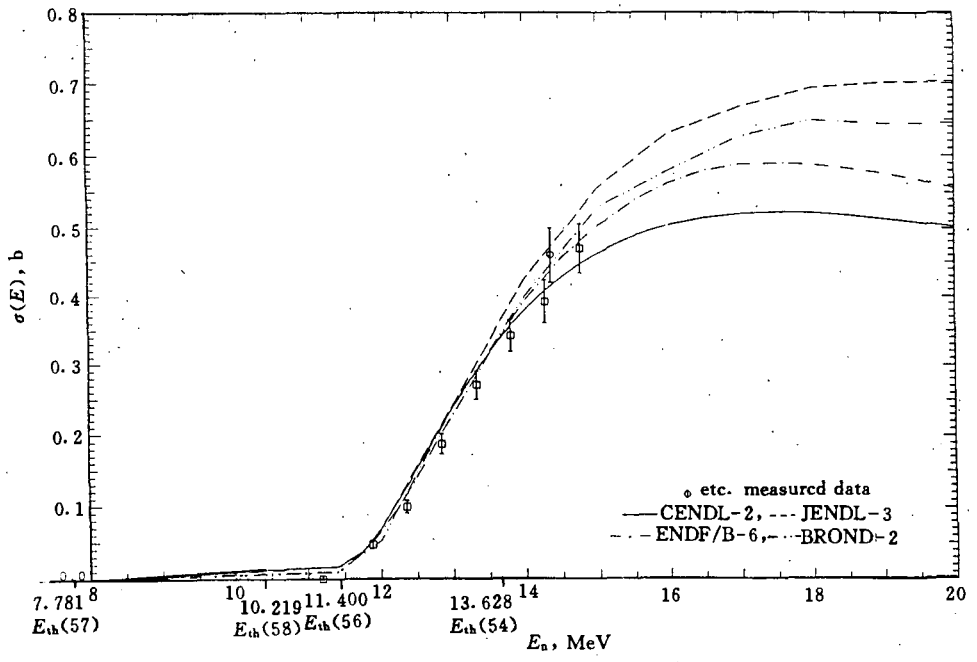

Fig. 1 Natural Fe(n,2n) cross section

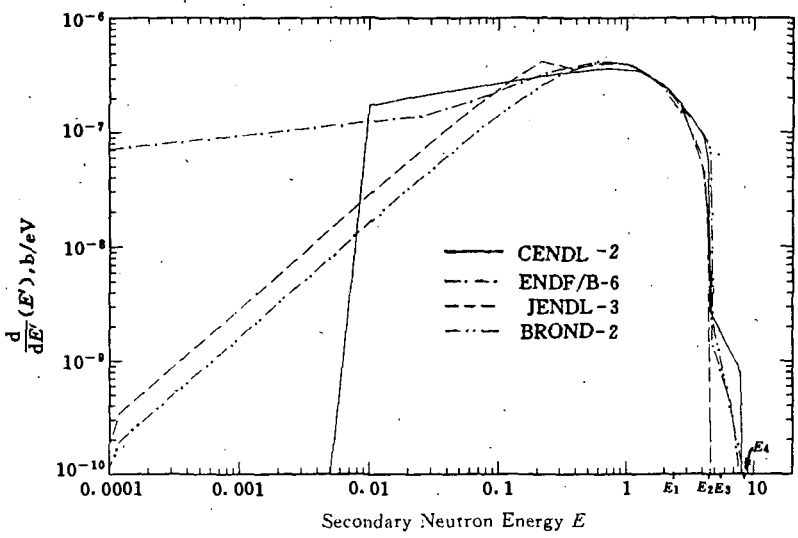

Fig. 2 The secondary neutron energy spectrum of natural Fe(n,2n) reaction at 18.0 MeV

E_1 : E_{max}(54) 2.331 MeV, E_2 : E_{max}(56) 4.521 MeV,

E_3 : E_{max}(58) 5.685 MeV, E_4 : E_{max}(57) 8.087 MeV.

References

[1] Science Press, "The Terms in Physics" (1990)

[2] P. F. Rose and C. L. Dunford, ENDF–102(1992)

[3] R. E. MacFarlane, Nuclear Data for Scie. & Tech., 780(1994)

[4] C. L. Dunford, IAEA–NDS–29 (1993)

Revision of the Inelastic Scattering Cross Section Evaluation of ^{238}U for CENDL-2.1

Tang Guoyou Zhang Guohui Shi Zhaomin Chen Jinxiang

(IHIP, Peking University, Beijing)

The evaluated neutron nuclear data set for ^{238}U is quite important for fission reactor technology. Maybe we can say that the available evaluations for ^{238}U in various libraries are in good agreement with each other and good enough for uses except the secondary neutron spectra and / or the inelastic scattering cross sections for which the discrepancies exist among the various evaluations. And to some extent, the discrepancies also exist between the evaluations and the experimental results of benchmark testing.

In our original evaluation of ^{238}U for CENDL-2[1, 2], the direct processes in inelastic scattering are only considered via coupled-channel optical model calculations for 0^+, 2^+ and 4^+ states[3]. From Refs. [1, 2] we can see that our evaluation is also in agreement with the other evaluations for various libraries except the total inelastic scattering cross sections for which large discrepancies exist especially below 6 MeV. Actually our total inelastic scattering cross section evaluations (see Fig. 1) are in good agreement with the recent experimental data provided by M. Baba[4] and previous data of R. Batchelor[5]. However, benchmark calculation for the evaluated data set of ^{238}U for CENDL-2 showed that the total inelastic scattering cross sections are too low and / or the secondary neutron spectra are too hard. Obviously, this problem may be resolved with enhancing the total inelastic scattering cross sections and reducing the elastic scattering cross sections or increasing the inelastic scattering cross sections to the lowest lying levels (2^+, 4^+ and 6^+). In this way, however, the secondary neutron spectra can not be changed essentially since the energies of the inelastic scattering groups from 2^+, 4^+, 6^+ states are nearly the same as the elastic groups. Actually, it is difficult to identify them in the experimental measurements. Fortunately, for application purposes, all of these groups can be approximately considered as elastic neutrons. In this sense, what we should do is to coincide the sums of the cross sections scattered to 0^+, 2^+, 4^+ and 6^+ states with the experimental values correspondingly. In this revision, such sums have been adjusted to the measured data by A. B. Smith et al.[6], as shown in Fig. 2.

Then, in order to improve the total inelastic scattering cross sections and / or the secondary neutron spectra essentially, we must enhance the inelastic scattering to the higher lying states, for example, 1^-, 3^-, 5^- and even more higher levels based on measured data. In this revision, direct components to 14 levels (6^+ and above) are calculated by using DWUCK4 in addition to the FMT (written by Zhang Jingshang based on semi-classical theory of multi-step nuclear reaction processes) calculations, and the β values was adjusted so that the calculations coincide with the measured data for discrete levels[7~10] and double-differential neutron emission cross sections at 14 MeV [11~13].

Some evaluated results are shown in the Figs. 1~9. For comparisons, the corresponding evaluated data of ENDF / B-6 and JENDL-3 and experimental data are also shown in these figures.

By using the present version for inelastic scattering of ^{238}U, the results of data testing for homogeneous fast benchmark assemblies are in better agreement with experimental values[14] than the others.

Acknowledgement

The authors would like to thank Dr. Zhou Delin for the beneficial discussions during this work and Drs. Zhang Jingshang and Shen Qingbiao for their helps in the model theory calculations.

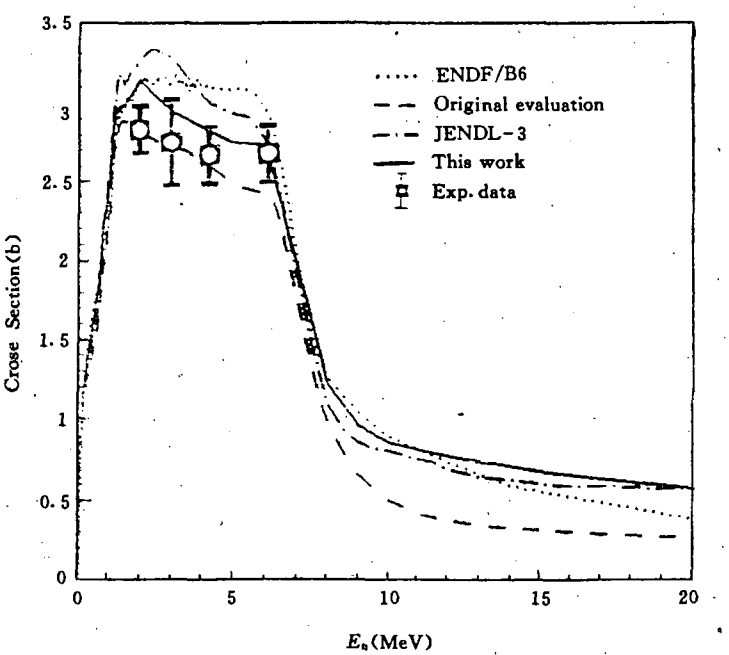

Fig. 1 Total inelastic scattering cross section

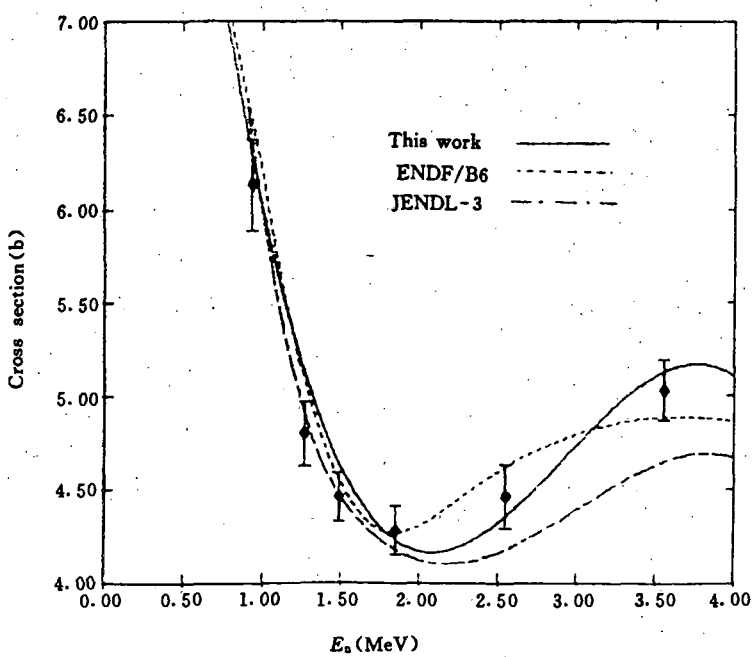

Fig. 2 Sum of the scattering cross sections to 0^+, 2^+, 4^+ and 6^+ states

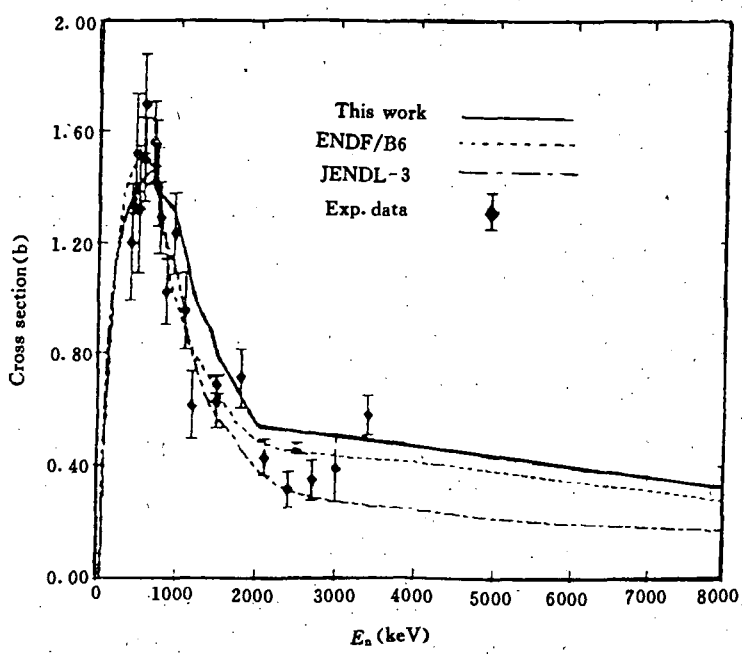

Fig. 3 Inelastic scattering cross section to 2^+ (44.89 keV) state

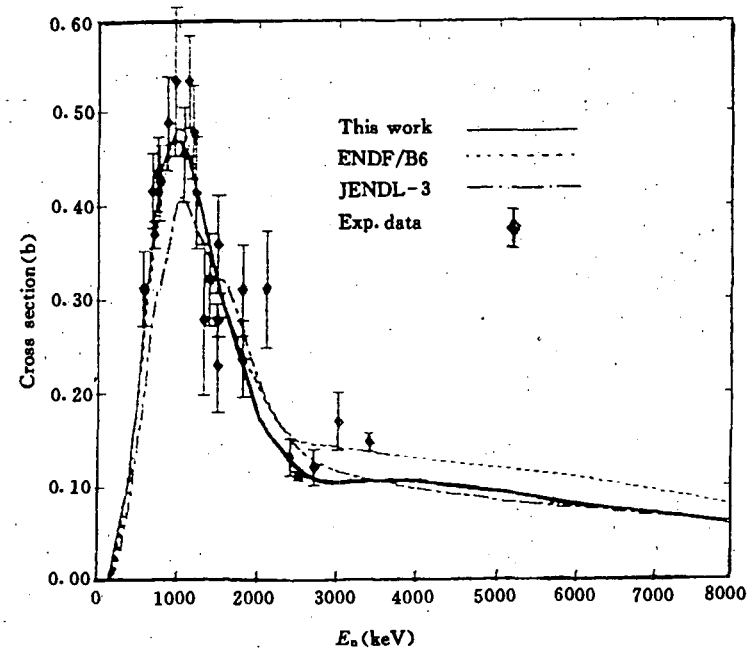

Fig. 4 Inelastic scattering cross section to 4^+ (148.4 keV) state

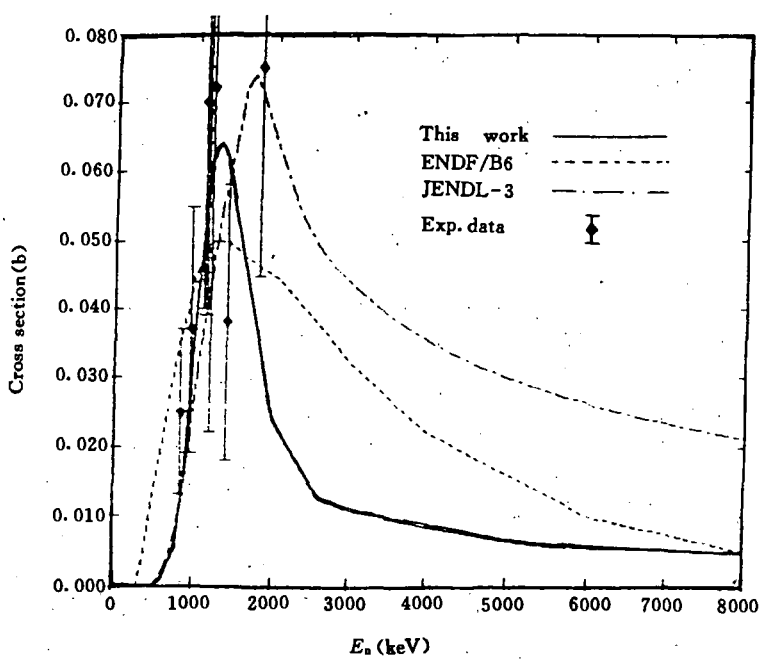

Fig. 5 Inelastic scattering cross section to 6^+ (307.2 keV) state

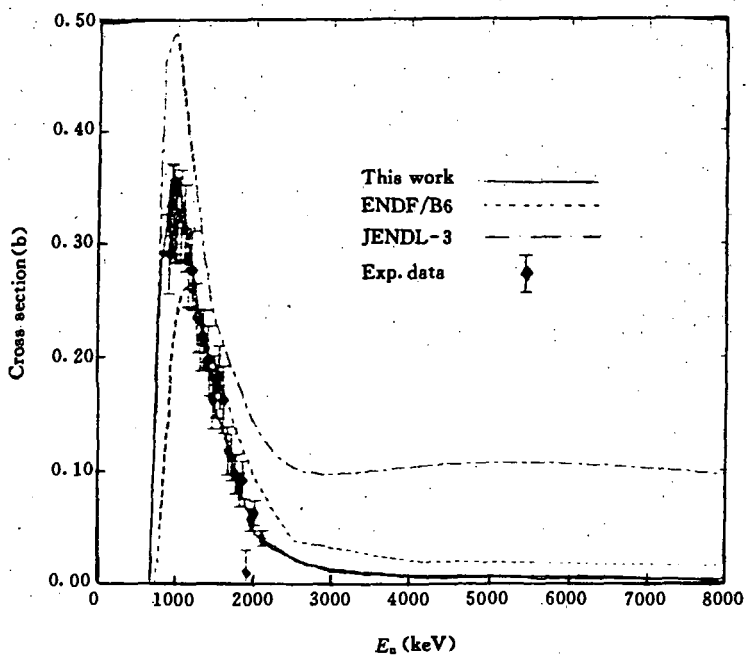

Fig. 6 Inelastic scattering cross section to 1^- (680.1 keV) state

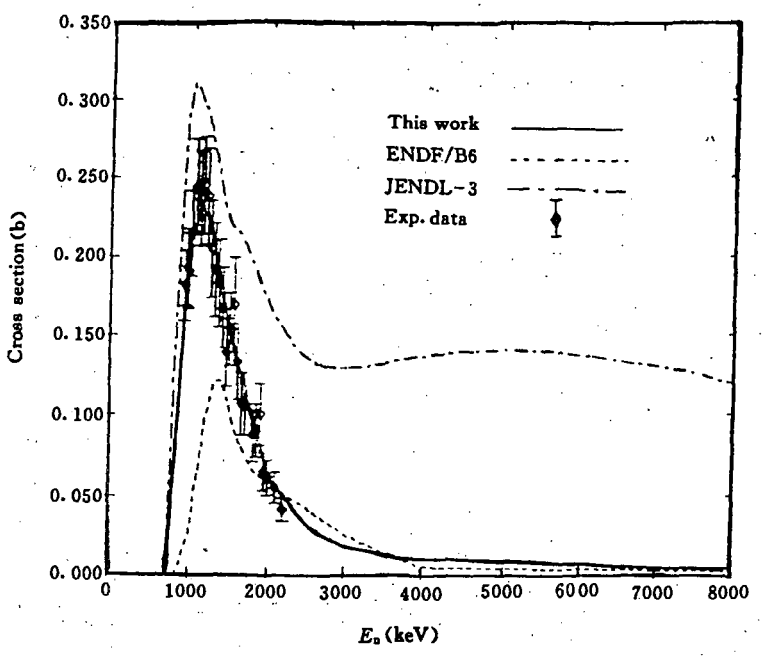

Fig. 7 Inelastic scattering cross section to 3^- (731.9 keV) state

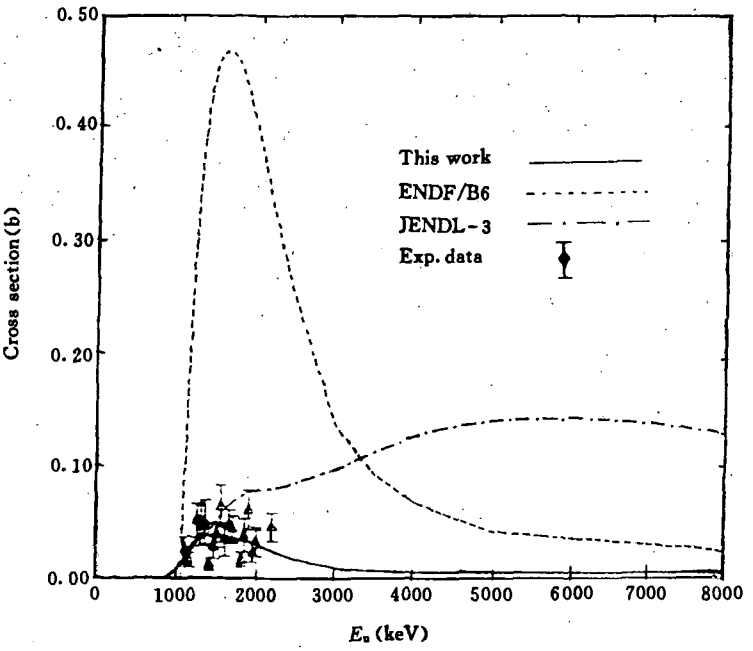

Fig. 8 Inelastic scattering cross section to 5^- (827.1 keV) state

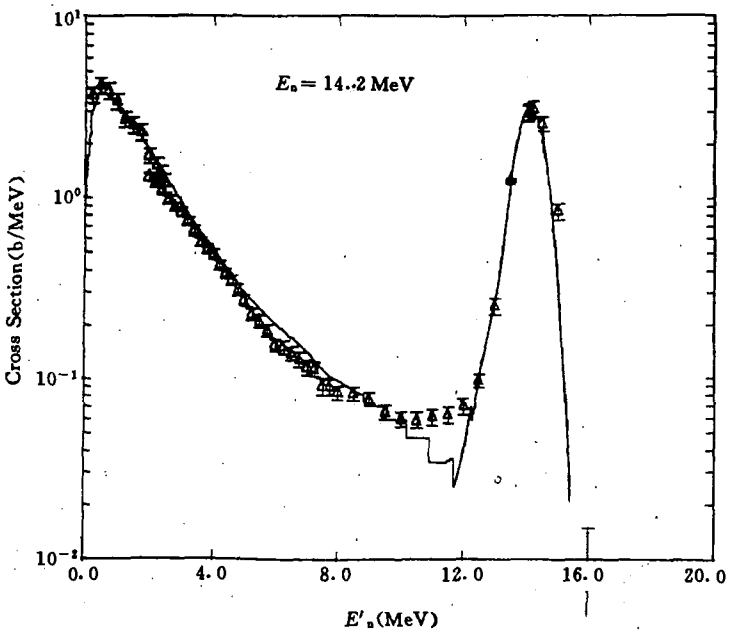

Fig. 9 Calculated secondary neutron spectrum at E_n = 14.2 MeV

References

[1] Tang Guoyou et al., CNDC–0008 p. 279 (1991)
[2] Tang Guoyou et al., CNDC–0012 p. 53 (1993)
[3] Shen Qingbiao, INDC(CPR)–029 / L p. 35(1992)
[4] M. Baba et al., J. Nucl. Sci. & Techn., 27, 601(1990)
[5] R. Batchelor et al., Nucl.Phys., 65, 236 (1965)
[6] A. B. Smith et al., Proc. of Inter. Conf. Nucl. Data for Sci. and Tech., Antwerp, Belgium, p. 39, 6～10 September, 1982
[7] L. E. Beghian et al., NSE, 69, 191(1979)
[8] P. Guenther et al., ANL–NDM–16 (1975)
[9] G. Haouat et al., NSE, 81, 491(1982)
[10] J. Q. Shao et al., NSE, 92, 350(1986)
[11] Shen Guanren et al., Proc.of Inter. Conf. Nuclear Data for Sci. and Tech., Mito, Japan, p. 201, 30 May ～ 3 Jun, 1988
[12] M. Baba et al., Proc. of Inter. Conf. Nucl. Data for Sci. and Tech., Julich, Fed. Rep. of Germany, p. 349, 13～17 May, 1991
[13] M. Baba et al., INDC(JPN)–153 / U p. 109(1991)
[14] Liu Guisheng CNDP, No. 13, 1995

Evaluation of Cross Sections for Neutron Monitor Reactions $^{54,56\sim58,Nat}Fe(n,x)^{51}Cr$, $^{52,54,56}Mn$ from Threshold to 60 MeV

Yu Baosheng Shen Qingbiao Cai Dunjiu

(Chinese Nuclear Data Center, IAE)

The cross sections for $^{54,56,Nat}Fe(n,x)^{51}Cr$, $^{52,54}Mn$ reactions from threshold to 50 MeV have been evaluated and published[1]. In order to extend the energy region up to 60 MeV, the pertinent methods have been provided. Because the knowledge of evaluated and calculated data below 50 MeV were described in previous works [1, 2], here we give the new data including the evaluation of the

cross section for $^{56}Fe(n,x)^{56}Mn$, which are shown in Figs. 1～8.

The $^{56}Fe(n,p)^{56}Mn$ reaction is as a neutron monitor reaction in intermediate energy region. There exist lots of experimental data from threshold to 20 MeV, especially at 14.6 MeV. Among them, the cross sections at 14.56 MeV and 13～18 MeV energy region were measured by Li Jizhou[3] in 1989 at CIAE, at 14.6 MeV by Zhou Muyao[4] at China Shanghai University of Science and Technology. The cross sections measured by Bao Zongyu[5] at CIAE in 1993 has been successfully examined through the international comparisons among several national standard laboratory.

These measured results at 14.6 MeV from different laboratories in China are in good agreement within the uncertainties. The recommended value at 14.6 MeV was obtained on the basis of Chinese measured data and the latest data from other laboratories abroad. In present work, the recommended value at 14.6 MeV is 109.02 ± 1.2 mb.

Above 13 MeV, the new measured data with small uncertainty are in agreement with the result of 14.6 MeV, they were measured by T. B. Ryves[6] from 15 to 19 MeV, K. Kudo[7] from 14 to 20 MeV, Y. Ikeda[8] from 12 to 14 MeV, Li Jizhou[3] from 13 to 20 MeV.

Below 13 MeV, the experimental data were measured by D. C. Santry[9], D. L. Smith[10], Yu. A. Nemilov[11], J. A. Grundl[12], S. K. Saraf[13]. The Santry's data covers energy region from 5.3 to 20 MeV, and it is in agreement with present data at 14.6 MeV. These data were adopted, they are in agreement with the precise value at 8 MeV measured by Saraf[13]. Therefore the recommended curve is reliable.

The measured data mentioned above can determine the curve shape of $^{56}Fe(n,p)^{56}Mn$ reaction from threshold to 20 MeV. The calculated data are close to the experimental data from 18 to 20 MeV energy region. The recommended cross section for $^{56}Fe(n,p)^{56}Mn$ reaction are based on the experimental data below 20 MeV and theoretical calculated data above 20 MeV, shown in Fig. 4.

The evaluated results of the natural iron are sum of the evaluated results of ^{56}Fe and the calculated results of $^{54, 57, 58}Fe$ according to the abundance of isotopes, the recommended data for $^{Nat}Fe(n,x)^{56}Mn$ reaction are shown in Fig. 5.

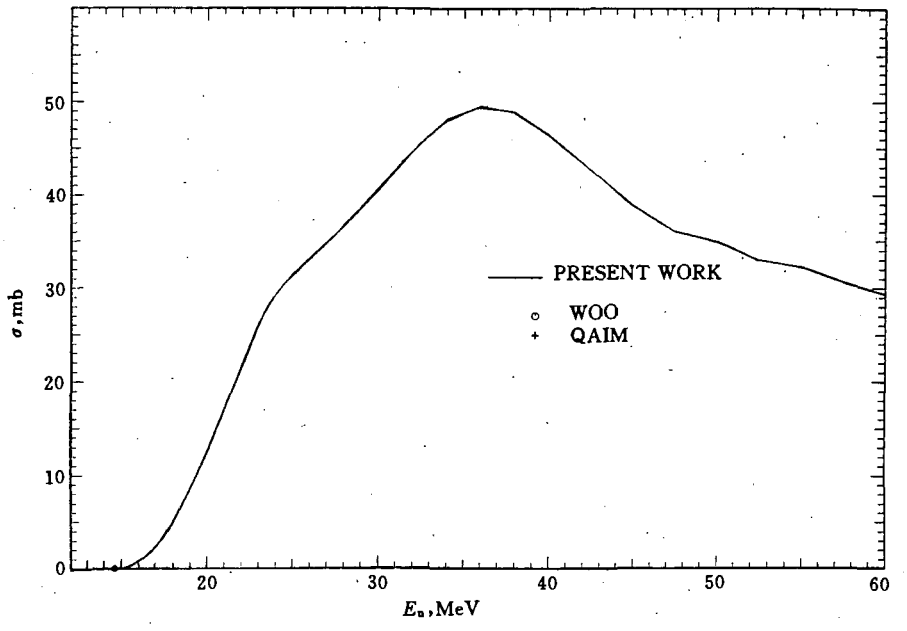

Fig. 1 Comparison of evaluated cross sections with experimental data for $^{54}Fe(n,x)^{52}Mn$ reaction cross sections

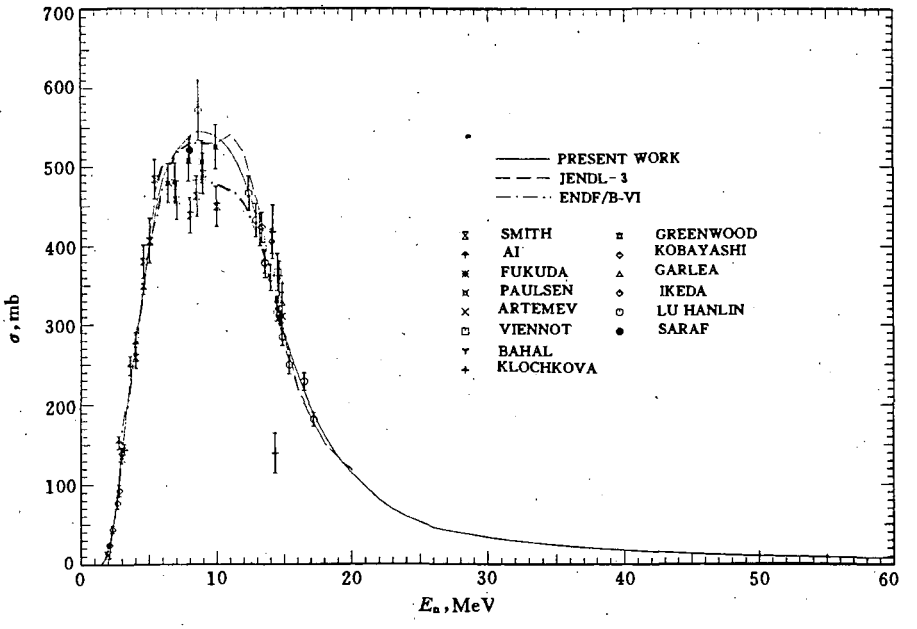

Fig. 2 Comparison of evaluated cross sections with experimental data for $^{54}Fe(n,x)^{54}Mn$ reaction cross sections

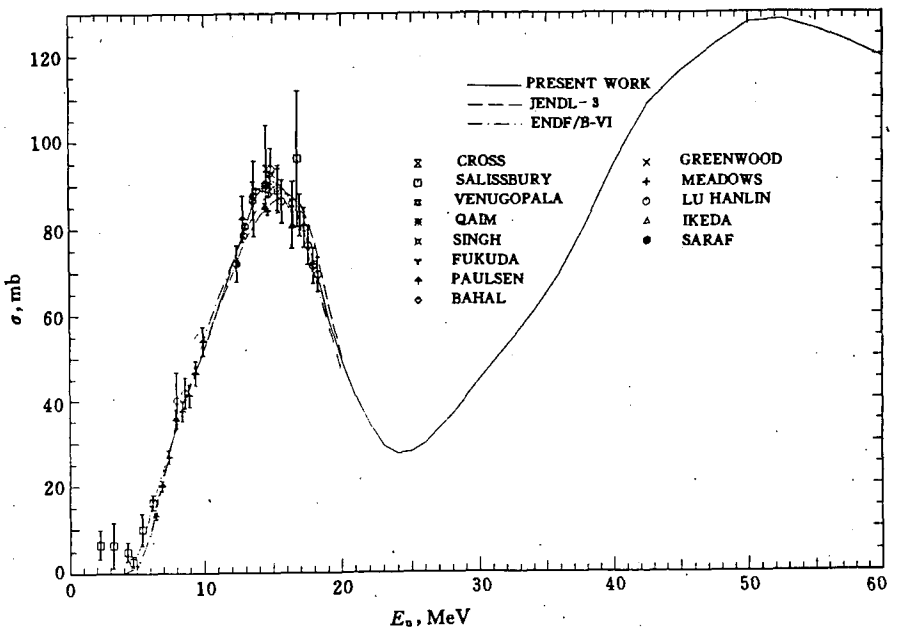

Fig. 3 Comparison of evaluated cross sections with experimental data for $^{54}Fe(n,x)^{51}Cr$ reaction cross sections

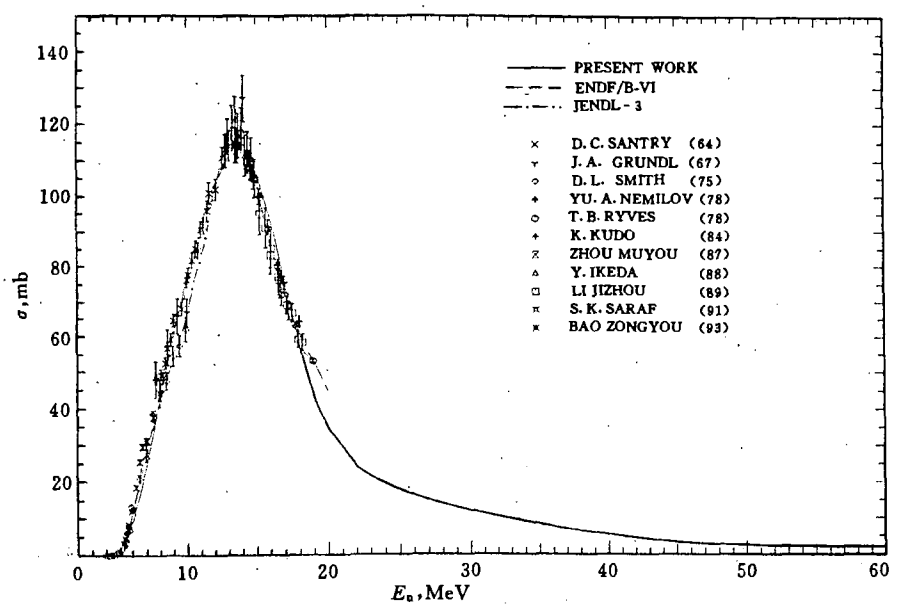

Fig. 4 Comparison of evaluated cross sections with experimental data for $^{56}Fe(n,x)^{56}Mn$ reaction cross sections

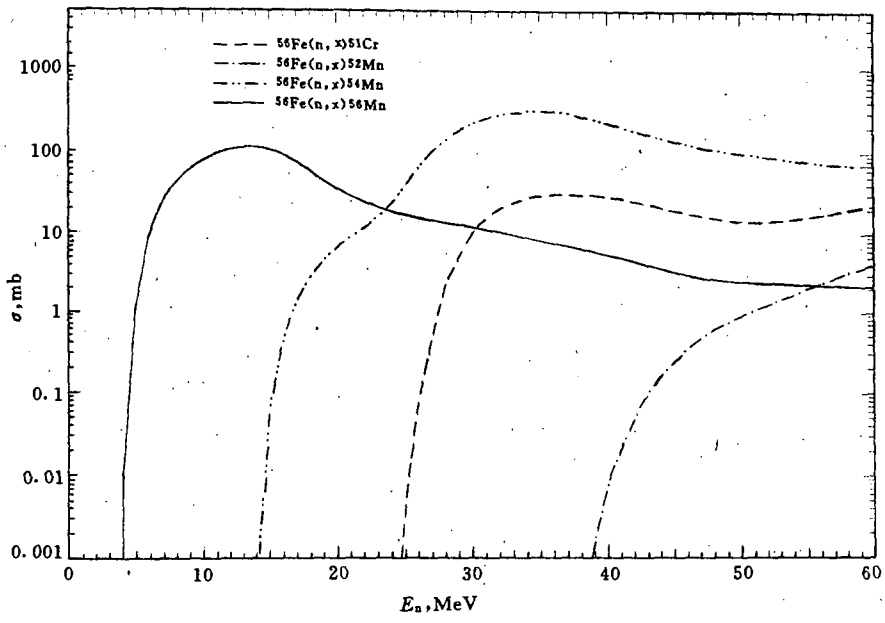

Fig. 5 Recommended cross sections for $^{56}Fe(n,x)^{51}Cr$, $^{52,54,56}Mn$ reactions

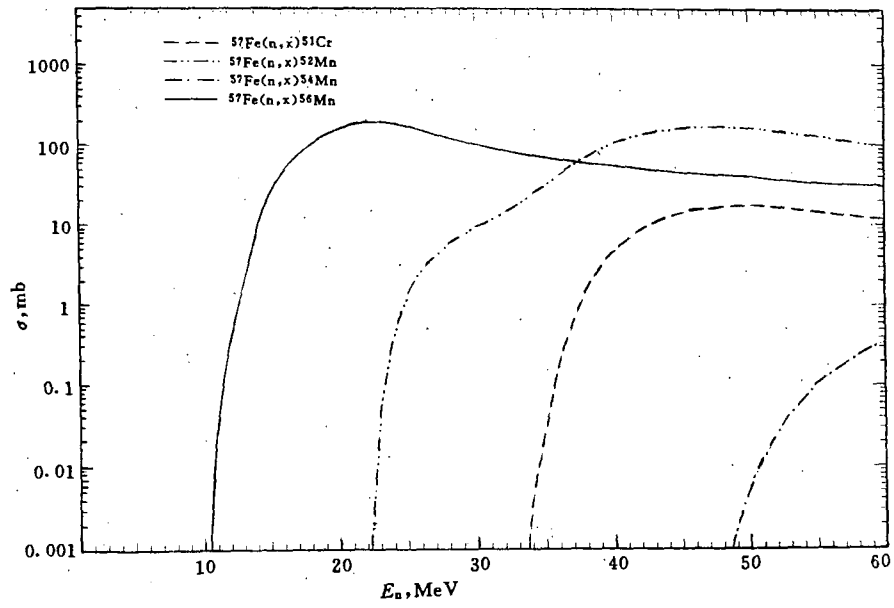

Fig. 6 Recommended cross sections for $^{57}Fe(n,x)^{51}Cr$, $^{52,54,56}Mn$ reactions

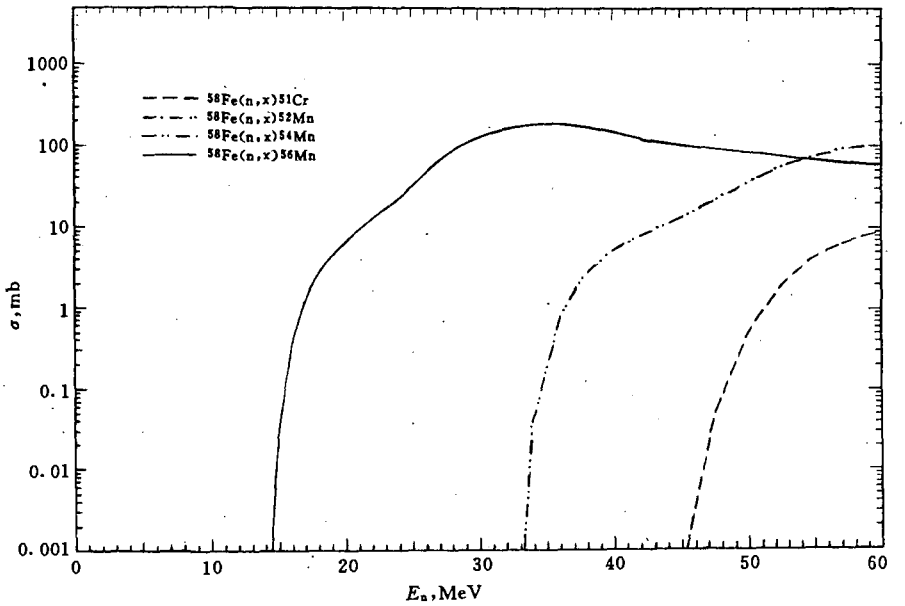

Fig. 7 Recommended cross sections for $^{58}Fe(n,x)^{51}Cr$, $^{52,54,56}Mn$ reactions

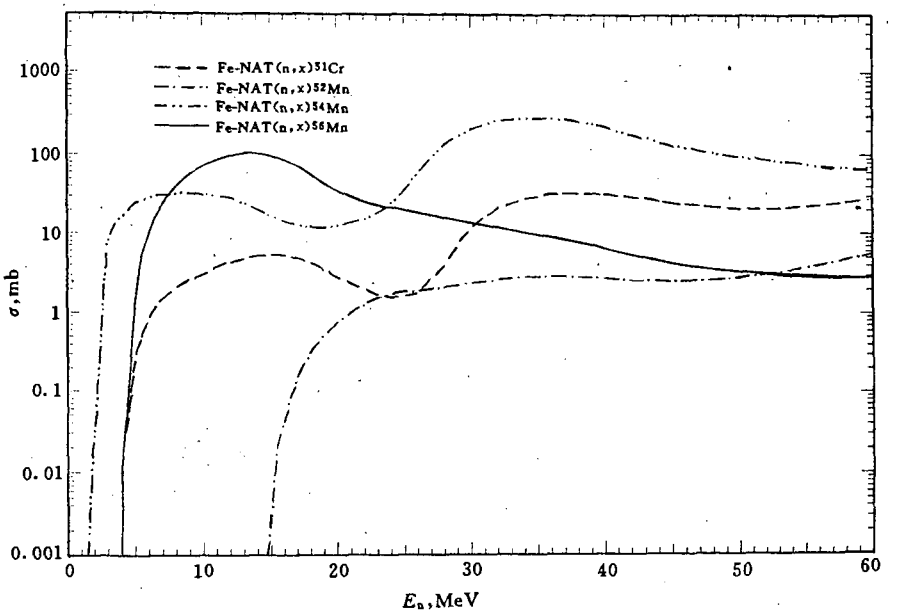

Fig. 8 Recommended cross sections for $^{Nat}Fe(n,x)^{51}Cr$, $^{52,54,56}Mn$ reactions

References

[1] Yu Baosheng et al., Evaluation of Cross Sections for Neutron Monitor Reactions $^{54, 56, Nat}Fe(n,x)^{51}Cr$, $^{52, 54}Mn$, INDC(CPR)–032 / L, p. 79(1993)

[2] Sheng Qingbiao et al., Calculation of $^{54, 56\sim 58, Nat}Fe(n,x)^{51}Cr$, $^{52, 54, 56}Mn$ Reaction Cross Sections up to 60 MeV, INDC(CPR)–032 / L, p. 31(1993)

[3] Li Jizhou et al., INDC(CPR)–16 (1989)

[4] Zhou Muyao et al., Chinese Journal of Nuclear Physics, 9, 34(1987)

[5] Bao Zongyu et al., Chinese Journal of Nuclear Physics, 15, 341(1993)

[6] T. B. Ryves et al., EXFOR Data 20772003

[7] K. Kudo et al., NEANDC(J)–83 / U (1984)

[8] Y. Ikeda et al., JAERI–1312 (1988)

[9] D. C. Santry et al., EXFOR Data 11701002

[10] D. L. Smith et al., Nucl. Sci. and Eng., 58, 314(1975)

[11] Yu. A. Nemilov et al., EXFOR Data 40485002 .

[12] J. A. Grundl et al., Nucl. Sci. and Eng., 30, 39(1967)

[13] S. K. Saraf et al., Nucl. Sci. and Eng., 107, 365(1991)

Evaluation of Neutron Monitor Cross Sections for $^{63, 65, Nat}Cu(n,x)^{56\sim 58, 60}Co$ Reactions from Threshold to 70 MeV

Yu Baosheng Shen Qingbiao Cai Dunjiu

(Chinese Nuclear Data Center, IAE)

Abstract

The cross sections for monitor reactions $^{63, 65, Nat}Cu(n,x)^{56\sim 58, 60}Co$ were analysed and evaluated based on measured data and theoretically calculated results from threshold up to 70 MeV. The recommended data could reproduce the experimental data very well. In higher energy region, the data were provided by theoretical calculation with adjusted model parameters based on measured

data.

Introduction

The neutron monitor cross sections for bombarding copper with intermediate energy are very important from the view point of monitoring high energy neutron field in the context of radiation induced material damage, radiation safety, neutron dosimetry, etc..

The natural copper consists of two isotopes, i. e. ^{63}Cu (69.17 %), ^{65}Cu (30.83 %). At present work, the monitor reactions, for which the cross sections were evaluated, are ^{63}Cu(n,x)$^{56\sim58,60}$Co, ^{65}Cu(n,x)$^{56\sim58,60}$Co and ^{Nat}Cu(n,x)$^{56\sim58,60}$Co.

For these cross section measurements there exist some difficulties for no good monoenergetic neutron source and numerous reactions in samples. Therefore, the experimental data are scarce in higher energy region. In order to recommend the cross sections of product nuclei mentioned above, the available experimental data were evaluated so as to guide the theory calculation for higher energy region. The parameters for the model calculation were adjusted refering to some measured data. The pertinent calculations[1] were performed.

1 Experimental Data Required for Adjusting Model Parameters

Based on the available experimental data of total and nonelastic cross sections and elastic scattering angular distributions data for natural copper and its isotopes ^{63}Cu and ^{65}Cu, a set of neutron optical potential parameters for ^{63}Cu and ^{65}Cu in energy region 2~ 80 MeV was obtained. Then, adjusting some charged particle optical potential and level density parameters as well as the exciton model constant, the calculated nuclear data, such as (n,2n), (n,d), (n,α) and (n,α–em) cross sections on ^{63}Cu and (n,2n), (n,d), (n,α), (n,α–em) and (n,p–em) cross sections on ^{65}Cu, are in good agreement with the experimental data. Therefore, the predicted cross sections and yields are reliable.

2 Evaluation of Cross Sections for Monitor Reactions ^{63,65,Nat}Cu(n,x)$^{56\sim58,60}$Co

2.1 ^{63}Cu(n,x)$^{56\sim58,60}$Co reactions

According to the analyses of the calculated results for producing activation products $^{56\sim58,60}$Co from ^{63}Cu(n,x) reactions, the contribution of the second

particle emission can be neglected when $E_n < 20$ MeV. The activation product ^{60}Co comes from $^{63}Cu(n,\alpha)$ reaction and $^{56\sim58}Co$ can not be produced below 20 MeV since their threshold values are higher than 20 MeV.

The available measured cross sections for $^{63}Cu(n,\alpha)^{60}Co$ reaction were collected and analysed. These data[2~17] are shown in Table 1 and Figs. 1.1, 1.2. Most of the experimental data up to 1993 have been included. Many data were retrieved from EXFOR files, enriched with new information as well as CIAE, LNE (Lanzhou University) experimental results.

There are 18 sets of data from 16 authors, which cover from threshold to 20 MeV. Among them, 15 sets provide the data around 14 MeV. For the cross section of activation product ^{60}Co from $^{63}Cu(n,\alpha)$ reaction, the measured data around 14 MeV exist large discrepancy. Recently, some new measurements for the data around 14 MeV were carried out by Wang Yongchang[13], Ikeda[14], Csikai[15], Meadows[16] and Lu Hanlin[17]. In order to reduce the discrepancy of the measured values around 14 MeV, the measured values were renormalized at 14.6 MeV.

For evaluating the data at 14.6 MeV, all collected cross sections around 14 MeV were adjusted for energy to equivalent 14.6 MeV cross section, which depends on the shape of the excitation curve for $^{63}Cu(n,\alpha)^{60}Co$ reaction. In order to obtain the factors of energy adjustment values, the data of Hetrick et al[18]. were used. The data around 14 MeV were also renormalized using the same standard cross section taken from Refs. [19] and [20]. The relevant cross section and energy adjusted factors R_1 and R_2 are also given in Table 1 separately, in which σ_0 and σ represent the original and adjusted cross sections, respectively.

The half–life of ^{60}Co is 5.271 years and the characteristic gamma ray of 1173 keV of the product has a branching ratio 99.89 %. The characters of gamma ray of ^{60}Co have not change to any significant extent for many years. The errors due to uncertainties in decay data were small and were within the quoted errors. Therefore, the half–life and branching ratio for this reaction were unnecessary to revise

After adjustment, the evaluation was done for 15 cross section values at 14.6 MeV. The data were rejected if there are larger discrepancies with others and exceed the averaged value by three standard deviation.

The second step, the remainder adjusted data were averaged with the weight factors based on the given errors by authors and quoted errors by us. Present evaluated value is 47.6 ± 2.1 mb at 14.6 MeV, as shown in Fig. 2.

In order to obtain the evaluated data from threshold to 20 MeV, The measured data by Paulsen[3], Wang Yongchang[13], Ikeda[14], Csikai[15], Lu Hanlin [17] were renormalized with our recommended value at 14.6 MeV. Only

the data obtained by Winkler[12] were adopted below 6.5 MeV.The measured data and the tend of evaluated data from ENDF / B–6 were considered in the energy region 8～12 MeV. The data were fitted with orthogonal polynomial.

The cross sections for $^{63}Cu(n,x)^{60}Co$ reactions were calculated from threshold to 70 MeV. The theoretically calculated values are very close to the experimental data, especially the calculated values consist with the experimental data between 18 and 20 MeV. Therefore, the calculated data above 20 MeV were recommended.

For $^{63}Cu(n,x)^{56\sim 58}Co$ reactions, the model parameters used in calculation are the same as for $^{63}Cu(n,\alpha)^{60}Co$. The recommended data for $^{63}Cu(n,x)^{56\sim 58, 60}Co$ reactions from threshold to 70 MeV were got, based on experimental and calculated data (Fig. 3).

2.2 For $^{65, Nat}Cu(n,x)^{56\sim 58, 60}Co$ reactions

The cross sections for monitor reactions $^{65}Cu(n,x)^{56\sim 58, 60}Co$ are belong to multi particles emission and the experimental data are very scarce. Therefore, the recommended data come from the theoretical calculations. The calculations were tested with other available experimental data, such as (n,tot), (n,el), (n,non), (n,2n), (n,γ), (n,d), (n,p), (n,α), (n,t) etc.. The recommended data are shown in Fig. 4.

For natural copper, the evaluation of cross sections are based on the evaluated values of $^{63}Cu(n,\alpha)^{60}Co$ reaction and the calculated result for $^{63, 65}Cu$. The data for the natural copper are sum of the calculated results of ^{65}Cu and the evaluated results of ^{63}Cu according to the abundance of isotopes. The recommended data for $^{Nat}Cu(n,x)^{56\sim 58, 60}Co$ reactions are shown in Fig. 5 .

3 Summary

The cross sections for monitor reactions $^{63, 65, Nat}Cu(n,x)^{56\sim 58, 60}Co$ have been evaluated, based on the experimental data below 20 MeV and the theoretically calculated values of multi–particle emission at higher energies. The used model parameters were determined based on experimental data. The recommended data are reliable. The present results for $^{63}Cu(n,x)^{60}Co$ monitor reactions were compared with ENDF / B–6 and JENDL–3 below 20 MeV. It was shown that our results could reproduce experimental data very well.

Acknowledgements

The authors are indebted to IAEA (International Atomic Energy Agency), CNNC (China National Nuclear Corporation) and CIAE for their supports, and thank to Drs. N. P. Kocherov, T. Benson, O. Schwerer, Lu Hanlin and Zhao Wenrong for their kind help and suggestions.

Table 1 Collected data and relevant information for $^{63}Cu(n,\alpha)$

Year	Author	E_n MeV	σ_0 mb	$\Delta\sigma$ mb	n flux	R_1	R_2	σ mb
1960	B. Czapp	14.0	47.0	9.4	$^{27}Al(n,\alpha)$	1.0873	1.0534	53.9
1967	A. Paulsen	5.8~20			H(n,n)			
1967	A. Paulsen	14.7	33.8	2.4	H(n,n)	0.9861		33.3
1969	R. C. Barrall	14.6	49.5	10	$^{27}Al(n,\alpha)$	1.0000		49.5
1972	M. Bormann	14.2	26.1	5.0	ACCOP	1.0534		27.5
1972	G. N. Maslov	14.6	53.5	6.0	$^{65}Cu(n.2n)$	1.0000	1.0387	55.6
1978	G. Winkler	14.8	40.7	1.0	$^{27}Al(n,\alpha)$	0.9721	1.0263	40.6
1979	K. Kayashima	14.6	50.4	5.7	$^{27}Al(n,\alpha)$	1.0000		50.4
1980	U. Garuska	14.6	43.0	2.0	$^{56}Fe(n,p)$	1.0000	1.0429	44.8
1980	O. I. Artem	14.8	41.0	8.0	$^{27}Al(n,\alpha)$	0.9721		39.9
1980	G. Winkler	3.6~5.3			$^{238}U(n,f)$			
1980	G. Winkler	5.1~9.9			$^{238}U(n,f)$			
1985	L. R. Greenwood	14.9	40.1	4.0	$^{93}Nb(n,2n)$	0.9577	0.9888	38.0
1990	Wang Yongchang	14.6	48.4	1.7	$^{27}Al(n,\alpha)$	1.0000		48.4
1991	Y. Ikeda	14.8	40.4	2.3	$^{58}Ni(n,p)$	0.9721		39.3
1991	J. Csikai	14.5	45.0	2.0		1.0139		45.6
1991	J. W. Meadows	14.8	43.5	1.0	$^{58}Ni(n,p)$	0.9721		42.3
1991	Lu Hanlin	14.58	49.0	1.7	$^{27}Al(n,\alpha)$	1.0028	1.0000	49.1

R_1 : Adjusted factor for neutron energy

R_2 : Adjusted factor for relevant cross section, half-life and gamma branching ratio.

σ_0 : Original cross sections

σ : Adjusted cross sections

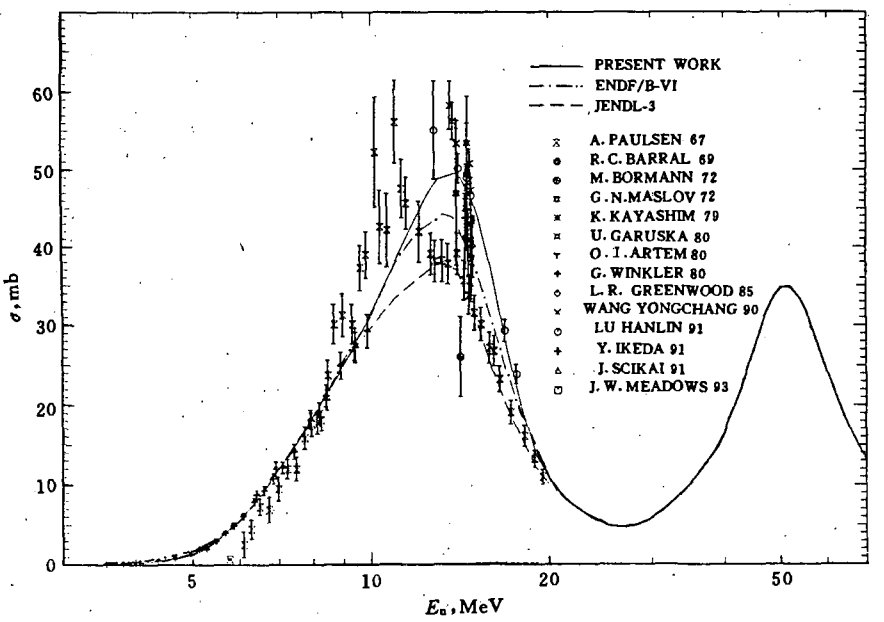

Fig. 1.1 Comparison of evaluated data with measured data for $^{63}Cu(n,x)^{60}Co$ reaction cross sections

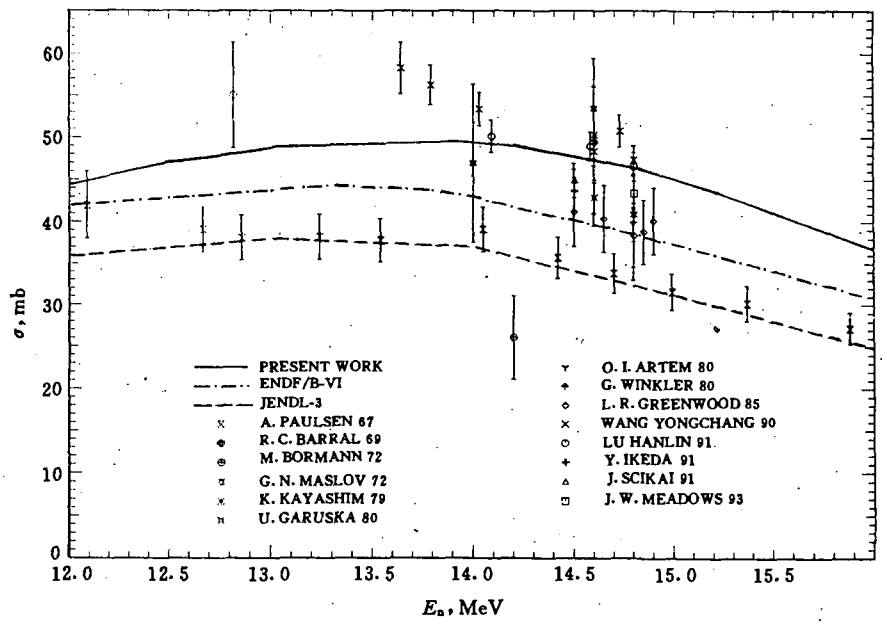

Fig. 1.2 Comparison of evaluated data with measured data for $^{63}Cu(n,x)^{60}Co$ reaction cross sections

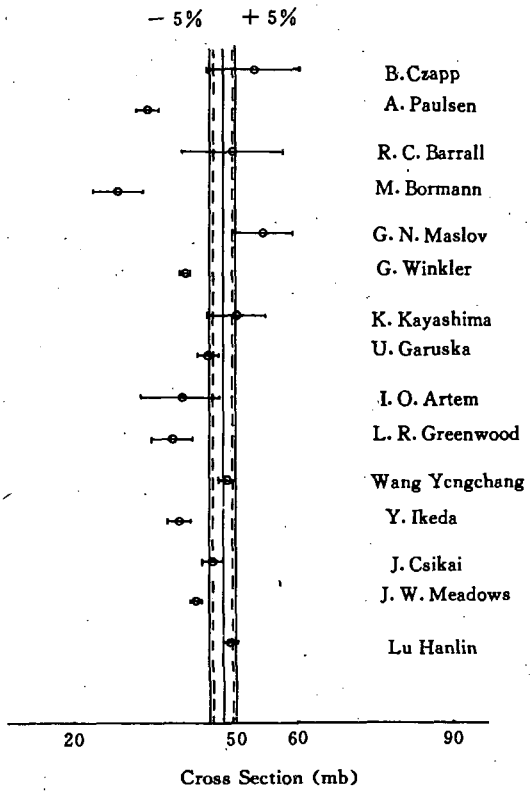

Fig. 2 The adjusted data of 14.6 MeV for $^{63}Cu(n,\alpha)^{60}Co$ reaction, evaluated cross sections (weighting average) at 14.6 MeV = 47.6 ± 2.1 mb

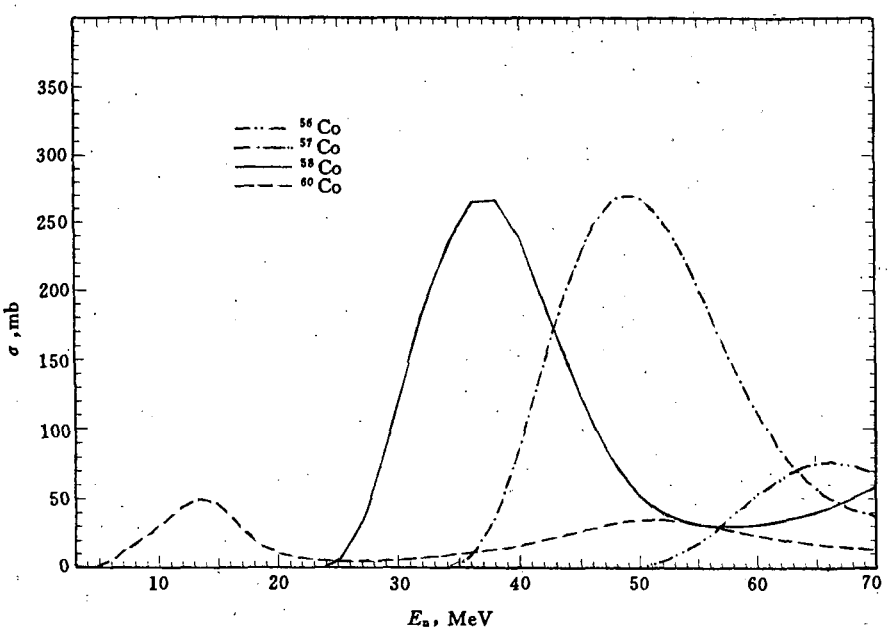

Fig. 3 Evaluated data for $^{63}Cu(n,x)^{56\sim58,60}Co$ reaction cross sections

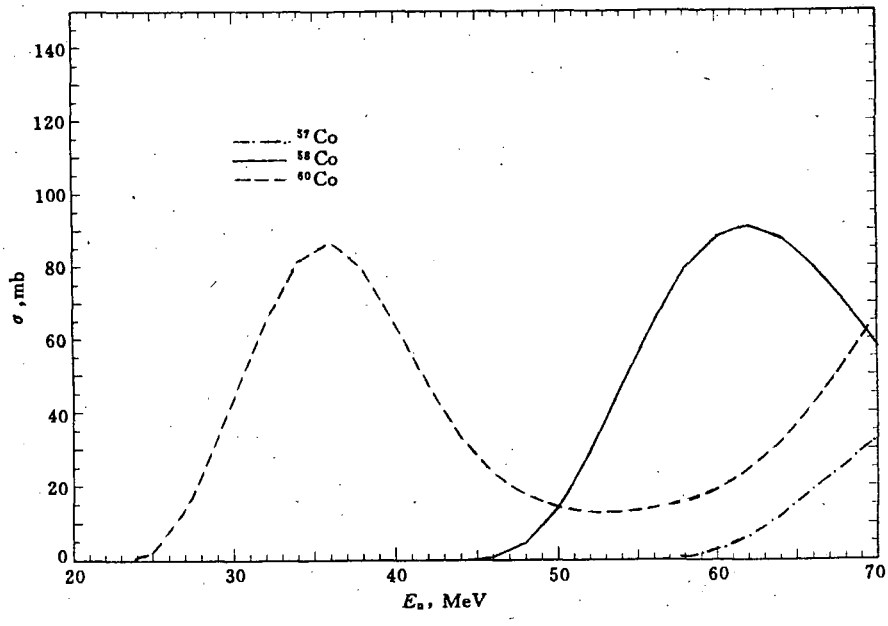

Fig. 4 Evaluated data for $^{65}Cu(n,x)^{56\sim58,60}Co$ reaction cross sections

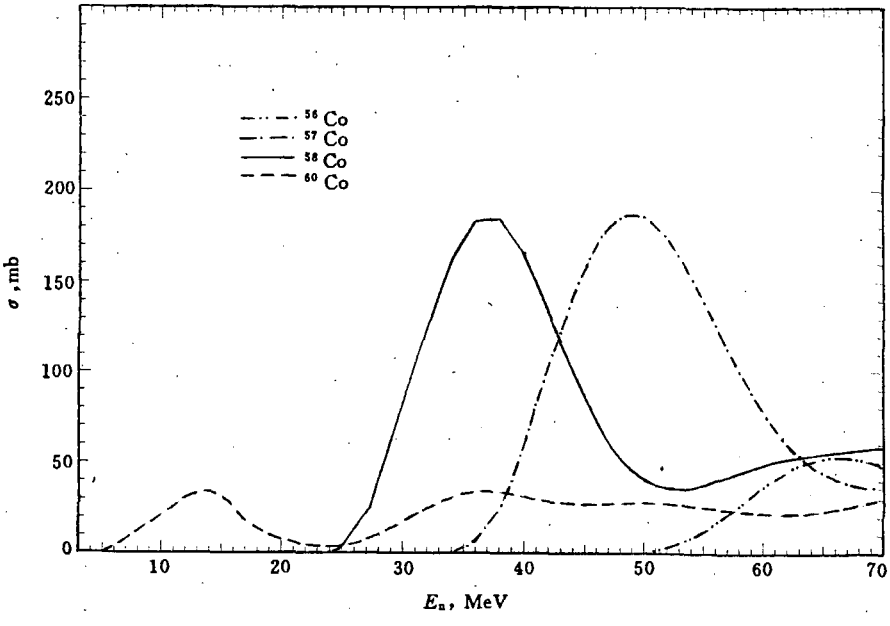

Fig. 5 Evaluated data for $^{Nat}Cu(n,x)^{56\sim58,60}Co$ reaction cross sections

References

[1] Shen Qingbiao et al., Calculations of Various Cross Sections for n +^{63,65}Cu Reactions

in Energy Region up to 70 MeV, to be published (1995)
[2] B. Czapp et al., EXFOR Data No. 20088004
[3] A. Paulsen et al., EXFOR Data No. 20388004
[4] R. C. Barrall et al., AFWL-TR-68-134 (1969)
[5] M.Bormann et al., Nucl. Phys., A 127, 81(1972)
[6] G. N. Maslov et al., EXFOR Data No. 21817011
[7] G. Winkler et al., Nucl. Sci. Eng., 67,260(1978)
[8] K. Kayashima et al., NEAND(J)-61U, 94(1979)
[9] U. Garuska et al., EXFOR Data No. 30553004
[10] O. I. Artem et al., Atomic Energy., 49, 195(1980)
[11] G. Winkler et al., Nucl. Sci. Eng., 76, 30(1980)
[12] L. R. Greenwood et al., DOE-ER-006-21 (1985)
[13] Wang Yongchang et al., Journal of Chinese High Energy Physics and Nuclear Physics., 14, 919(1990)
[14] Y. Ikeda et al., INDC-263-91(1991)
[15] J. Csikai et al., INDC-263-91(1991)
[16] J. W. Meadows et al., INDC(NDS)-286 (1993)
[17] Lu Hanlin et al., Private Communication (1994)
[18] D. M. Hetrick et al., ENDF-201, p. 198(1991)
[19] Zhao Wenrong et al., INDC(CRP)-16 (1989)
[20] A. Smith et al., ENDF-201, p. 216 (1991)

IV BENCHMARK TESTING

Homogeneous Fast Reactor Benchmark Testing of CENDL–2 and ENDF / B–6

Liu Guisheng

(Chinese Nuclear Data Center, IAE)

Abstract

How to choose correct weighting spectrum has been studied to produce multigroup constants for fast reactor benchmark calculations. A correct weighting option makes us obtain satisfying results of K_{eff} and central reaction rate ratios for nine fast reactor benchmark testings of CENDL–2 and ENDF / B–6.

Introduction

Recently, the revised nuclear data file[1] of ^{238}U was produced for CENDL–2.1. In order to do the validation for CENDL–2, especially ^{238}U, it should be necessary to choose several sets of benchmark experiments which includes homogeneous and heterogeneous fast reactors, thermal reactors, fusion reactors and others. First of all, homogeneous fast reactor benchmark testing of CENDL–2 and ENDF / B–6 are given in this paper. The remainder of data testing will be released in the Communication of Nuclear Data Progress one after another.

Nine homogeneous fast assemblies with simple compositions and geometries are used in this data testing. They are recommended by CSEWG inthe United States[2]. The effective multiplication factors and central reaction rate ratios of these assemblies were calculated and compared with others. It is worth notice that correct option of weighting spectrum used in generating multigroup constants is very important. The concerned calculational results are discussed.

1 Description of Benchmark Assemblies

Nine fast critical reactors were used in this study. Their main characteristics are given in Table 1. All of these assemblies have simple geometry and uniform compositions, they facilitate calculational testing, especially for the uranium and plutonium isotope cross sections in the fission source range. Besides, BIG-10 with larger core volume and softer core spectrum is best suited to test ^{238}U cross sections of resonance region and above fission threshold.

Table 1 Critical assembly characteristics

	CORE		REFLECTOR	
ASSEMBLY	FUEL	RADIUS (cm)	MATERIAL	THICKNESS (cm)
GODIVA	Enriched U 92% ^{235}U	8.741	No	0.0
FLATTOP-25	Enriched U 91% ^{235}U	6.116	Natural U	18.041
BIG-10	Enriched U 10% ^{235}U	30.480	Depleted U	15.240
JEZEBEL	Pu	6.385	No	0.0
JEZEBEL-Pu	Pu, 20% ^{240}Pu	6.65985	No	0.0
FLATTOP-Pu	Pu	4.533	Natural U	19.597
JEZEBEL-23	^{233}U	5.983	No	0.0
FLATTOP-23	^{233}U	4.371	Natural U	19.520
THOR	Pu	5.310	^{233}Th	24.570

2 Theoretical Method

2.1 Generations of Multigroup Constants

NJOY-91.91[3] and MILER[4] code system were applied to processing evaluated nuclear data and generating 175 group cross sections with VITAMIN-J energy structure in the AMPX master library format from CENDL-2 and ENDF / B-6. NJOY-91.91 can produce infinitely multigroup averaged cross sections, transfer matrices and self-shielding factors dependent on reactions, temperature and σ_0. The output data file of multigroup cross sec-

tions from module GROUPR of NJOY is called the GENDF in ENDF / B format. The MILER read two GENDF data files independent and dependent on temperature, respectively. And then the two files are converted into a multigroup cross section data file with Bondarenko self–shielding factors in the AMPX master library format.

In order to test the weighting spectrum effect on generating averaged cross–sections, three weighting functions, i. e. W–A (thermal maxwellian + $1/E$ + fission spectrum), W–B (thermal + $1/E$ + fast reactor + fission + fusion) and W–C (VITAMING–E weighting function, described in the option 11 of module GROUPR in the NJOY–91.91), were used in running code NJOY, respectively. From our calculational results it has been shown that the more close to the calculated reactor core spectrum the weighting function is, the more accurate values calculated integral parameters of the reactor become.

2.2 Benchmark Calculations

First of all, a problem–dependent AMPX working library is produced from the AMPX master library by such modules as AJAX–C, BONAMI–C, and NITWAL–S in the modified code system PASC–1[5].

The module AJAX–C can select the concerned multigroup data from AMPX master library to produce a new master library. The BONAMI–C performs a resonance self–shielding calculation based on the Bondarenko method and generates problem–dependent master data set. The NITAWL–S converts the AMPX master library into a AMPX working library. The XSDRNPM–C is a modified version of one–dimensional transport code XSDRNPM–S in the PASC–1 code system[6]. The modified XSDRNPM–C can calculate central reaction rate ratios of fast critical reactors.

Finally, the XSDRNPM–C was used in calculating K_{eff} and central reaction rate ratios with 175 groups in P_3 S_{32}.

3 Weighting Spectrum Effect

As mentioned above three weighting spectra have already specified to generate three sets of 175 group cross sections in the VITAMIN–J energy structure from CENDL–2. Three weighting functions, which are called weighting *A*, *B*, and *C*, respectively, are shown in Fig. 1. Three uranium fuel assemblies were used in this study. The calculated results are listed in Table 2.

Table 2 Effects of weighting spectra on integral parameters

ASSEMBLY	GODIVA		FLATTOP–25		BIG–10		
	K_{eff}	F28	K_{eff}	F28	K_{eff}	F28	C28
EXP.	1.00000 ± 0.1%	0.1647 ± 1.1%	1.00000 ± 0.1%	0.149 ± 1.34%	0.996 ± 0.2%	0.0373 ± 1.07%	0.1100 ± 2.73%
W–A C	0.99681	0.1594	0.99737	0.1462	0.99415	0.03726	0.1103
C/E	0.99681	0.9678	0.99737	0.9812	0.99814	0.9989	1.0027
W–B C	0.99656	0.1588	0.99753	0.1457	0.99541	0.03747	0.1104
C/E	0.99656	0.9642	0.99753	0.9779	0.99940	1.0046	1.0032
W–C C	1.00003	0.1625	1.00142	0.1489	1.00211	0.03799	0.1100
C/E	1.00003	0.9866	1.00142	0.9991	1.00800	1.0161	1.0000

We also drew a picture with three reactor core spectra shown as Fig. 2, so as to further clarify the effects of different weighting function on integral parameters and to better understand the relationship between weighting and reactor spectrum. For convenience, all of the spectra of weighting and reactor cores were normalized to the flux of the fission threshold energy group of ^{238}U.

As the core of GODIVA is a very small bare metal sphere assembly of high enriched uranium, its spectrum is very hard and very close approximation to weighting spectrum *C*. The volume of core of FLATTOP–25 is only 0.96 liters. Therefore the core spectrum of FLATTOP–25 is also hard and the same spectrum as GODIVA has. Consequently, the calculated results for the harder weighting *C* are reasonable. Fortunately, they are also better than that using weighting *A* and *B*. Owing to the fact that the weighting *B* is softer, the fission contribution of ^{238}U in the high energy range has been underestimated. It is the reason why K_{eff} and F28 for the weighting *B* have been decreased by about 0.4% and 2%, respectively, as compared with that for weighting *C*. At the same time, weighting *A* is hard, too. The excessive hard spectrum results in that fission contributions of ^{235}U are underestimated and secondary fission spectrum neutrons are decreased so as to decrease fission rate of ^{238}U. And the value of K_{eff} for system is underestimated, too.

Because the BIG–10 has the larger core volume of 119 liters, its core spectrum is softened. It is a very famous intermediate energy standard neutron field. It is necessary that we should make use of the weighting *B* with softer fast re-

actor spectrum to generate multigroup cross sections. Obviously, the calculated results for the weighting B are reliable. Using the harder weighting C, the K_{eff} and F28 were overestimated by 0.8% and 1.2%, respectively. It was unexpected that using the hardest weighting A we obtained the lowest value of K_{eff}. In fact, the hard core spectrum results in increasing leakage neutrons from core and decreasing fission contribution of ^{235}U.

It is seen from these results that a good selection of weighting function should be suitable to the calculated reactor spectrum. That is to say, the weighting function used in generating multigroup cross sections must approximate to the spectrum of the assembly as far as possible, especially for benchmark testing of nuclear data. It is the correct weighting option that makes us obtain satisfying results about the benchmark testing of CENDL–2 for three homogeneous uranium fuel assemblies.

4 Calculational Results of Integral Parameters

According to analyses in the preceding paragraph, three weighting functions were used for generating 175 group cross sections from CENDL–2 and ENDF / B–6. Transport calculations of 175 groups in P_3 S_{32} for nine fast critical assemblies listed in the Table 1 were carried out using the benchmark calculational method described in the paragraph 2.2. The values of K_{eff} and central reaction rate ratios for these assemblies were obtained.

4.1 Effective Multiplication Factors

Table 3 presents the calculated values of K_{eff} of nine homogeneous assemblies for CENDL–2 and ENDF / B–6 obtained by CNDC along with the values of K_{eff} published for benchmark testing of ENDF / B–6, JEF–2 and JENDL–3[7, 8].

The results of first two columns are right, because the correct weighting options were used and the transport calculations with resonance self–shielding processing are rigorous, too. Naturally, these are results of homogeneous fast reactor benchmark testing of CENDL–2 and ENDF / B–6. It may be true that the results from CENDL–2 are better than others. The data of the new evaluated ^{238}U of CENDL–2 used calculations lead to good results for all of uranium fuel assemblies with hard and soft spectra. The K_{eff} value of BIG–10 for ENDF / B–6 was overestimated by 2 %, because the calculated spectrum is too hard.

The calculated K_{eff} values of two plutonium metal bare sphere assemblies

for CENDL–2 were overestimated by about 0.4 percent. However, the good results of that for ENDF / B–6 were obtained. It is interesting that the calculated value of K_{eff} of FLATTOP–Pu with natural uranium reflector for CENDL–2 is much better than that for all of other evaluated libraries.

Table 3 Results of K_{eff} calculations

	C N D C				Ref. 7		Ref. 8
Assembly	CENDL–2*	ENDF / B–6*	ENDF / B–6△	ENDF / B–6□	ENDF / B–6	JEF–2	JENDL–3
GODIVA	1.00003	0.99946	0.99626	0.99626	0.9954	0.9934	1.0066
FLATTOP–25	1.00142	1.00785	1.00356	1.00101	1.0007	0.9898	1.0033
BIG–10 C	0.99541	1.01576	1.01693	1.00555	1.0063	0.9928	1.0038
C / E	0.99940	1.01984	1.02101	1.00959			
JEZEBEL	1.00430	1.00056	0.99753	0.99753	0.9960	0.9952	1.0001
JEZEBEL–Pu	1.00391	1.00261	1.00040	1.00040	0.9893	0.9898	0.9963
FLATTOP–Pu	1.00066	1.00886	1.00424	1.00742	1.0025	0.9887	0.9974
JEZEBEL–23	0.99463	0.99458	0.99301	0.99301	0.9929	0.9756	1.0206
FLATTOP–23	1.00187	1.00645	1.00341	1.00470	1.0026	0.9836	1.0175
THOR	1.00925	1.00721	1.00389	1.00719	1.0056	0.9797	0.9985

Note :

* W–C was used in generating multigroup constants for assemblies, except W–B for BIG–10. Transport calculations with resonance self–shielding.

△ W–A was used in generating multigroup constants with resonance self–shielding processing.

□ W–A was used in generating multigroup constants without resonance self–shielding processing.

4.2 Central Reaction Rate Ratios

The Table 4 presents the calculated results of central reaction rate ratios for nine assemblies. The reaction rates are all relative to that of fission of ^{235}U.

Table 4 Central reaction rate ratios (C/E)

			C N D C			Ref. 7		Ref. 8
ASSEMBLY		EXP.	CENDL-2*	ENDF/B-6*	ENDF/B-6△	ENDF/B-6	JEF-2	JENDL3
GODIVA	F28	0.1647	0.9866	0.9879	0.9686	0.9541	0.9535	1.0006
	F49	1.402	0.9971	0.9883	0.9871	0.9860	0.9922	
	F37	0.837	0.9719	0.9883	0.9805	0.9742	0.9609	
	F23	1.590	0.9999	1.0002	1.0010	1.0016	0.9676	
FLATTOP-25	F28	0.149	0.9993	0.9968	0.9759	0.9655	0.9708	1.0697
	F49	1.370	1.0020	0.9953	0.9945	0.9936	0.9983	
	F37	0.760	0.9937	1.0141	1.0069	1.0016	0.9868	
	F23	1.600	0.9920	0.9936	0.9947	0.9949	0.9621	
BIG-10	F28	0.0373	1.0046	1.0512	1.0657	1.0519	1.0142	1.0195
	C28	0.110	1.0032	0.9475	0.9818	0.9836	0.9998	
	F49	1.185	0.9704	0.9948	0.9992	0.9985	0.9872	
	F37	0.316	0.9410	1.0639	1.0780	1.0724	0.9720	
	F23	1.580	0.9850	0.9954	0.9973	0.9972	0.9773	
JEZEBEL	F28	0.2137	0.9708	0.9839	0.9736	0.9600	0.9528	0.9944
	F49	1.448	0.9941	0.9818	0.9838	0.9836	0.9893	
	F37	0.962	0.9828	0.9874	0.9932	0.9889	0.9624	
	F23	1.578	1.0016	0.9987	0.9998	1.0005	0.9659	
JEZEBEL-Pu	F28	0.206	0.9861	0.9941	0.9888	0.9675	0.9651	1.0063
	F37	0.920	1.0116	1.0164	1.0226	1.0169	0.9903	
FLATTOP-Pu	F28	0.180	0.9733	0.9909	0.9817	0.9730	0.9734	1.0117
	F37	0.840	0.9821	0.9987	1.0050	1.0042	0.9766	
JEZEBEL-23	F28	0.2131	1.0588	1.0560	1.0192	1.0081	0.9348	1.0619
	F37	0.977	0.9821	1.0256	1.0128	1.0079	0.9393	1.0192
FLATTOP-23	F28	0.191	1.0473	1.0453	1.0099	1.0030	0.9384	1.0696
	F37	0.890	1.0111	1.0331	1.0209	1.0184	0.9483	1.0300
THOR	F28	0.195	0.9620	0.9760	0.9657	0.9559	0.9781	1.0034
	C28	0.083	0.8471	0.8413	0.8471	0.8500	0.8301	
	F37	0.920	0.9512	0.9548	0.9605	0.9580	0.9633	

Note : '*' and '△' represent the same meaning as that in the Table 3.

Considering calculational results for CENDL–2, very satisfactory results were obtained for three uranium fuel assemblies. Especially, F28 and C28 for BIG–10 are much better than that from other evaluated libraries. F49 for BIG–10 is about 3 percent less than experimental value, although that for other assemblies with harder spectra are satisfactory. The calculated values of F37 for CENDL–2 are generally underestimated, as compared with that for ENDF / B–6.

The calculated central reaction rate ratios for all the enriched uranium and plutonium fuel assemblies for ENDF / B–6 are good, except that for BIG–10. Our calculated values of F28 and C28 for BIG– 10 are 5.1% higher and 5.2% lower than experimental values, respectively. It may result from that slowing–down power of ^{238}U in high energy region is too weak. The calculated reaction rate ratios for assembly THOR are underestimated, especially, the calculated C28 is about 15 percent lower than the experimental value.

Acknowledgement

The author is greatly indebted to Dr. Zhang Baocheng for his help.

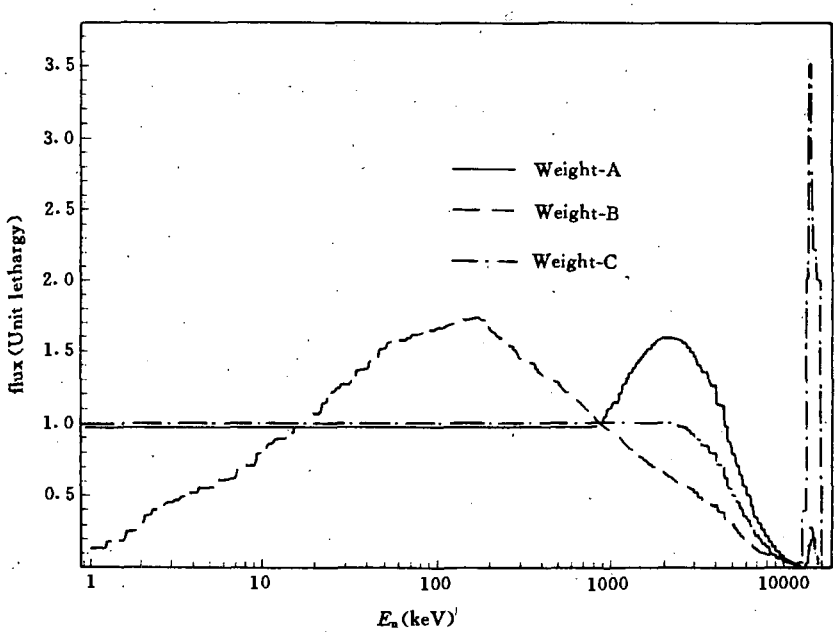

Fig. 1 Comparison of neutron weighting spectrum

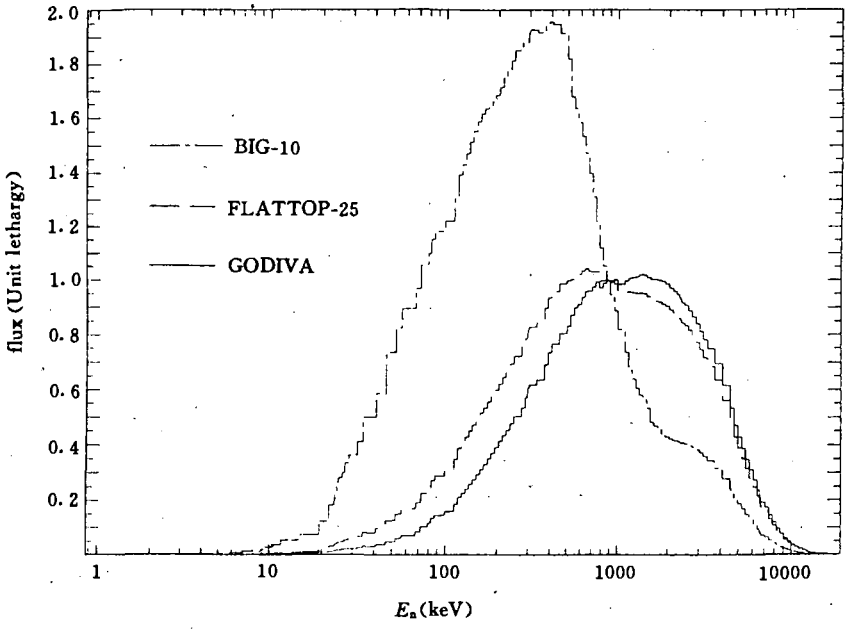

Fig. 2 Comparison of neutron flux spectrum

References

[1] Tang Guoyou, et al., CNDP, No. 13, 1995

[2] Cross Section Evaluation Working Group, Benchmark Specifications, BNL-19302 (ENDF-202), 1981

[3] R. E. MacFarlane and D. W. Muri, LA-9303-M, 1982

[4] P. F. A. de Leege, IRI-131-091-003, Delft University, Netherlands, 1991

[5] Liu Guisheng et al., Chinese Journal of Nuclear Science and Engineering, Vol. 13 No. 3, p. 9, Sep., 1993

[6] Wang Yaoqing et al., ECN-89-005, 1989

[7] M. Caro et. al., Proceedings of International Conference on Nuclear Data for Science & Tech., p. 214, Berlin, Germany, May 13~17, 1991

[8] D. Tian, et al., JAERI-M 91-032, p. 148, March, 1991

Benchmark Testing of CENDL-2 for U-Fuel Thermal Reactors

Zhang Baocheng Liu Guisheng Liu Ping

(Chinese Nuclear Data Center, IAE)

Abstract

Based on CENDL-2, NJOY-WIMS code system was used to generate 69-group constants, and do benchmark testing for TRX-1, 2; BAPL-UO_2-1, 2, 3; ZEEP-1, 2, 3. All the results proved that CENDL-2 is reliable for thermal reactor calculations.

Introduction

Recently, many new evaluated nuclear data libraries, such as ENDF / B-6, JEF-2, JENDL-3.1, BROND-2 and CENDL-2, are released. As a rule, these data should be tested before being used in reactor analysis. The Cross Section Evaluation Group (CSEWG) is composed of representatives from United States laboratories, which has chosen a number of integral experiments[1] for checking the data of interest.

Now CENDL-2 is being used to update WIMS 69-group library. To ensure that the new library is reliable for thermal reactor calculations, it is necessary to do benchmark testing. All these work have been done with NJOY-WIMS code system[2].

1 Description of Benchmark Experiments

In order to test CENDL-2 data, 8 benchmark lattices containing ^{235}U and ^{238}U, which include TRX-1, 2; BAPL-UO_2-1, 2, 3; and ZEEP-1, 2, 3; are chosen.

TRX used U metal fuel in ^{235}U enriched to 1.305 wt.%; BAPL uranium oxide to 1.311 wt.%; ZEEP natural uranium. TRX and BAPL were H_2O-moderated, and ZEEP were D_2O-moderated. Details of these lattices are given in Tables 1 and 2.

Table 1 Brief characteristics of TRX−1,2; BAPL−1, 2, 3

Lattice	Fuel	Cladding	Moderator	Rod Radius (cm)	Pitch (cm)
TRX−1	1.3 wt. % U−metal	Al	H_2O	0.4915	1.8060
TRX−2		Al	H_2O	0.4915	2.1740
BAPL−1	1.3 wt. % UO_2	Al	H_2O	0.4864	1.5578
BAPL−2		Al	H_2O	0.4864	1.6523
BAPL−3		Al	H_2O	0.4864	1.8057

Table 2 Brief characteristics of ZEEP−1, 2, 3

Region	Outer Radius (mm)	Composition	
		Isotope	Concentration 10^{24} atoms / cm^3
Fuel	16.285	^{235}U	3.454E−4
		^{238}U	4.760E−2
Air Gap	16.470	O	5.0E−5
Cladding	17.490	Al	6.025E−2
Moderator		^{1}H	1.529E−4
		^{2}H	6.633E−2
		O	3.324E−2

For these lattices, experimental buckling values are available. So it is easy to do leakage calculation with input buckling values.

Besides K_{eff}, parameters ρ^{28}, δ^{25}, δ^{28} and C^* were measured for TRX and BAPL, δ^{28} and RCR for ZEEP. All the parameters are defined as following:

ρ^{28} — epithermal / thermal captures for ^{238}U

δ^{25} — epithermal / thermal fissions for ^{235}U

δ^{28} — ^{238}U / ^{235}U fissions

C^* — ^{238}U captures / ^{235}U fissions

RCR — $C^*_{lattice} / C^*_{Maxwellian}$.

2 Generation of 69−Group Constants Library

In CENDL–2, ENDF / B–6 format and Reich–Moore resonance parameters were widely used. NJOY is an useful code to process this kind of data.

In order to use WIMS / D4[3] to do cell calculation, 69–group WIMS library, 14 fast, 13 resonance and 42 thermal energy groups, was generated with NJOY, WIMSR code. In this library, only one fission spectrum was given. General, ^{235}U fission spectrum was used. It is reasonable for most U–fuel thermal reactor because only less than 10% fission neutron derives from ^{238}U. In this work, ^{235}U and ^{238}U mixed spectrum was used[2].

For 69–group WIMS library the upper boundary of thermal energy group is 4.0 eV. It is possible that resonance construct exits in thermal group for some nuclide. Besides in WIMS 69–group library, only absorption and neutron yield per fission integrals were tabulated and all the other cross sections were entered corresponding to a σ_0, which was chosen from input values. Clearly, the results of benchmark calculations are sensitive to the selection of σ_0. In this work, σ_0 was derived from calculation according to normal reactor cells.

For generating the group constants, CPM averaging spectrum was used. This spectrum is an option in NJOY.

The group constants of hydrogen bounded in water and deuterium in heavy water were calculated using the scattering law data of ENDF / B–6.

3 Methods of Cell Calculation

The cell calculations were made using WIMS / D4 code. At first, according to real cell composition, intermediate approximation was used to calculate resonance self–shielding. The main transport equation was solved using Sn method, and the cylindrical cell approximation was used to simplify the geometry of the cell. Leakage calculations have been done with input buckling values and B1 method. The reaction rates of ^{235}U and ^{238}U were given in output files for two groups.

4 Results and Discussions

The comparison between the values of calculations and experiment for TRX–1, 2 and BAPL–UO_2–1, 2, 3 is shown in Table 3. The results of IAEA are also based on CENDL–2[4]. The calculated results with CENDL–2 are much better than those from old library associated with WIMS / D4. In this work, JEF–1 was calculated in same way, and the results are listed in Table 4.

The K_{eff} values from our calculations are in good agreement with experiments. Only the value of TRX–1 is lower than 0.1%. The values of ρ^{28} for TRX–2, BAPL–UO_2–1 and 3 are well predicted within the uncertainty interval of the measurements values, for TRX–1 and BAPL–UO_2–2, the results are higher than 3% (1.6% uncertainty in measurement) and 3.59% (0.89% uncertainty), respectively. All the values of δ^{25} are lower from 0.679% to 2.39% than experimental ones. For δ^{28} parameter the calculated values are generally within the uncertainty interval of the measurements values, except for BAPL lattices, for which the prediction values are underestimated about 5.9% to 9%. The agreement for parameter C^* is very good.

Table 3 Comparison of calculation and experimental lattice parameters for TRX–1, 2 and BAPL–UO_2–1, 2, 3

	Parameter	Experiment	Calculation of CNDC	Calculation of IAEA	WIMS / D4
TRX–1	K_{eff}	1.0000	0.9975	0.9996	1.0023
	ρ^{28}	1.320 ± .021	1.3608	1.336	1.279
	δ^{25}	0.0987 ± .0010	0.09803	0.0988	0.0990
	δ^{28}	0.0946 ± .0041	0.09622	0.0978	0.0965
	C^*	0.797 ± .008	0.7922	0.793	0.780
TRX–2	K_{eff}	1.0000	0.9998	0.9984	0.9965
	ρ^{28}	0.837 ± .016	0.8530	0.842	0.808
	δ^{25}	0.0614 ± .0008	0.06021	0.0608	0.0610
	δ^{28}	0.0693 ± .0035	0.06811	0.0699	0.0695
	C^*	0.647 ± .006	0.6387	0.643	0.636
BAPL–1	K_{eff}	1.0000 ± .00065	1.0010	1.0057	1.0029
	ρ^{28}	1.39 ± .01	1.3923	1.385	1.358
	δ^{25}	0.084 ± .002	0.08199	0.0832	0.0840
	δ^{28}	0.078 ± .004	0.07362	0.0758	0.0755
	C^*	———	0.7972	0.803	0.800
BAPL–2	K_{eff}	1.0000 ± .00062	1.0003	1.0043	1.0005
	ρ^{28}	1.12 ± .01	1.1602	1.156	1.133
	δ^{25}	0.068 ± .001	0.06695	0.0679	0.0687
	δ^{28}	0.070 ± .004	0.06327	0.0653	0.0652
	C^*	———	0.7274	0.734	0.732
BAPL–3	K_{eff}	1.0000 ± .0005	1.0007	1.0034	0.9981
	ρ^{28}	0.906 ± .010	0.9130	0.911	0.894
	δ^{25}	0.052 ± .001	0.05150	0.0523	0.0529
	δ^{28}	0.057 ± .003	0.05184	0.0536	0.0538
	C^*	———	0.6511	0.0657	0.657

Table 4 Comparison of results based on CENDL-2 and JEF-1

	Parameter	Experiment	Calculation	
			CENDL-2	JEF-1
TRX-1	K_{eff}	1.0000	0.9975	0.9952
	ρ^{28}	1.320 ± .021	1.3608	1.3531
	δ^{25}	0.0987 ± .0010	0.09803	0.09907
	δ^{28}	0.0946 ± .0041	0.09622	0.09826
	C^*	0.797 ± .008	0.7922	0.7971
TRX-2	K_{eff}	1.0000	0.9998	0.9972
	ρ^{28}	0.837 ± .016	0.8530	0.8463
	δ^{25}	0.0614 ± .0008	0.06021	0.06073
	δ^{28}	0.0693 ± .0035	0.06811	0.06978
	C^*	0.647 ± .006	0.6387	0.6424
BAPL-1	K_{eff}	1.0000 ± .00065	1.0010	1.0020
	ρ^{28}	1.39 ± .01	1.3923	1.3857
	δ^{25}	0.084 ± .002	0.08199	0.08290
	δ^{28}	0.078 ± .004	0.07362	0.07559
	C^*	———	0.7972	0.8022
BAPL-2	K_{eff}	1.0000 ± .00062	1.0003	1.0014
	ρ^{28}	1.12 ± .01	1.1602	1.1538
	δ^{25}	0.068 ± .001	0.06695	0.06763
	δ^{28}	0.070 ± .004	0.06327	0.06507
	C^*	———	0.7274	0.7318
BAPL-3	K_{eff}	1.0000 ± .0005	1.0007	1.0014
	ρ^{28}	0.906 ± .010	0.9130	0.9070
	δ^{25}	0.052 ± .001	0.05150	0.05198
	δ^{28}	0.057 ± .003	0.05184	0.05341
	C^*	———	0.6511	0.06548

From Table 3, the difference of calculated results between CNDC and IAEA can be found, especially δ^{25} and δ^{28} for BAPL lattices. Generally, the results of IAEA are little higher than those of CNDC. The difference may come

from using different fission spectrum and scattering law data (IAEA using ENDF / B–3). Fig. 1 shows that the fission spectrum used by CNDC is the softest one above ^{238}U fission threshold energy.

For ZEEP–1, 2 and 3 the results of CENDL–2, JEF–1 and ENDF / B–5[5] are summarized in Table 5. Because WIMS / D4 code can calculate $C^*_{Maxwellian}$ directly, the value of ENDF / B–5 given in Ref. [4] (0.654) was used to observe RCR.

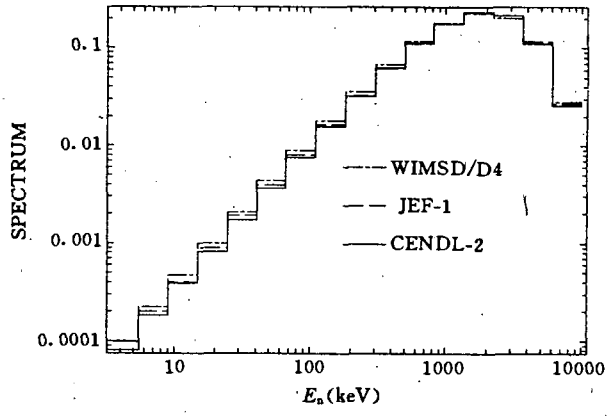

Fig. 1 The comparison of fission spectrum

Table 5 Comparison of calculated and experimental lattice parameters

Lattice	Parameter	Experiment	ENDF / B–5	CENDL–2	JEF–1	WIMS / D4
ZEEP–1	K_{eff}	1.0000	1.00360	1.00290	1.00278	0.99155
	ρ^{28}	——	0.282	0.287	0.274	0.263
	δ^{25}	——	0.0263	0.0256	0.0262	0.0258
	δ^{28}	0.0675	0.0682	0.0679	0.0690	0.0648
	RCR	1.260	1.281	1.274	1.275	1.279
ZEEP–2	K_{eff}	1.0000	1.00161	0.99973	1.00270	0.99695
	ρ^{28}	——	0.516	0.527	0.497	0.472
	δ^{25}	——	0.0502	0.0488	0.0497	0.0489
	δ^{28}	——	0.0725	0.0719	0.0735	0.0691
	RCR	——	1.491	1.489	1.476	1.467
ZEEP–3	K_{eff}	1.0000	1.00089	0.99734	1.00337	1.00138
	ρ^{28}	——	0.688	0.704	0.660	0.623
	δ^{25}	——	0.0674	0.0655	0.0666	0.0654
	δ^{28}	——	0.0764	0.0758	0.0777	0.0730
	RCR	——	1.640	1.643	1.619	1.599

Although there are no quite enough experimental data with heavy water moderated lattices, the available data have shown that the results calculated by

using CENDL–2 are within or close to the experimental uncertainty limits.

All the lattice parameters calculated by using CENDL–2 data are in well agreement with experiment.

References

[1] Cross Section Evaluation Working Group Benchmark Specifications, ENDF–202, Nov. 1974

[2] Zhang Baocheng, Liu Guisheng et al. A Data Processing and Critical Safety Analyzing Code System, CNDP, No. 12, p. 66(1994)

[3] M. J. Halsall, A Summary of WIMS / D4 Input Options. AEEW–M1327, July, 1980

[4] T. Zidi, Nuclear Data Processing and Applications, p. 214

[5] D. S. Craig, Testing ENDF / B–5 Data for Thermal Reactors, AECL–7690 (Rev.1) p. 53, June, 1984

V DATA, PARAMETER AND PROGRAM LIBRARIES

Modification and Improvement of CENDL–2

Liang Qichang Liu Tingjin Zhao Zhixiang Liu Tong Sun Zhengjun

(Chinese Nuclear Data Center, IAE)

Since CENDL–2 was finished in 1992, it has been modified and improved as follows :

1. The characteristic values (thermal cross section, resonance integrals, etc.) have been added in the text in MF1 MT451 for all evaluations of CENDL–2.
2. The secondary neutrons energy spectra have been modified for ^{16}O, ^{23}Na, Mg, Si, ^{31}P, S, K, Ti, ^{51}V, Zr, Cd, In, Sb, Hf, W, ^{197}Au, Pb, ^{237}Np, ^{239}Pu.
3. The total cross sections for natural S, K, Ti, Ni, Zr, Sb, Hf, Pb have been updated.
4. The gamma–production data have been supplemented in the data files for Ti, Zn, Zr, Mo, Cd, In, Sn, Sb, Hf, ^{181}Ta, W, ^{197}Au, Pb.
5. The re–evaluations for Ca and ^{238}U by using new model theory codes have replaced the old one in CENDL–2.
6. The new evaluations for ^{56}Fe and natural Lu, Hg, Tl have been added in CENDL–2.

Progress on Chinese Evaluated Nuclear Parameter Library (CENPL) (IV)

Su Zongdi Ge Zhigang Zhang Limin
Sun Zhengjun Wang Chengxiang

(Chinese Nuclear Data Center, IAE)

Huang Zhongfu Dong Liaoyuan Qiu Guochun

(Dept. of Phys., Guangxi University)

Liu Jianfeng

(Zhengzhou University)

Yu Ziqiang Zuo Yixin

(Nankai University)

Ma Gonggui

(Sichuan University)

Chen Zhenpeng

(Tsinghua University)

Some progress on setting up of the CENPL and studies of the relevant model parameters have been made for the past period.

1 Setting up of the CENPL

1.1 The MCC, GDP and FBP Sub-Libraries

Three sub-libraries (the first edition), the atomic masses and characteris-

tic constants of nuclear ground states (MCC)[1], the giant dipole resonance parameters for gamma–ray strength function (GDP) [2], the fission barrier parameters (FBP)[3], including their data files and the management–retrieval code systems have all been finished and used to serve the users in different research fields.

1.2 The DLS Sub–Library

The data file of the sub–library of the discrete level schemes and gamma radiation branching ratios (DLS)[4] has been set up, and the management–retrieval code system is being programmed. The data and information in the DLS data file were translated from the Evaluated Nuclear Structure Data File (ENSDF).

1.3 The NLD Sub–Library

The nuclear level density (NLD) sub–library includes two data files : the data relative to the level density (LRD) and the level density parameters (LDP). The LRD file contains S–wave average resonance level spacing D_0, strength function S_0 and radioactive capture width at neutron separation energy, as well as the cumulative number N_0 of low–lying levels. The D_0 and S_0 values were recommended by us in 1993[5]. The LDP file[6] contains eight sets of the level density parameters corresponding to three kinds of popular level density formulas, which are the composite four–parameter (GC) formula, the back–shifted Fermi gas (BS) formula, the generalized superfluid model (GSM). The management–retrieval code system of this sub–library was finished.

1.4 The OMP Sub–Library

The data file of the optical model parameter (OMP) sub–library includes the following two parts.

A. Global and regional optical model potential parameter sets (OMPP)

Six types of projectiles are collected and compiled in the first part respectively. For each type of projectile there is a brief information table on authors, published date, nuclear region, energy region, spherical or deformed (S / D), local or nonlocal (L / N), fitting experimental data types and so on. There is an entry for each set of the OMPP, it contains 13 subjects denoted by different keywords. They are "Entry", "Title", "Authors", "Affil.", "Ref.", "Projectile", "Nucleus Region", "Energy Region", "Potential", "Parameters",

"Primary Data", "Optim. Method", and "Comments". This part has reached a specific scale till now.

B. Nucleus–specific optical model potential parameter sets

The nucleus–specific OMPP sets for neutron projectile only are collected and compiled in the second part. A standard OMPP form has been determined. It not only can cover most of the OMPP sets existing in the literature at present, but also can be suit for future possible development tendency of the optical model potential. A related computer format has been fixed to set up this file. Each set of OMPP and its brief information are listed. The information contains target nucleus, neutron incident energy, spherical or deformed (S / D), fitting experimental data types and made model calculations, deformed parameter and standard abbreviation of reference. So far, about 75 sets of optimum optical model parameters which were used in calculations of complete neutron data in CENDL–1, 2 have been collected and compiled. The data file is in an embryonic form.

The great progress has been made for management–retrieval code system of the OMP sub–library . It not only can retrieve the OMPP sets for a single reaction channel and several related channels in a neutron induced reaction respectively, but also can calculate the cross sections and compare the results of the optical model calculations from the different OMPP sets with input experimental data.

2 Studies of the Relevant Model Parameters

2.1 In the studies on the nuclear level density, a new set of the level density parameters a_s and energy shifts E_{sh} [7] of the generalized superfluid model (GSM) for 249 nuclides ranging from ^{41}Ca to ^{250}Cf has been obtained by fitting the D_0 and N_0 valuesrecommended by us in 1993. A set of a_s and E_{sh} values has been compiled in the LDP data file of the NLD sub–library.

The intercomparison[8] of three kinds of popular level density formulas, i. e. the GC, BS and GSM formulas, for 49 nuclides ranging from ^{46}Sc to ^{247}Cm has been made to compare the ability describing the low–lying levels for the three level density formulas. Theirparameters were obtained by fitting D_0 and N_0 values. The D_0 values of the 49 nuclides are consistent within the errors of available D_0 values. The N_0 values were taken from the ENSDF and have further been corrected and supplemented according to the recent data from "Nuclear Data Sheets" (until 1993). Considering the missing of excited levels, the cut–off energy has been chosen by means of the histogram of the low–lying levels. Below the cut–off energy we have counted up the number of levels in group,

and the histogram until the cut–off energy has been fitted in order to obtain the best level density parameters.

Analyzing these results, it seems that the results of only 11 nuclides (about 22%) are identical within the statistical error for the three formulas. For other nuclides, the results of the GC formula to reproduce the discrete levels seem better than others.

2.2 The S–wave neutron average resonance level spacing D_0 is the most fundamental and important data, which characterizes the average properties of the resolved resonance region and can be used to obtain the level density parameters. Presently, by using the average resonance parameters of the resolved resonance region from ENDF / B–6, JEF–2 and JENDL–3, the D_0 values are estimated and recommended again[9]. The evaluation methods, such as the moment method, maximum likelihood method and Beyes method and so on are applied. Considering the imperfection of the experimental sample, the Wigner distribution has been used to make the X^2 statistical check. From the comparison and analysis of the estimated values of the three methods mentioned above and the checked results and the histogram drawn for neutron reduction width, a new set of D_0 values for 252 nuclideshave been evaluated finally. In addition, the D_0 values of other 84 nuclides have been collected and recommended.

2.3 The giant dipole resonance parameters (GDRP) for only 102 nuclides from ^{51}V to ^{239}Pu compiled by Dietrich and Berman are available and there are no GDRP for nuclides with $A < 50$. In addition, the systematics researches of the GDRP were mainly done for the single peak of spherical nuclei, therefore GDRP systematics formulas should be developed for deformed nuclei especially. In view of the requirement the following respects of the researches have been done.

A. By fitting the excitation curves of the photo–nuclear reactions for nuclides ^{12}C, ^{14}N, ^{16}O, ^{27}Al and ^{28}Si, the GDRP for these nuclides have been estimated reasonably[10]. The integrated total cross sections, the first moments and second moments of the integrated total cross sections for the photo–nuclear reactions have been calculated. The results are in good agreement with the experimental data.

B. Based on the hydrodynamical model and the experimental results of the giant dipole resonances of the photo–nuclear reactions, a semi–empirical formula to calculate the giant dipole resonance peak energies for the nuclides with $A > 50$ has been proposed and it has the following form[11]

$$E_{g1} = 45.0\ Z^{-1/3}\ A^{0.05} / (\ 1 + 2/3\ \delta\ ),$$

$$E_{g2} = 45.0\ Z^{-1/3}\ A^{0.05} / (\ 1 - 1/3\ \delta\ )$$

Where δ is the deformation parameter. When $\delta = 0$, the formula becomes

$$E_{g1} = E_{g2} = 45.0\ Z^{-1/3}\ A^{0.05}$$

i. e. a single peak formula for the spherical nuclei is obtained. These formulas could reproduce the experimental results very exactly and can be used to calculate the giant dipole resonance peak energies for both spherical and deformed nuclei.

3 The Activities on CENPL

In order to review the work progress, discuss some problems in constructing CENPL, propose and arrange the tasks for the next period, we held the 2nd Working Meeting on CENPL (July 1994, Chengde), as well as two Workshops on the level density (June 1994, Nanning) and the 2nd optical model parameters (Dec. 1994, Tianjin).

We also participated the 1st Research Coordinated Meeting on "Development of Reference Input Parameter Library for Nuclear Model Calculations of Nuclear Data" organized by the International Atomic Energy Agency (Cervia, Italy, 19～23, Sep. 1994)[12].

The project is supported in part by the International Atomic Energy Agency and the National Natural Science Foundation of China.

References

[1] Su Zongdi et al., CNDP, 11, 103(1994)
[2] Zuo Yixin et al., CNDP, 11, 95(1994)
[3] Zhang Limin et al., CNDP, 10, 88(1993)
[4] Su Zongdi et al., CNDP, 12, 83(1993)
[5] Huang Zhongfu et al., "Four Kinds of Data Related to Level Density", Report of CNDC in 1993

[6] Su Zongdi et al., CNDP, 13(1995)
[7] Lu Guoxiong et al., to be published
[8] Dong Liaoyuan et al., to be published
[9] Huang Zhongfu et al., to be published
[10] Liu Jianfeng et al., to be published
[11] Liu Jianfeng et al., to be published
[12] P. Oblozinsky, INDC(NDS)-321

The Sub-Library of Nuclear Level Density — The Data File of Nuclear Level Density Parameters (CENPL.LDP)

Su Zongdi

(Chinese Nuclear Data Centre, IAE)

Huang Zhongfu Dong Liaoyuan

(Department of Physics, Guangxi University)

Introduction

One of the basic statistical properties of the excited nuclear levels is the nuclear level density, which are a crucial ingredient in the nuclear reaction models and neutron transport calculations. For example, the level densities are needed in the calculations of the widths, cross sections, spectra etc. for various reaction channels, and the requirements of their accuracy and reliability are ever higher in the practical calculations. Since they have played a very important role in both fundamental nuclear physics and different kinds of applications, a level density parameter data file (LDP), the nuclear level density sub-library of the Chinese Evaluated Nuclear Parameter Library (CENPL), has been set up at the Chinese Nuclear Data Center (CNDC). Some valuable sets of the level density parameters for the popular level density models have been collected and

compiled in the LDP–1 (Version 1) data file. These models and corresponding parameters are all used widely in practical applications.

1 Contents

The LDP–1 data file contains eight sets of level density parameters for three kinds of level density formulas, i. e. the composite formula of the constant temperature–Fermi gas (Gilbert–Cameron approch), the back–shifted Fermi gas model and generalized superfluid model. They were obtained by fitting the related data, such as the average resonance level spacing D_0 and the cumulative number N_0 of low–lying levels. They are contained in Tables 1, 2 and 3 respectively, this paper has omitted these tables.

In Table 1, three sets of level density parameters for the composite four–parameter level density formula recommended by Gilbert and Cameron (G–C)[1] in 1965, Cook et al.[2] in 1967 and Su et al.[3] in 1985 have been compiled respectively. The parameters of G–C and Su et al. are from $Z=11$, $N=11$ to $Z=98$, $N=150$; the Cook's are from $Z=28$, $N=33$ to $Z=95$, $N=150$.

Table 2 consists of three sets of level density parameters for back–shifted Fermi gas model recommended by Dilg et al. (the half– rigid body parameter and rigid body parameter for the moment of inertia)[4] in 1973 and Huang et al.[5] in 1991. The former contains 219 nuclides ranging from ^{41}Ar to ^{249}Cm, and the latter contains 321 nuclides ranging from ^{17}O to ^{253}Cf.

Table 3 consists of two sets of level density parameters for generalized superfluid model formula recommended by Ignatyuk et al.[6] in 1991 and Lu et al.[7] in 1994. They contain 249 nuclides ranging from ^{40}Ca to ^{250}Cf.

2 Format

Each record in Table 1 contains N or Z, $P(N)$, $S(N)$, $P(Z)$ and $S(Z)$. They are the neutron or charge number (column 1～4), pairing energy of neutron in MeV (7～11 for Su et al., 33～36 for G–C, and 57～61 for Cook et al.), shell correction of neutron in MeV (12～17 for Su et al., 37～42 for G–C, 62～67 for Cook et al.), pairing energy of proton in MeV (18～23 for Su et al., 43～47 for G–C, 68～73 for Cook et al.), shell correction of proton in MeV (24～30 for Su et al., 48～54 for G–C, 74～80 for Cook et al.), respectively.

Each record in the Table 2 contains Z, EL, A, a, and BSE. They are the charge number (column 1～3), element symbol (5～6), mass number (8～10), level density parameter in 1 / MeV (13～17 for Huang et al., 26～30 for half–rigid body parameter, 39～43 for rigid body parameter) and back–shift

energy in MeV (19～23 for Huang et al., 32～36 for half–rigid body parameter, 45～49 for rigid body parameter), respectively.

Each record in Table 3 contains Z, EL, A, Esc, $E2^+$, Dp, as, E_{sh}. They are the charge number (column 1～3), element symbol (5～6), mass number (8～10), shell correction in nuclear binding energy in MeV (13～18), experimental value of energy for the first 2^+ level of the even–even nuclei and extrapolation of those values for the neighboring odd and odd–odd nuclei in MeV (20～23), deformation parameter for nucleus (25～28), asymptotic value of the level density parameter at high excitation energy in 1 / MeV (31～35 for Lu et al., 44～48 for Ignatyuk et al.), supplementary shift in the excitation energy in MeV (37～41 for Lu et al., 50～54 for Ignatyuk et al.).

Acknowledgments

The authors would like to thank Dr. Ge Zhigang and Mr. Jin Yongli for their participation in a part of the work.

The project is supported in part by the International Atomic Energy Agency and the National Natural Science Foundation of China.

References

[1] A. Gilbert and A. G. W. Cameron, Can. J. Phy., 43, 1446(1965)

[2] J. L. Cook, H. Ferguson and A. R. de L. Musgrove, Aust. J. Phys., 20, 477(1967)

[3] Su Zongdi et al., INDC (CPR)–2, 1985

[4] W. Dilg et al., Nucl. Phys., A217, 269(1973)

[5] Huang Zhongfu et al., Chinese J. Nucl. Phys., 13, 147(1991)

[6] O. T. Grudzevich et al., 《Systematics of level densities》, Private communication, Nov.'1991

[7] Lu Guoxiong et al., to be published

Program MADEX Creating Index for CPL in CNDC

Liu Ruizhe

(Chinese Nuclear Data Center, IAE)

Due to the fact that the computer programs, which are from Chinese and foreign programmers and have been registered in Computer Program Library (CPL) in Chinese Nuclear Data Center (CNDC), are getting more and more, the number of users is on increasing. On the one hand, it is difficult for users to search codes they need without index especially the user have no exact information, on the other hand, the information on programs collected by CPL should be shown to domestic and foreign users for exchanging and using. Obviously varied indexes of codes are needed. In order to meet the needs, program MADEX was developed.

Three executable codes are contained in MADEX. They are ORDEL, SUBDEX and KEYDEX which are used to create alphabetical index, subject index and keyword index, which are in the same format as that of NEA Data Bank, and allow the user to look up programs according to program name, program category and program keyword.

The functions of the three programs are described below.

1 ORDEL

ORDEL is a program for creating alphabetical index files CNDCP.DAT and CNDCB.DAT. They are the indexes for programs written by Chinese and foreigner, respectively. MADEX is also for adding new, modifying and deleting old program index. CNDCP.DAT and CNDCB.DAT are in alphabetical order of domestic and foreign program names, respectively. The index files are with fixed record length 100 bytes on Micro VAX–II. One record is for one program index. Every index line has the following format :

Column 1–77 : program name(s) followed by a short descriptive text. The abbreviations used here are as same as that in publication of NEA Data Bank[1].

Column 78–87 : abstract identification number which is reference number under which the abstract and the program can be found.

Column 88–91 : Date (mmyy) : the date when the program is tested by

expert invited by CNDC.

2 The Function of SUBDEX

SUBDEX is used to establish subject index file, when a new program is registered. The input data are abstract file and alphabetical index file, so SUBDEX must be executed after ORDEL execution. The programs written by Chinese are grouped in fifteen categories according to the subject. The 15 categories are as follows :

CC–Coupled Channel;
DI–Direct Interaction;
DWBA–Distorted Wave Born Approximation;
EDP–Experimental Data Process;
FKK–Feshbach–Kerman–Loonin;
GMC–Generations of Multigroup Constants;
INCM–Intra–Nuclear Nucleon Cascade Model;
OM–Optical Model;
PEM–Pre–Equilibrium Model;
PLT–Plot;
RC–Reactor Calculations;
RM–R–Matrix;
RP–Related Program;
SM–Statistical Model;
SYS–Systematics.

One or several category abbreviations can be written for one program which based on how many subjects the program refer to.

The subject index file named SUBDEX.CHA is divided into fifteen parts and in the order of abbreviation letter. In each part, the indexes, which have the same format as alphabetical index, are in order of program name. Every program index line is grouped under one or several categories, which depends on how many categories written in the 17th term of the program abstract.

3 The Function of KEYDEX

KEYDEX is used to establish the program keyword index file. Entries are in alphabetical order of the keyword. The format of index line is as follows :

Column 1–30 : Keyword, in alphabetical order;

Column 31–120 : Index, the same as in alphabetical index.

This index is convenient for users if they do not know the program name, author or the category.

Reference

[1] Abstract Index, N. E. A. Data Bank

VI ATOMIC AND MOLECULAR DATA

Radiative Loss for Carbon Plasma Impurity

Yao Jinzhang Tian Wei

(Chinese Nuclear Data Centre, IAE)

There are a number of particles such as atoms, ions and electrons in fusion plasma. The radiation with electronic and magnetic wave will occur when the status in kinematics and dynamics of particles are changed. Radiative loss can make a singnificant contribution to the local power balance and the total energy losses in present Tokamak. They should also play an important role in physics and design of future reactors, especially in the plasma edge and diverter regions. For example, line radiation by light impurities in the edge region can help distribute the exhausted power over a large area of the neutralizer plates and alleviate the erosion in the core. But it always is detrimental. In addition to diluting the fuel there, strong line radiation by not full stripped ions will make the conditions required for ignition more difficult to achieve.

We calculate the radiative loss for carbon plasma impurity by modified coronal model[1] with metastable state effects. The present calculation is based on the following assumptions : (1) There may be long lived metastable states for which the largest transition probability is smaller than, or comparable to, the largest collisional rate to the ground state or to other metastable states. (2) For metastable states, the relative densities n_{qf} for given ionization state q are determined by the excitation or deexcitation between the ground state and metastable states, radiative decay ionization from the ground state and metastable states, and excitation from the ground state and metastable state to non–metastable states. (3) The multistep processes are neglected for excited nonmetastable states. (4) The recombination of more than eight radiations or dielectrons from metastable states may take place. (5) For the relatively low densities of interest to Tokamak plasma less than $10^{14}/\mathrm{cm}^3$, three–body recombination is neglected. With this model, the radiative loss rate P_r is

$$P_r = \sum_q \{ \sum_{fi} n_{qf} A^q_{fi} \varepsilon^q_{if} + \sum_{ifj} n_{qi} \int dV^3 \varepsilon_j^{q-1} V \sigma^q_{dr,ifj}(V) f(V)$$
$$+ \sum_{if} n_{qi} \int dV^3 \left(\frac{1}{2} M V^2 + \varepsilon^q_{0i} + \varepsilon_0^{q-1} \right) V \sigma^q_{rr,if}(V) f(V)$$
$$+ n_H \sum_{if} n_{qi} T^q_{if} \varepsilon^{q-1}_{0f} + \sum n_{qi} P^q_i \} \qquad (1)$$

In the equation n_H is the density of neutral hydrogen. The coefficient A^q_{fi} is the transition probability for the transition from state i to f. The $\sigma^q_{dr,ifj}(V)$ is the cross section for dielectronic recombination into the Rydberg state of ionization state $q-1$, associated with a core transition to state f, from an ion initially in state i of stage q. The $\sigma^q_{rr,if}(V)$ is the cross section for radiative recombination into state f of stage $q-1$, from stage q in state i. The T^q_{if} is the rate of charge transfer between neutral hydrogen and an impurity initially in state i of stage q resulting in stage $q-1$ in state f. The $f(v)$ is a Maxwellian electron distribution function normalized and its integral over velocitiesis equal to unity. The P^q_i is the rate of bremsstrahlung associated with stage q in state i. Many atomic processes involved in the calculation of radiative loss for fusion plasma. Excitation, ionization, radiative recombination, dielectron recombination and transition probabilities data are included in Eq. (1). Most of excitation rates of carbon ions used in this calculation are those recommended by Phanef et al[2]. Ionization rate from the ground state are calculated from analytic integration of the cross sections recommended by Lennon et al[3]. Ionization from metastable state is calculated with the Lotz semiempirical formula[4]. Radiative recombination from the ground state is calculated so as to reproduce recommended total recombination rates. The rates of radiative recombination to specific all rates are then multiplied by a constant which is chosen so that the normalized rates correctly reproduce the recommended rate for total radiative recombination rates. The total recombination rate used is calculated by Aldrovandi et al[5]. No recommended data have been found for radiative recombination from metastable states. The rate is calculated from scale hydrogenic expression. The rate of dielectronic recombination is calculated empirically and normalized so as to reproduce recommended rates for specific groups of transitions[6~12]. Most transition probabilities used in the calculations have been provided by Wiese et al[13]. For forbidden transitions in hydrogen- and helium-like ions, we use the transition probabilities calculated by Drake et al[14, 15]. For beryllium-like ions are complemented by the transition probabilities of Shevelko et al[16].

Calculation Result and Discussion

The results calculated for various stages of carbon are shown in Fig. 1. The CI is for neutral carbon and CVII is for full stripping. The result indicates that radiative loss depends on the charged stages q of ions. Radiative loss for neutral Carbon is maximum and decreasing with q increasing. The situation becomes very complication in a region of electron temperature less than 100 eV due to internal configuration of ions. Computational error is 50%. The correctness of result is poorer if the isotopic abundance would be considered.

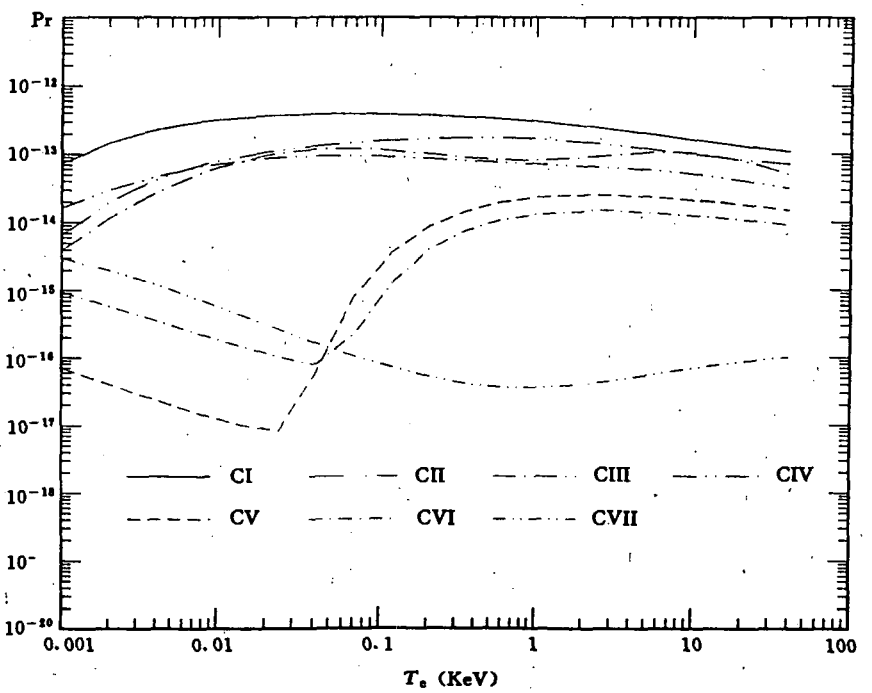

Fig. 1 Radiative loss coefficients for carbon plasma impurity

References

[1] H. P. Summers and R. W. P. Mcwhirter, J. Phys., B12, 2387(1979)

[2] R. A. Phaneuf et al., Rep. ONRL–6090 (1987)

[3] M. A. Lennon et al., J. Phys. Chem. Ref. Data 17, 1285(1988)

[4] W. Lotz, Z. Phys., 206, 205(1967)

[5] S. M. V. Aldrovandi et al., Astrophys, 25, 137(1973)

[6] S. Datz and P. F. Dittner, Z. Phys., D 10, 187(1988)

[7] N. R. Badnell, J. Phys., B 20, 2081(1987)

[8] N. R. Badnell, J. Phys., B 21, 749(1988)
[9] N. R. Badnell, Phys. Scr., T28, 33(1989)
[10] D. C. Griffin, Phys. Scr., T28, 17(1989)
[11] Y. Hahn, Phys. Scr., T28, 25(1989)
[12] L. Roszman, J. Phys. Scr., T28, 36(1989)
[13] W. L. Wiese et al., At. Trans. Prob. Vol.1 Hydrogen through Neon (1966)
[14] G. W. F. Drake, Phys. Rev., A34, 2871(1986)
[15] G. W. F. Drake, Phys. Rev., A3, 908(1971)
[16] V. P. Shevelko et al., Phys. Scr., T28, 39(1989)

VII NUCLEAR DATA NEWS

Activities and Cooperations on Nuclear Data in China During 1994

Zhuang Youxiang

(Chinese Nuclear Data Center, IAE)

1 The Meetings were Held by CNDC in 1994 :

1) "The Third Meeting for Reviewing Codes Related to Nuclear Data", July 15～16, Chengde City, Hebei Province; 12 codes were reviewed and accepted into the computer program library at CNDC. They are related to nuclear model calculation, experimental data compilation and evaluation, plotting, management codes of computer program library and Chinese evaluated nuclear parameter library.

2) "The Second Working Meeting of Chinese Evaluated Nuclear Parameter Library (CENPL)", July 17～18, Chengde City, Hebei Province; exchanged and reviewed the progress on CENPL as well as CRP, discussed some technical problems and possible international cooperation, arranged the future work for recent three years (1995～1997).

3) "The Meeting of Chinese Nuclear Data Evaluation Working Group", July 19～21, Chengde City, Hebei Province; exchanged the progress on CENDL-2.1, reviewed the evaluations of 8 nuclides completed newly, and discussed the future work.

4) " The Symposium on Nuclear Data Measurement, Evaluation and Benchmark Testing", Oct. 6～11, Huangshan City, Anhui Province; some great progresses on nuclear data measurements were made, such as fission product yield, double differential cross section of secondary neutron and (n,α), (n,xp) reactions, and activation cross section of long-lived nuclides; interchanged the progresses on CENDL-2.1, charged particle and decay data, nuclear model parameter library, medium-high energy, four bodies and fission mechanism re-

searches, communicated the progress on integral fusion experiment, discussed the benchmark testing work in the future.

2 The International Meetings and Workshops in Nuclear Data Field Attended by Staff Members of CNDC in 1994:

1) "13th Advisory Group Meeting on the Coordination of Nuclear Reaction Data Center", April 25~27, Paris, France.

2) "Workshop on Nuclear Reactor — Physics, Design and Safety", April 7 ~ May 7, ICTP, Italy.

3) " Meeting of NEA Working Party on International Evaluation Cooperation", May 4~6, Oak Ridge, USA.

4) "International Conference on Nuclear Data for Science and Technology ", May 9~13, Gatlinburg, USA.

5) " IAEA Advisory Group Meeting on the Coordination of the Nuclear Structure and Decay Data Evaluation Network" , May 16~ 20, Lawrence Berkeley Lab., USA.

6) "First Research Coordination Meeting on Development of Reference Input Parameter Library for Nuclear Model Calculations of Nuclear Data", Sept. 19 ~23, Cervia, Italy.

7) "IAEA Research Coordination Meeting on Establishment of an International Reference Data Library of Nuclear Activation Cross Sections", Oct. 4 ~ 7, Debrecen, Hungary.

8) "Research Coordination Meeting on Compilation and Evaluation of Fission Yield Nuclear Data", Oct. 17~20, Vienna, Austria.

3 The Foreign Scientists in Nuclear Data Field Visited CNDC / CIAE in 1994:

Dr. E. T. Cheng, San Diego, USA, June 1~2;
Dr. H. Takano, JAERI / NDC, Japan, Sept. 8~11;
Dr. C. Y. Fu, ORNL, USA, Oct. 24~29.

4 One staff member of CNDC as a visiting scientist has worked at Kentucky University, USA, for one year.

CINDA INDEX

Nuclide	Quantity	Energy (eV)		Lab	Type	Documentation			
		Min	Max			Ref	Vol	Page	Date
^{7}Li	(n,n′)	9.0 +6	1.0 +7	BJG	Expt	Jour CNDP	13	1	Jun 95
^{9}Be	(n,n)		1.47+7	SIU	Expt	Jour CNDP	13	19	Jun 95
^{11}C	(p,x)	5.0 +6	2.5 +7	AEP	Theo	Jour CNDP	13	47	Jun 95
	(d,x)	1.0 +6	2.5 +7	AEP	Theo	Jour CNDP	13	47	Jun 95
^{58}Ni	(n,α)	6.0 +6	7.0 +6	BJG	Expt	Jour CNDP	13	10	Jun 95
Ni	(n,xp)		1.46+7	STC	Expt	Jour CNDP	13	25	Jun 95
^{54}Fe	(n,x)	Thrsh	6.0 +7	AEP	Eval	Jour CNDP	13	92	Jun 95
^{56}Fe	(n,x)	Thrsh	6.0 +7	AEP	Eval	Jour CNDP	13	92	Jun 95
^{57}Fe	(n,x)	Thrsh	6.0 +7	AEP	Eval	Jour CNDP	13	92	Jun 95
^{58}Fe	(n,x)	Thrsh	6.0 +7	AEP	Eval	Jour CNDP	13	92	Jun 95
Fe	(n,x)	Thrsh	7.0 +7	AEP	Eval	Jour CNDP	13	92	Jun 95
	(n,xp)		1.46+7	STC	Expt	Jour CNDP	13	92	Jun 95
^{63}Cu	(n,x)	Thrsh	7.0 +7	AEP	Eval	Jour CNDP	13	98	Jun 95
		Thrsh	7.0 +7	AEP	Theo	Jour CNDP	13	53	Jun 95
^{65}Cu	(n,x)	Thrsh	7.0 +7	AEP	Eval	Jour CNDP	13	98	Jun 95
		Thrsh	7.0 +7	AEP	Theo	Jour CNDP	13	53	Jun 95
Cu	(n,x)	Thrsh	7.0 +7	AEP	Eval	Jour CNDP	13	98	Jun 95
		Thrsh	7.0 +7	AEP	Theo	Jour CNDP	13	53	Jun 95
^{106}Cd	(n,2n)	1.34+7	1.48+7	LNZ	Expt	Jour CNDP	13	13	Jun 95
^{110}Cd	(n,2n)	1.34+7	1.48+7	LNZ	Expt	Jour CNDP	13	13	Jun 95
^{111}Cd	(n,p)	1.34+7	1.48+7	LNZ	Expt	Jour CNDP	13	13	Jun 95
^{116}Cd	(n,2n)	1.34+7	1.48+7	LNZ	Expt	Jour CNDP	13	13	Jun 95
^{196}Hg	(n,p)	1.41+7	1.48+7	LNZ	Expt	Jour CNDP	13	16	Jun 95
	(n,d)	1.38+7	1.48+7	LNZ	Expt	Jour CNDP	13	16	Jun 95
^{198}Hg	(n,p)	1.41+7	1.48+7	LNZ	Expt	Jour CNDP	13	16	Jun 95
^{199}Hg	(n,p)	1.45+7	1.48+7	LNZ	Expt	Jour CNDP	13	16	Jun 95
^{238}U	(n,n′)	1.0~5	2.0 +7	BJG	Eval	Jour CNDP	13	86	Jun 95

STC = University of Science and Technology of China

Author, Comments
Chen Jinxiang+, ANG DIST, TOF
Zhang Kun+, ANG DIST, TOF
Shen Qingbiao+, SIG, p+ C−1
Shen Qingbiao+, SIG, d+ C−1
Fan Jihong+, SIG, ANG DIST, GIS
Ye Bangjiao+, SIG, DDCS, EΔE
Yu Baosheng+, SIG, CR−51, MN−52, 54
Yu Baosheng+, SIG, CR−51, MN−52, 54, 56
Yu Baosheng+, SIG, CR−51, MN−52, 54, 56
Yu Baosheng+, SIG, CR−51, MN−52, 54, 56
Yu Baosheng+, SIG, CR−51, MN−52, 54, 56
Ye Bangjiao+, SIG, DDCS, EΔE
Yu Baosheng+, SIG, CO−56～58
Shen Qingbiao+, SIG, n+ Cu−63
Yu Baosheng+, SIG, CO−56～58, 60
Shen Qingbiao+, SIG, n+ Cu−65
Yu Baosheng+, SIG, CO−56～58, 60
Shen Qingbiao+, SIG, n+ Cu
Kong Xiangzhong+, SIG, TBL, ACTIV
Kong Xiangzhong+, SIG, TBL, ACTIV
Kong Xiangzhong+, SIG, TBL, ACTIV
Kong Xiangzhong+, SIG, TBL, ACTIV
Yuan Junqian+, SIG, TBL, ACTIV
Yuan Junqian+, SIG, TBL, ACTIV
Yuan Junqian+, SIG, TBL, ACTIV
Yuan Junqian+, SIG, TBL, ACTIV
Tang Guoyou+, FOR CENDL−2.1

（京）新登字 077 号

图书在版编目 (CIP) 数据

核数据进展通讯 (13) = COMMUNICATION OF NUCLEAR DATA PROGRESS NO. 13 : 英文 / 中国核数据中心编. —北京 : 原子能出版社, 1995, 6
ISBN 7-5022-1365-1

I. 核 … II. 核 … III. 核技术—数据—进展—通讯—英文 IV. TL-37

中国版本图书馆 CIP 数据核字 (95) 第 06797 号

原子能出版社出版发行
责任编辑 : 李乾坤
社址 : 北京市海淀区阜成路 43 号 邮政编码 : 100037
核科学技术情报研究所印刷
开本 787×1092 1/16 • 印张 8 1/2 • 字数 140 千字
1995 年 6 月北京第一版 • 1995 年 6 月北京第一次印刷

COMMUNICATION OF NUCLEAR DATA PROGRESS

ISBN 7-5022-1365-1